Investigating Proteomic Profiles of Rainbow Trout (*Oncorhynchus mykiss*) Kidney and Liver Tissues Exposed to Low Concentrations of Waterborne Nickel

by

Kylee Ronnenberg

A thesis submitted to the
School of Graduate and Postdoctoral Studies in partial
fulfillment of the requirements of the degree of

Master of Science in Applied Bioscience

Faculty of Science

University of Ontario Institute of Technology (Ontario Tech University)

Oshawa, Ontario, Canada

August 2023

THESIS EXAMINATION INFORMATION

Submitted by: **Kylee Ronnenberg**

Master of Science (MSc) in **Applied Bioscience**

Thesis title: Investigating Proteomic Profiles of Rainbow Trout (*Oncorhynchus mykiss*) Kidney and Liver Tissues Exposed to Low Concentrations of Waterborne Nickel

An oral defense of this thesis took place on August 23, 2023 in front of the following examining committee:

Examining Committee:

Chair of Examining Committee	Dr. Bernadette Murphy
Research Supervisor	Dr. Denina Simmons
Examining Committee Member	Dr. Andrea Kirkwood
Thesis Examiner	Dr. Sean Forrester

The above committee determined that the thesis is acceptable in form and content and that a satisfactory knowledge of the field covered by the thesis was demonstrated by the candidate during an oral examination. A signed copy of the Certificate of Approval is available from the School of Graduate and Postdoctoral Studies.

ABSTRACT

Nickel has become a component of natural freshwater that may pose serious ecological risks to aquatic wildlife. Due to Canada's significant presence in producing and exporting nickel, the country has the opportunity to negatively impact aquatic watersheds and the surrounding environment. We examined changes in protein profiles of kidney and liver tissues of rainbow trout using untargeted proteomics to study the impacts of low concentration nickel (1 - 46 ppb). Findings suggest that the organs' proteomes showed fewer significant protein changes compared to non-lethal and non-invasive sample types (e.g. epidermal mucus and blood plasma) with regard to nickel toxicity. The proteome of the kidney as compared to the liver was more significantly affected by nickel. Additionally, findings suggest that proteins involved in the regulation of biological and cellular processes were impacted and that the kidney proteome of rainbow trout is sensitive to low concentrations of nickel.

Keywords: Nickel; rainbow trout; liver; kidney; sampling

AUTHOR'S DECLARATION

I hereby declare that this thesis consists of original work of which I have authored. This is a true copy of the thesis, including any required final revisions, as accepted by my examiners.

I authorize the University of Ontario Institute of Technology (Ontario Tech University) to lend this thesis to other institutions or individuals for the purpose of scholarly research. I further authorize the University of Ontario Institute of Technology (Ontario Tech University) to reproduce this thesis by photocopying or by other means, in total or in part, at the request of other institutions or individuals for the purpose of scholarly research. I understand that my thesis will be made electronically available to the public.

The research in this thesis that was performed in compliance with the regulations of the Animal Care Committee under **16421**.

_____ KYLEE RONNENBERG

STATEMENT OF CONTRIBUTIONS

Urvi Pajankar MSc designed the nickel exposure study on rainbow trout, performed the analytic calculations to determine the appropriate nickel sulphate hexahydrate salt quantities for the appropriate aquatic nickel concentration, and performed the nickel exposure study on rainbow trout. She completed protein preparation pertaining to skin mucus and blood plasma for her research, titled “Investigated proteomic profiles of skin mucus and blood plasma of rainbow trout (*Oncorhynchus mykiss*) exposed to low concentrations of waterborne nickel”.

I completed the protein preparation pertaining to liver and kidney tissues, the appropriate statistics, and the proteomic analysis of the liver and kidney tissues and skin mucus and blood plasma of rainbow trout exposed to low concentrations of waterborne nickel.

I hereby certify that I am the sole author of this thesis and that no part of this thesis has been published or submitted for publication. I have used standard referencing practices to acknowledge ideas, research techniques, or other materials that belong to others. Furthermore, I hereby certify that I am the sole source of inventive knowledge described in this thesis.

ACKNOWLEDGEMENTS

I am sincerely grateful to my research supervisor, Dr. Denina Simmons, for giving me the opportunity to complete this research, providing invaluable mentorship and guidance throughout my time at Ontario Tech University. She convincingly transferred enthusiasm, compassion, excitement, and adventure in regards to research and science. Without her guidance, passion, and motivation, this work or my time at Ontario Tech University would not have been possible. I am forever indebted to the kindness and gentleness that she has shown me and I hope to be a fraction of the role model that she has continued to be. She will forevermore be an inspiration in which I aspire. I cannot thank her enough for the time and patience that she has shown me as a mentor, as a professor, and as a friend.

I would like to acknowledge with gratitude, the support and love from my husband. His constant encouragement and motivation kept me going during times of considerable difficulty and stress. I experienced a number of personal and academic struggles but his encouragement never wavered. I am beyond thankful that I have been able to emotionally and financially rely on my best friend during my time at school.

I would like to thank all my peers for their constant friendship during my time at Ontario Tech University. I would not be here today if it was not for the care of my fellow graduate students that showed me perseverance along the way. I am so grateful for all that I have learned in the Aquatic Omics Laboratory. In particular, I want to thank Urvi Pajankar for her eagerness to expand her study and for her contributions to non-invasive sampling. I would also like to thank my committee member, Dr. Andrea Kirkwood, for providing constructive feedback and continual support during my research. She allowed me freedom

and accommodations that have permitted me to succeed in a dependable environment. I am looking forward to utilizing my knowledge and skills in my future career.

TABLE OF CONTENTS

LIST OF TABLES

LIST OF FIGURES

LIST OF ABBREVIATIONS

AB	Ammonium bicarbonate
ACC	Animal Care Committee
AUP	Animal Utilization Protocol
BLAST	Basic Local Alignment Search Tool
$CaCO_3$	Calcium carbonate
Cl	Chloride
CTDbase	Comparative Toxicogenomic Database
DDA	Data Dependent Acquisition
DO	Dissolved Oxygen
DOC	Dissolved Organic Content
GO	Gene Ontology
HDPE	High-density polyethylene
HPLC	High-Performance Liquid Chromatography
IAA	Iodoacetamide
LC-HR-MS/MS	Liquid Chromatography High Resolution Tandem Mass-Spectrometry
LC-MS	Liquid Chromatography Mass Spectrometry
LOQ	Limit of Quantification
Ni or Ni^{2+}	Nickel
$NiCl_2$	Nickel chloride
Ni_3S_2	Nickel sulphide
$Ni(SO_4)$	Nickel sulphate
$NiSO_4.6H_2O$	Nickel sulphate salt
OROF	Ontario Ring of Fire
pH	Potential Hydrogen
PTFE	Polytetrafluoroethylene
Q-TOF	Quadruple Time-of-Flight
SGS	Standard Global Services
TECP	Tris(2-carboxyethyl) phosphine hydrochloride

Chapter 1. Introduction

1.1 Nickle: Overview and Importance

Nickel (Ni) is a stable, malleable, conductive, and non-corrosive metal that is in high demand due to its commercial applications (Barceloux and Barceloux 1999). Ni has an atomic and mass number of 28 and 58.69, respectively (Hausinger 2013). It is a hard and ductile transition metal and exists as several isotopes, such as ^{58}Ni, ^{60}Ni, ^{61}Ni, ^{62}Ni ^{64}Ni, with ^{58}Ni being the most naturally abundant (Barceloux and Barceloux 1999; Templeton 1994; Hausinger 2013). Ni occurs in a few oxidative states; the most common oxidative state is +2, with compounds 0, +1, and +3 being well documented (Barceloux and Barceloux 1999; Couture and Pyle 2011). Pure Ni was first produced by Torbern Bergman in 1775, although the use of Ni has been traced back to 3500 BC (Hausinger 2013).

Commercially, Ni is used as an alloy in the formation of stainless-steel and nichrome, an alloy of Ni and chromium (Nash 1986; Basketter et al. 2003). Ni plates other metals as corrosion-resistant protection and has the ability to tolerate high temperatures. Ni has been used as a prevalent component in the manufacturing of batteries, including rechargeable batteries and batteries used in hybrid and electric vehicles (Fraser et al. 2021). The commercial uses of Ni can be divided into a few groups, with engineering and metal goods being in the highest demand and construction and electronic goods following in demand. Metallic Ni is present in more than 3,000 different alloys which are used in the manufacturing of kitchen utensils, coins, car parts, paints, solvents, and some pesticides, in addition to the manufacturing of batteries (Tomei et al. 2004). The frequent use of commercial chemicals by industrial companies is a prominent source of aquatic pollution.

Additionally, there are a variety of diffuse sources, such as atmospheric deposition, natural weathering, and/or surface runoff, that contribute to environmental Ni accumulation.

Plants and limited terrestrial animals rely on Ni as an essential trace metal. Plants rely on Ni for growth and development as it is integral for the activation of several enzymes required for nitrogen metabolism (Mustafiz et al. 2014; Shahzad et al. 2018). Ni is classified as an essential nutrient in 17 animal species, including chicken, cow, goat, pig, rat, and sheep; furthermore, at very low levels, Ni is essential to humans (Wintz, Fox, and Vulpe 2002; Poonkothai and Vijayavathi 2012). As an essential nutrient, Ni functions in the action and formation of cyclic guanosine monophosphate (cGMP), a messenger signal that regulates various physiological processes (Poonkothai and Vijayavathi 2012). Naturally occurring concentrations of Ni in soil (100 mg/kg) and water (5 μg/L) have been accelerated in accumulation in recent years due to anthropogenic activities (Shahzad et al. 2018). Despite Ni being an essential element required for the healthy growth of plants, animals, and soil microbes, excess Ni affects the photosynthetic functions of plants, causes acute and chronic diseases in humans, and reduces soil fertility (Seregin and Kozhevnikova 2006; Poonkothai and Vijayavathi 2012; Shahzad et al. 2018). However, the essentialness of Ni in aquatic animals has remained unestablished. Based upon the toxic effects of Ni to animals, including skin allergies, carcinogenesis, cardiovascular, and renal disorders (Denkhaus and Salnikow 2002), it is clear that understanding the significance of Ni to environmental ecosystems is required for water quality guidelines and improving policies to prevent contamination.

1.2 Environmental Nickel in Canada

Nickel is listed as a contaminant of concern in the Priority Substances List and Toxic Substances List under the Canadian Environmental Protection Act, 1999 (CEPA 1999). Additionally, Ni is listed as a top six priority critical mineral in Canada for both domestic and international markets to spur Canadian economic growth (CCMS 2022). Ni is not used solely for domestic manufacturing, as there is economic value by increasing exports for allies, and expanding domestic refining, processing and components manufacturing (CCMS 2022). Ni is present in Canadian freshwater and terrestrial environments due to a variety of human activities in addition to mining and smelting, such as fuel combustion, scrap metal reprocessing, and waste incineration (Chau and Kulikovsky-Cordeiro 1995). Collective studies from 1981-1992 indicate that most unpolluted rivers and lakes in Canada contained between 0.1 and 10 μg/L Ni while industrial sites generally contained between 50 and 2000 μg/L Ni (Chau and Kulikovsky-Cordeiro 1995). Additionally, collective studies on Ni levels in sediment collected from 1983-1992 from polluted sites such as the Welland River, some Sudbury lakes, and Hamilton and Toronto Harbours ranged between 20 and 5000 μg/g Ni dry weight (Chau and Kulikovsky-Cordeiro 1995). Furthermore, collective studies from 1984-1991 showed that the more urbanization and industrialization associated with the city, the higher the means and medians of Ni levels in air (Chau and Kulikovsky-Cordeiro 1995). With the increasing use of Ni for economic and commercial purposes, the mining and extraction of Ni is projected to increase.

A large area of untouched natural resources is found in the James Bay Lowland region, located in Northern Ontario, Canada. This area of the Hudson Bay Lowlands is the

second largest peatland ecosystem worldwide, behind the Cuvette Centrale swamp forest in the Congo Basin (Dargie et al. 2017). Peatlands are a type of wetland system that are extremely rich in organic carbon, as the released carbon dioxide from decaying vegetation and animal matter is trapped and unable to enter the atmosphere (Dise 2009). The classification distinction between the bogs, fens, swamps, and marshes of the James Bay Lowlands is based on soil nutrients, moisture regime, and water chemistry (Preston et al. 2012). Most peat is found in cool climatic regions where unconstrained decomposition is slower. Biotic and abiotic carbon sequestration have the potential to mitigate climate change risks. Climate change models predict the James Bay Lowland region will experience warmer and drier conditions, potentially shifting the region from a long-term carbon sink to a source, which could be exasperated due to the development of mineral extraction (Preston et al. 2012; Dise 2009).

The Ontario Ring of Fire (OROF) region has a vast abundance of naturally occurring metals, such as chromite, cobalt, nickel, copper, platinum, and plentiful other mineral deposits. While these minerals have great significance to modern society, future mineral extraction has the potential to endanger the surrounding ecosystems. As an example, lead accumulates in soil with high organic content, such as peatland. Lead is a relatively unreactive post-transition metal that is a known neurotoxin that accumulates in soft tissues and bones, causing damage to the nervous system and interferes with biological functions (Rogers, Richards, and Wood 2003; Javed 2012; Paul, Chakraborty, and Sengupta 2014). Environmental contamination from metals such as nickel and cobalt are a real danger to aquatic organisms due to their ability to bioaccumulate in the aquatic food chain (Ubaid-ullah, Javed, and Abdullah 2004; Javed 2013). Proposed mineral extraction

in the OROF endangers the stability of this ecosystem, namely the large nickel deposit in the “Eagle’s Nest”. Currently, the measured Ni concentrations in the rivers near the OROF are 0.2 μg/L. Aqueous Ni can threaten the entire ecosystem, from soil to plants to wildlife, accelerating harmful effects on aquatic populations. The impacts of various metal contaminants on Canadian wetlands and surrounding ecosystems have not been investigated in depth.

1.2.1 Nickle in Aquatic Environments

As previously discussed, Ni is an essential trace metal and acts as a cofactor for hydrogen metabolism and nitrogen fixation in aquatic plants (Mustafiz et al. 2014; Shahzad et al. 2018). However, the essentialness of Ni in humans is debated and unestablished in aquatic animals. The World Health Organization’s admissible Ni concentration in drinking water is 20 μg/L (WHO; Organization 2021). The Canadian Council of Ministers of the Environment has set the Canadian water quality guideline for nickel at 25 to 150 μg/L for aquatic life (CCME; SQGHH and Provisional 2015). Previous research from our lab indicated that Ni concentrations detected in the Oshawa, Ontario drinking water is consistently 0.5 μg/L (Pajankar 2022). Various studies that have investigated Ni homeostasis have determined that Ni is comparable to other essential metals (Sreedevi et al. 1992; Chowdhury, Bucking, and Wood 2008) while contrariwise, other studies have determined that Ni is non-essential in fish (Denkhaus and Salnikow 2002). The toxicity of metals in fish is reliant on various factors, including temperature, dissolved oxygen content (DOC), pH, the presence of other metal ions, hardness, and salinity (Binet et al. 2018; Garai et al. 2021). A change in any of these factors has the potential to affect the oxidative state of the metal. The most bioavailable form of nickel in water is free divalent Ni^{2+}, which can

be absorbed at the gills and skin or ingested by fish and enter the bloodstream and digestive tract. After this uptake of Ni^{2+}, it can bind and interfere with biomolecules, making it the most toxic form of Ni in aquatic wildlife (Hoang, Tomasso, and Klaine 2004; Alsop and Wood 2011). A reduction in Ni toxicity can occur with increasing DOC and water hardness (Hoang, Tomasso, and Klaine 2004).

Historically, in Canada, Sudbury, Ontario, was the leading producer of Ni. The local mining and smelting activities in Sudbury notoriously caused large-scale contamination of water and the surrounding environment. Due to this contamination, surrounding lake water samples contained Ni concentrations around 131 μg/L, with the extensively contaminated areas having Ni concentrations close to 2000 μg/L (Dixit, Dixit, and Smol 1992), while the Ni concentration of unaffected natural water ranges from 1 to 10 μg/L (Chau and Kulikovsky-Cordeiro 1995). Water-soluble Ni compounds are nickel chloride ($NiCl_2$), nickel sulphate ($Ni(SO_4)$), and the hydrates ($NiCl_2.6H_2O$, $Ni(SO_4).6H_2O$, $Ni(SO_4).7H_2O$), that are typically used in research when examining the impact of Ni in aquatic environments (Templeton 1994). In Sudbury, there was documented loss of local fish, fish habitat, and destruction of vegetation due to the contaminated watershed ecosystems and polluted lands, which created toxic conditions for aquatic and terrestrial wildlife (Chau and Kulikovsky-Cordeiro 1995). In the late 1970s, after decades of Ni mining and smelting, Sudbury initiated restoration of land and watershed ecosystem projects (Chau and Kulikovsky-Cordeiro 1995). After several decades of remedial efforts, Sudbury has successfully restored the damaged environment and is now in recovery.

1.3 Fish Exposed to Nickel

1.3.1 Uptake

Transition metals have been known to negatively affect aquatic organisms through toxicity. Biological effects, such as deformities or mortality, can occur after chronic exposure to the free ion Ni^{2+}. Aqueous Ni is known to bind to the gills of fish, causing metal accumulation at the gill surface binding site (Meyer et al. 1999; Blewett and Leonard 2017). Fish gills are in constant contact with the external environment; thus, this organ is the primary route for Ni exposure. Additionally, fish are exposed to aqueous Ni during ingestion of contaminated food and sediments, which is absorbed through gut epithelial cells. Although the regulatory mechanisms that control Ni absorption in the intestine are not well understood (Ptashynski et al. 2001; Tjälve, Gottofrey, and Borg 1988), fish residing in Ni-contaminated environments showed high Ni concentrations in the contents of their gastrointestinal tract, which confirmed Ni exposure through ingestion of contaminated diet items (Chowdhury, Bucking, and Wood 2008). As Ni^{2+} is chemically similar to iron (Fe), the molecules compete for the same carrier proteins in the intestinal mucosa, leading to the saturation of the carrier proteins, limiting the uptake of Ni and reducing Ni accumulation in the intestinal tissues (Tallkvist, Bowlus, and Lönnerdal 2003).

1.3.2 Storage and Accumulation

Kidney and liver are the predominant sites of Ni accumulation in fish (Eisler 1998; Eric F Pane et al. 2005; Chowdhury, Bucking, and Wood 2008; Driessnack, Jamwal, and Niyogi 2017). A previous study on Lake whitefish (*Coregonus clupeaformis*) determined that fish fed medium and high doses of Ni (100 and 1000 μg Ni/g of $NiSO_4$) accumulated significant amounts of Ni in the intestinal tissues and a dose- and duration-dependent

accumulation in the stomach, kidney, liver, gill, and skin tissues (Ptashynski and Klaverkamp 2002). Brown trout (*Salmo trutta*) exposed to water-borne Ni for 3 weeks accumulated the highest concentrations of Ni in their kidneys, gills, and liver, respectively (Tjälve, Gottofrey, and Borg 1988; Ptashynski et al. 2001). Ni accumulation in the fish liver, gallbladder, and bile suggests the liver plays a role in detoxification and elimination of dietary Ni (Ptashynski et al. 2001).

1.3.3 Excretion

The kidney is the primary site of reabsorption and excretion of Ni in rainbow trout (Eisler 1998; Eric F Pane et al. 2005). Water temperature is vital for the transport of Ni, as increased water temperatures induce oxidative stress, generating ROS and inhibiting antioxidant enzyme activities, leading to nickel-induced toxicity in the aquatic mollusk, Pacific abalone (*H. discus hannai*) (Min et al. 2021). Primary nickel excretion sites, such as the liver, gills, and kidney, experience increased activity in response to nickel exposure. The remainder of the ingested, unabsorbed Ni is excreted via feces or eliminated through urine (Chowdhury, Bucking, and Wood 2008).

1.3.4 Effects of Nickel

1.3.4.1 Acute

Acute toxicity is defined as an adverse effect occurring within 24-hours following the ingestion or absorption of a substance. Acute exposure to waterborne Ni can affect respiration, renal function, circulation, protein metabolism, and ionoregulation. Water-insoluble nickel sulfide (Ni_3S_2), water-soluble nickel sulphate ($NiSO_4$) and nickel chloride ($NiCl_2$) are all known carcinogens, as the Ni ions induce heterochromatinization by binding to DNA-histone complexes and inhibiting chromatin condensation (Athikesavan et al.

2006; Blewett and Leonard 2017; Denkhaus and Salnikow 2002). Ni disrupts magnesium (Mg^{2+}) homeostasis and inhibits uptake at the organ and cellular levels of the rainbow trout kidney (Athikesavan et al. 2006; Blewett and Leonard 2017; Denkhaus and Salnikow 2002). The disruption in Mg^{2+} is due to Ni^{2+} competing through antagonism in the kidney, causing an increased loss of Mg^{2+} in the urine and overall decreasing the Mg^{2+} levels in rainbow trout blood (Eric F Pane et al. 2005). Rainbow trout acutely exposed to Ni presented kidney lesions (Eric F Pane et al. 2005), Nile tilapia (*Oreochromis niloticus*) exhibited dose-dependent increases of iron (Fe) ions in the kidney (Oliveira-Filho et al. 2010), and zebrafish (*Danio rerio*) experienced Na^{+} ion loss throughout the whole body (Alsop and Wood 2011). Structural damages of the gill lamellae due to increased Ni burden decrease the ventilation rate and cause blood hypoxia in trout (Eric F Pane, Haque, and Wood 2004; Svecevičius 2010). Prominent evidence of nickel poisoning in fish include altered behaviours such as surfacing, rapid opercular movement, convulsions, and loss of equilibrium prior to death (Svecevičius 2010). A study of acute nickel toxicity in five fish species found that the less obvious poisoning signs include decreased concentrations of glycogen in muscle and liver with increased levels of lactic acid and glucose in the blood, leading to contractions of vascular smooth muscle, typically associated with hypertension in mammals (Svecevičius 2010). Acute Ni toxicity causes noticeable deleterious effects in tissues such as the gills, liver, and kidney in a number of fish species.

1.3.4.2 Chronic

Chronic toxicity is defined as an adverse effect that spans lifetimes occurring following the repeated ingestion or absorption of a substance. Chronic exposure to waterborne Ni can cause a large range of toxic effects on fish physiological and

biochemical functions, such as damage to organs like the gills, liver, and kidney. Liver and kidney tissues are known to be the target organs for inducing toxic effects by heavy metal exposure, such as nickel, lead, or arsenic, and chronic heavy metal exposure leads to accumulation in these organs (Dave and Xiu 1991), as the kidney and liver function for detoxification and releasing toxic substances (Eisler 1998; Eric F Pane et al. 2005). The liver releases metals into the body through the circulatory system, while the kidney is responsible for external excretion of metals, although accumulated metals can also be stored in these tissues (Eisler 1998; Ptashynski et al. 2001; Eric F Pane et al. 2005). A bioindicator of contaminant exposure is the hepatosomatic index (HSI) used to determine energy reserves in the liver by comparing the weight of the liver to the total body weight of the fish (Pandit and Gupta 2019).

Similar to acute Ni toxicity, chronic Ni exposure significantly decreases Na^+ and Cl^- ions, elevates Mg^{2+} ion concentration, and increases ammonia and protein levels in the plasma of rainbow trout (Eric F Pane, Haque, and Wood 2004). In rainbow trout, chronic Ni exposure is known to affect epithelial cells through proliferation and fusion of secondary lamellae in the gills, causing hypertrophy of the epithelial cells and impairing oxygen consumption and substance exchange (Eric F Pane, Haque, and Wood 2004). Silver carp (*Hypophthalmichthys molitrix*) exposed to chronic $NiCl_2$ concentrations experienced enlargement of the lumen in the proximal and distal tubules of the kidney due to hypertrophy as the kidney was under pollution stress to eliminate the excess toxins (Athikesavan et al. 2006). Fathead minnows (*Pimephales promelas*) experienced a significant decrease in egg production (Driessnack, Jamwal, and Niyogi 2017; Pickering 1974) and zebrafish experienced delays and inhibition during the hatching of embryos

(Dave and Xiu 1991), suggesting harmful effects on the fertility of fish. These deleterious effects on embryo hatching have been documented in Atlantic salmon (*Salmo salar*), carp, and fathead minnows (Grande and Andersen 1983; Blaylock and Frank 1979; Driessnack, Jamwal, and Niyogi 2017). Rainbow trout in chronic Ni exposure situations exhibit a significant increase in antioxidant enzymatic activity with decreased enzymatic activity in regards to catalyzing the decomposition of hydrogen peroxide to water and oxygen in the brain, gills, and kidney (Topal et al. 2015). Additionally, chronic Ni exposure is a suspected neurotoxin because it impairs the nervous system of fish and causes altered behaviour (E F Pane, Richards, and Wood 2003). Chronic Ni can cause signs of demyelination in the brain and brain tissue and cause neurotic changes (Topal et al. 2015), although there is no evidence that Ni accumulates in brain tissue (Kubrak et al. 2014). Chronic Ni toxicity causes antagonistic effects at the organismal, tissue, cellular, and organelle levels in a variety of fish.

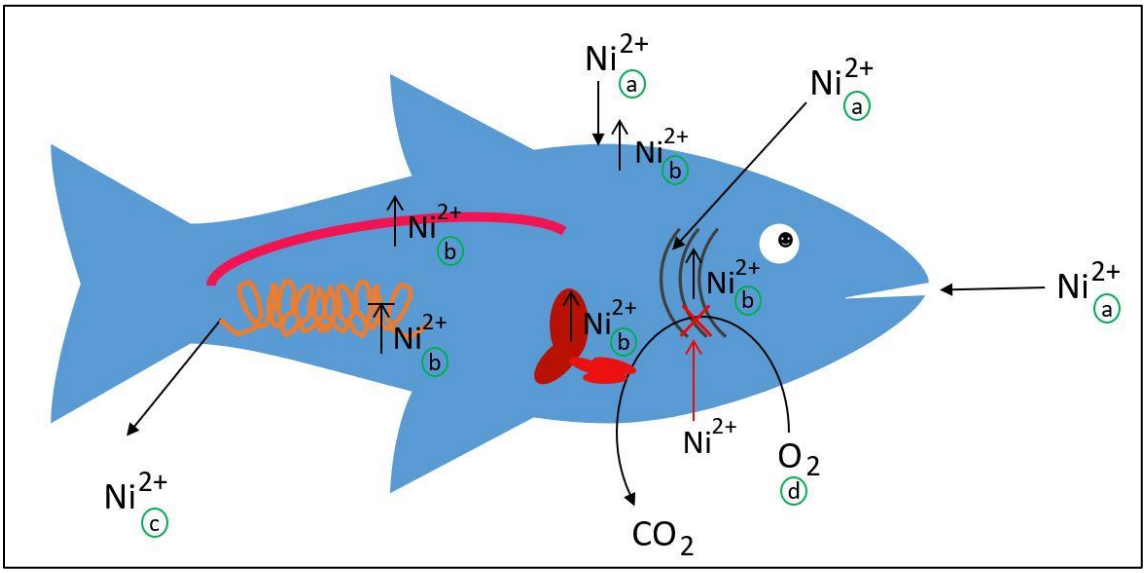

Figure 1. Schematic of fish exposed to aquatic nickel: a) uptake; b) storage and accumulation; c) excretion; d) effects.

1.4 Rainbow Trout

Rainbow trout (*Oncorhynchus mykiss*) belong to the family Salmonidae and are thus related to Pacific salmon (*Oncorhynchus keta*), Atlantic salmon, various trout (*Salvelinus sp.*), and Arctic grayling (*Thymallus arcticus*). While rainbow trout are native to the North Pacific Ocean, they have been introduced and cultivated in freshwater lakes all throughout Canada, in particular in the freshwater systems surrounding the Great Lakes. Rainbow trout are the most commonly farmed fish worldwide, as they rely on freshwater systems and can tolerate a wide range of water temperatures and environmental factors. The growth rate of rainbow trout depends on water temperature, quality, and food abundance (McLaren et al. 1947; Hardy 2002). As opposed to domestic monogastric animals, rainbow trout have the ability to obtain a substantial portion of their required minerals from their encompassing water (Hardy 2002). Due to this absorption of minerals from the water, fish, specifically rainbow trout, experience toxicity to environmental contaminants, including metals, which can be absorbed via the same transporters as other elemental nutrients.

1.5 Proteomics

Proteomics is the study of proteins, which are multifunctional macromolecules involved in all cellular processes. Proteins are involved in every biological process, thus understanding how these molecules interact is vital to research. Proteins control various levels of phenotypic expression, such as signaling proteins, ion pumps, transporters, and transcription factors, to control gene expression (Liang, Martyniuk, and Simmons 2020). Proteomics studies the ‘proteome’, an entire set of proteins expressed by an organism at any point in time (Wasinger et al. 1995). The proteome is not static but rather a fluctuation

and adaptation of protein expression caused by internal and external influences, such as environmental exposure. Proteomics employs a high-throughput system to attempt to identify and quantify the proteins in a biological sample. Proteomics investigates the information provided by genomic sequences, such as structure, function, and/or biological pathways, in order to understand the systemic analysis of proteins expressed in a cell, tissue, or organism (Liang, Martyniuk, and Simmons 2020). The plethora of information found in an organism's proteome can reveal details about the organism's health as well as the changes caused by environmental toxins or communicable diseases. The abundance of proteomic information has been a collaborative scientific effort regarding the extensive range of organisms that can be accessed freely online (Apweiler et al. 2004; Consortium 2018). The abundance of proteomic information is more readily available for commonly studied organisms for medical research, such as humans, mice, and zebrafish, while less information is available for environmentally relevant species. The human proteome contains over 51,000 reviewed proteins (Apweiler et al. 2004), however, zebrafish, being the most commonly studied fish relevant to medical research, only has around 3,000 reviewed proteins on Uniprot, limiting research in an environmentally relevant species.

Proteomics has two functional uses; qualitative (non-targeted) or quantitative (targeted) analysis of proteins. Utilizing proteomics for a non-targeted application examines the whole set of proteins present in a sample as opposed to a targeted proteomic approach, which examines and quantifies a specific protein (Covey et al. 1986). Non-targeted proteomics requires the biological samples to go through reduction, alkylation, and fragmentation of the proteins into peptides. The peptides are further separated using a liquid chromatogram and recognized using a mass spectrometer. Spectral peaks obtained

from liquid chromatography-mass spectrometry (LC-MS) are used to identify the peptide sequences and cross-referenced to reference proteomes using special software to identify proteins present in the biological sample.

Proteomics is used to identify potential biomarkers of effect when an organism is exposed to contaminants. To identify potential biomarkers, examine the alterations in the abundance of various proteins exposed to that distinct contaminant, and then associate the proteins with toxicological or physiological pathways. This important application of proteomics aids in identifying pathways and proteins due to the observed effects of the contaminant. Proteomics was employed to investigate pathways affected due to herbicide contaminant exposure in goldfish (*Carassius auratus*) revealing impacts on cellular stress response, carbohydrate, protein and lipid metabolisms, the methionine cycle, and cellular functions and structure (Gandar et al. 2017). Proteomics was able to identify the adverse effects of pollutants in the goldfish central nervous system (Gandar et al. 2017). Proteomics is a necessary tool to determine pathways and establish biomarkers and should be used to predict exposure for environmental biomonitoring programs.

1.6 Significance

The development of mining, smelting, and refining of minerals has been a significant reason for heavy-metal contamination in aquatic watersheds. Aquatic wildlife is threatened by many human pollutants, such as the run-off from industrial activities regarding heavy metal mining. The proposed development of the nickel-rich Ontario Ring of Fire mining site (Figure 2), located in the James Bay Lowlands, could cause nickel contamination to the surrounding ecosystem. The James Bay Lowlands drain into the Hudson Bay through various lakes, rivers, and streams. Thus, contamination of this

massive peatland could also impact marine life in the Arctic Ocean. It is vital to determine and understand the environmentally relevant concentrations of potential metal contaminants to monitor the health of aquatic wildlife in the Ring of Fire mining region. The primary objective of this thesis is to understand the proteomic responses in the liver and kidney of fish exposed to environmentally relevant nickel concentrations. The secondary objective is to compare those responses to the proteome of blood plasma and skin mucus from the same fish to support the use of non-lethal sampling in environmental monitoring.

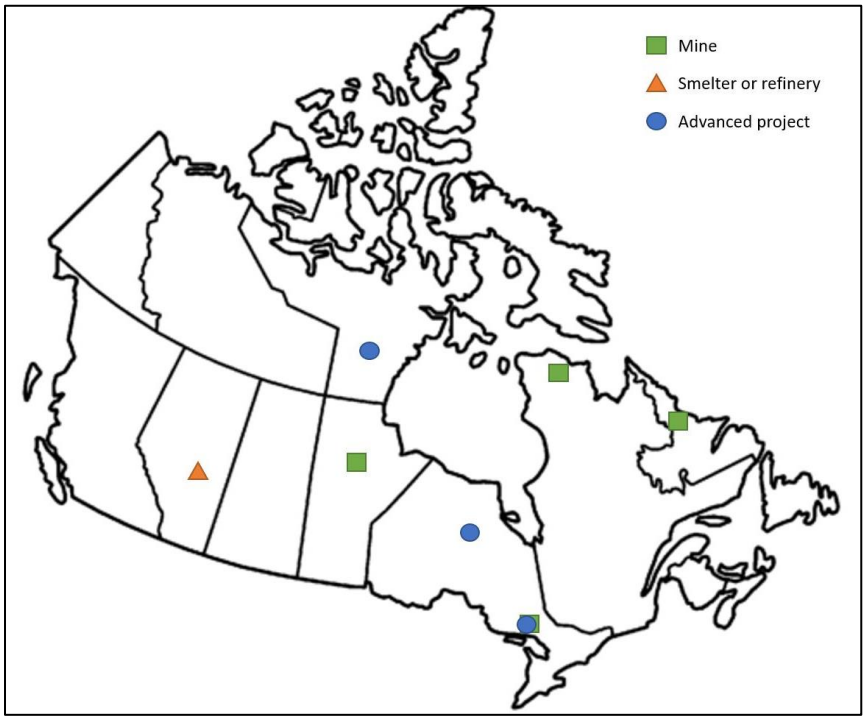

Figure 2. Canada's nickel-rich regions. Encompassing nickel opportunities spanning all regions of Canada. Adapted from The Canadian Critical Mineral Strategy (CCMS 2022).

1.7 Research Objectives

The intention of my thesis was to identify protein biomarkers sampled from fish that indicated exposure and/or adverse effects at environmentally relevant concentrations of aqueous nickel. Expanding the knowledge of rainbow trout (*Oncorhynchus mykiss*) liver

and kidney tissue specificity in relation to environmental toxins could help drive future research in biomarker discovery, progress current proteomic databases, and improve environmental health monitoring. To achieve this, I proposed the following objectives:

Objective 1: To investigate effects of nickel exposure in rainbow trout kidney and liver tissues. From previous studies, the kidney and liver of fish typically contain an array of proteins circulating from various organs of the body and should provide a wealth of information about the biological response to fish exposed to nickel.

Objective 2: To examine any differences in pathways effected by nickel exposure in rainbow trout with regard to non-lethal and lethal sampling types. The fish biofluids can be sampled with minimal impact to fish health while traditional organ sampling requires exsanguination of the fish.

Objective 3: To identify potential biomarkers of chronic waterborne nickel exposure. Using data obtained in objective 1, I examined differentially abundant proteins among the protein profiles in both the kidney and liver to identify potential adverse outcome pathways of nickel exposure.

Chapter 2. Methodology

Rainbow trout exposures were conducted during a previous master' study and were performed by Urvi Pajankar (MSc) under the supervision of Dr. Simmons, with approval from the Ontario Tech University Animal Care Committee.

2.1 Fish Maintenance and Acclimation

Healthy rainbow trout (25-35 cm; 200-450 g) were obtained from Linwood Acre Trout Farms (Izumi Aquaculture Inc., Campbellcroft, Ontario) and acclimated the fish in 1000 L fiberglass holding tanks (10 tanks, 15 fish each) for 3 weeks. Municipal water was supplied to the tanks from the City of Oshawa, drawn from Lake Ontario (hardness = 108-125 mg/L $CaCO_3$, pH = 7.5, Cl = 0 ppm, DO = 11 mg/L, Ni = 0.5 μg/L). The water was filtered, dechlorinated, and maintained at 12 ±2°C via a chiller. The trout were maintained in flow-through systems obtaining water at four turnovers per day, with a photoperiod of 16 hours light; 8 hours dark. Fish were fed 1.6% of their weight on alternate days with Corey Aquafeed Optimum™ 4 mm trout food. Tanks were cleaned and drained daily to remove waste accumulated from uneaten food or fecal matter. Fish health and behavior was monitored daily, with no mortalities observed during the acclimation and experimental period.

2.2 Experimental Exposure

2.2.1 Nickel Treatments

Urvi Pajankar determined three nickel (Ni) concentrations based on levels present in the OROF (detected average of 0.2 μg/L; PWQMN, 2021), Canadian Water Quality Guidelines for Ni (25 μg/L; CCME, 1987), and previous Ni toxicology studies conducted on rainbow trout (24-2000 μg/L). Solutions were prepared by dissolving nickel sulphate

hexahydrate salts ($NiSO_4.6H_2O$, CAS# 10101-97-0, Fisher Scientific, 99.97%) in distilled water. Significantly lower to environmentally relevant concentrations of Ni were used. The three Ni treatments were 0.45, 4.5, and 44.5 ppb (or µg/L) along with the control of 0 ppb. The study concentrations are approximately 2x, 20x, and 200x the detected levels of Ni in the OROF. The actual measurement of dissolved and total Ni concentrations levels (by SGS, Lakefield, Ontario) were 0.5 (control), 1.5, 4.9, 45.7 ppb (or µg/L) respectively. The measured Ni treatment concentrations are the values which will be referred to throughout this thesis.

2.2.2 Nickel Concentration Preparation

Urvi Pajankar determined the flow through rate for the aquatic facility exposure tanks and prepared the stock nickel solutions for exposure. Each experimental treatment consisted of two replicate 1000 L tanks with 15 fish each, containing a total of 30 fish dosed with the same Ni treatment. The fish were exposed to their associated Ni concentration for a duration of 30 days, at which time the fish were euthanized and dissected. Housing tanks were maintained at four turnovers per day, with an inflow rate of 166.67 L/hr or 2.78 L/min. These flow rates were manually verified by Urvi Pajankar before the experiment by measuring the flow rates every 10 seconds. To ensure that the water flow rates were maintained between 2.7-2.8 L/min, a water flow meter (Dewenwils, ASIN #B08TC4QYC2) was implemented. A peristaltic pump (250U/CA multi-channel cartridge pump; Watson-Marlow Bredel Pumps) supplied stock Ni concentrations to each tank, with a flow rate of 0.088 mL/min at 1.1 rpm (5.28 mL/hr) with the tubing of bore size 1.42 mm. The pump flow was manually validated by running water through the pump to monitor hourly flow rates for each tank. Urvi Pajankar, calculated the mean flow rate of

water being pumped into each tank for 5 separate days to then calculate the dilution factor required to make stock concentrations and the number of Ni moles present in the nickel sulphate salt used in preparations (Table 1).

Nickel stock concentrations were prepared by dissolving the salt into 500 mL of distilled water and stirred for 15 minutes before the solution was transferred to a 1 L volumetric flask. The Ni solution was diluted to 1 L and transferred to Nalgene™ amber high-density polyethylene (HDPE) bottles, connected to the peristaltic pump for tank dosing. Stock bottles were replaced every six days and were prepared prior to dosing.

Table 1. Various equations used by Urvi Pajankar to determine appropriate nickel stock concentrations for experimental exposure study on rainbow trout.

Equation	Formula	Variable
Dilution factor	$\mathbf{D} = \frac{\boldsymbol{P_f}}{\boldsymbol{P_f + W_i}}$	D = dilution factor P_f = peristaltic pump flow rate to the tank W_i = rate of water inflow to the tank, assumed constant rate of 2.77 L/min or 166.67 L/hr
Stock concentration	$\mathbf{C} = \frac{\boldsymbol{N}}{\boldsymbol{D}} \times \frac{\mathbf{1}}{\boldsymbol{n}}$	C = stock concentration N = nominal Ni concentration of each tank D = dilution factor of each tank n = number of moles of nickel in $NiSO_4.6H_2O$
Number of moles	$\boldsymbol{n} = \frac{\boldsymbol{mass\ of\ substance}}{\boldsymbol{mass\ of\ one\ mole}}$ $n = \frac{58.69}{262.85}$ $n = 0.223$	n = number of moles of nickel in $NiSO_4.6H_2O$ mass of Ni = 58.69 g molar mass of $NiSO_4.6H_2O$ = 262.85 mol/g

2.3 Tissue Collection

Prior to the Ni treatment and twice during the treatment period, non-lethal skin mucus was obtained from each individual fish. Then, following the 30-day treatment, fish were anaesthetized, skin mucus was sampled and blood was drawn from the caudal vein.

Fish were euthanized by exsanguination and cervical dislocation. Liver and head kidney were removed by dissection. The length (cm) of the fish was measured and the liver weight (g) was recorded to calculate the hepatosomatic index and Fulton's condition factor (K). All cryovials containing the tissues were immediately flash frozen in liquid nitrogen and stored at -80°C until further analysis.

$$Hepatosomatic\ Index = \frac{Liver\ weight\ (grams)}{Somatic\ weight\ (grams)} \times 100$$

$$Fulton's\ Condition\ Factor\ (K) = \frac{Somatic\ weight\ (grams)}{Length\ of\ fish\ (cm)^3} \times 100$$

2.4 Tissue Homogenization and Protein Concentration

Kidney and liver tissues were allowed to thaw completely on ice after being removed from the -80°C freezer. Approximately 100 mg of each tissue was dissected from the entire organ and placed into a 2 mL microcentrifuge tube. Each individual weight was recorded and 5 times the volume (v/w) of 200 mM ammonium bicarbonate (AB) buffer was added to each tube. To homogenize the tissue, a pair of metal beads were added to each tube and placed in the ball mill (TissueLyser II, Qiagen) for 1 minute at 20 Hz. The homogenized samples were centrifuged to separate the pellet and the supernatant, the latter of which approximately 500 µL was transferred into low-retention microcentrifuge tubes. The rough protein concentration was estimated using the Qubit 4 Fluorometer (Invitrogen, Thermo Fisher Scientific) using the average of 10 homogenates sub-sample. For Standard 1, Standard 2, and a blank consisting of 200 mM of AB buffer, 20 µL was added to three separate 0.5 mL tubes. Of the 10 homogenate sub-samples, 20 µL was separately added to 0.5 mL tubes. Every tube had 150 µL of Qubit™ Protein BR Assay Buffer and 30 µL of Qubit™ Protein BR Assay Reagent added, vortexed and then allowed to incubate for 10

minutes at room temperature. The tubes were inserted into the Qubit 4 Fluorometer spectrophotometer and the protein concentration was recorded. The average protein concentration was taken from the homogenate sub-samples and approximately 1 mg of total protein was transferred to a low-retention microcentrifuge tube for each sample. The samples were evaporated to 50 uL in SpeedVac (SPD 1030/2030 Thermo Scientific) in 5-minute intervals. Samples were then processed by protein digestion and extraction.

2.5 Protein Digestion and Extractions

To reduce the proteins, 2.65 μL of 100 mM tris(2-carboxyethyl) phosphine hydrochloride (TCEP) in 200 mM AB was added to the tubes, vortexed and allowed to incubate for 45 minutes at room temperature. To alkylate the proteins, 2.8 μL of 200 mM iodoacetamide (IAA) in 200 mM AB buffer was added to the solutions, vortexed, and allowed to incubate for 45 minutes at room temperature in the dark. Digestion of the proteins was performed by adding 50 μL of 20% (v/v) formic acid in Milli-Q water to the tubes and incubated at 115°C on a heating block for 30 minutes. Once cooled to room temperature, the samples were evaporated to near dryness in SpeedVac (SPD 1030/2030 Thermo Scientific). The dried samples were reconstituted with 20 μL HPLC buffer containing 95% water, 5% acetonitrile and 0.1% formic acid (v/v). The reconstituted samples were vortexed until a homogenous mixture then centrifuged to separate the pellet and the supernatant. The supernatant (~ 20 μL) was aspirated into 250 μL inserts of 2 mL screw thread HPLC vials capped with 9 mm blue PTFE/silicone/PTFE screw caps. The final peptide solutions were stored in 4°C for immediate LC-MS instrumental analysis.

2.6 Liquid Chromatography Mass Spectrometry Analysis

The HPLC sample vials were placed in the autosampler to allow 2 μL of digested protein solution to be injected and separated by reverse phase liquid chromatography using a Zorbax, 300SB-C18 1.0 x 50 mm 3.5 μm column with an Agilent 1260 Infinity Binary Liquid Chromotogram (Agilent Technologies Canada Inc., Mississauga, ON). Samples were separated with a gradient using solvent A (95% H_2O, 5% acetonitrile, and 0.1% formic acid) and solvent B (5% H_2O, 95% acetonitrile, and 0.1% formic acid). Liquid chromatography was coupled with the Agilent 6545 Accurate-Mass Quadrupole Time-of-Flight (Q-TOF) mass spectrometer in tandem to the Agilent 1200 series liquid chromatography system to detect and identify the separated peptides. Each analytical run included a solvent blank and a BSA (bovine serum albumin) digest standard (Agilent Technologies Canada Inc., Mississauga, ON) injection every 12 samples to monitor the baseline, carry-over, drift, sensitivity, and instrumental variation during the runtime. The samples were injected once per individual fish. All samples collected from fish exposed to Ni treatments were randomized and analyzed together, and the control samples were randomized and separately analyzed.

2.7 Protein Identification and Quantification

Spectral files were obtained for each sample from the LC-MS/MS run and analyzed using the Spectrum Mill software (Agilent Technologies, Version B.04.01.141) to identify detected peptides. Proteins were identified by cross-comparing detected peptides against known proteins found in the Uniprot Reference Proteome for rainbow trout (Proteome ID: UP000193380). Proteins were manually validated and accepted when the following criteria were met: 1) peptide score (quality match between observed spectrum and theoretical

spectrum) was greater than 6 in at least one peptide; and 2) a percent of the spectral intensity accounted for by the theoretical fragments (%SPI) was greater than 70%, following the recommended Agilent Q-TOF mass spectrometer validation. Spectrum Mill identified peptides at the MS/MS level, which were then imported into Skyline 20.2 (MacCoss Lab software) to perform MS1 filtering to quantify protein abundance based on chromatogram peak intensities. Quantification at the MS1 level were imported into Skyline 20.2 to perform a data-dependent acquisition (DDA) workflow with the criteria of a cut-off score of 0.9, 2-minute retention time window, and 5 missing cleavages with transition settings for the Q-TOF (Pino et al. 2020). The list of identified rainbow trout protein accession numbers were searched using the Basic Local Alignment Search Tool (BLAST) against human genes using Uniprot Proteome (Proteome ID: UP000005640) to obtain their orthologous gene symbols based on sequence similarity. The proteins that were not matched using the script were mapped manually. Redundancies in orthologous gene symbols were consolidated on Microsoft Excel using the consolidation feature to select the row containing the maximum value. Protein abundances (peak areas) with mean intensity values <5000 were removed.

2.8 Statistical Data Analysis and Visualization

Proteins in liver and kidney were analyzed using the online software Metaboanalyst 5.0 (https://www.metaboanalyst.ca/home.xhtml). Proteins with missing values were removed. Pre-processing of the one-factor and two-factor data involved normalization by median, cube root transformation, and pareto scaling. Normalized concentrations for each individual protein were visualized as box plots in Metaboanalyst 5.0 using Fisher's least significant differences (LSD; p-value < 0.05). For liver analysis, due to the statistical

limitation of less than 10 proteins using an FDR < 0.25 (p-value < 0.05) on Metaboanalyst 5.0, an FDR < 0.50 (p-value < 0.05) was initially used before the re-implication of an FDR < 0.05 (p-value < 0.05), to allow for a larger dataset for comparison. Two-factor data was interpreted to ensure no cofounding male or female factors effected the treatment groups, by performing a Principle Component Analysis (PCA).

Rainbow trout hepatosomatic index (HSI) and condition factors (K) were calculated using liver weights, whole-body weights, and fork length. The data was tested for significance using a Kruskal-Wallis test, with a Dunn's multiple comparison test with an alpha value of 0.05. The condition factor data set was only normal when transformed using a natural logarithm. A two-way ANOVA was performed along with Tukey's test for multiple comparisons with an alpha value of 0.05.

2.9 Pathway and Network Analysis

From the main effects of nickel treatment for liver and kidney samples, an overrepresentation analysis of proteins was performed on ConsensusPathDB-human (CPDB) and Cytoscape (version 3.9.1). Human orthologous gene symbols were used along with human as the selected species. No background protein lists were used. All pathway and Gene Ontology (GO) biological processes (p-value < 0.10) were selected and manually arranged to produce a network established on the overlap between processes and pathways as a result of shared genes. Protein lists attained from pairwise comparisons for liver or kidney were analyzed using GO enrichment with no multiple test correction (p-value < 0.05). The terms for GO were manually selected for relevance and uniqueness to eliminate redundancy.

The significantly affected proteins from the liver and kidney were uploaded to the Comparative Toxicogenomics Database (CTDbase) using the gene set analyzer to determine the enriched diseases and enriched pathways. The selected enriched diseases (p-value < 0.05) were selected and manually arranged to establish the overlap of shared genes. The enriched diseases were manually selected for relevance and uniqueness to eliminate redundancy. Likewise, the enriched pathways (p-value < 0.05) were manually arranged to establish the pathway groupings.

This entire pathway and network analysis process was repeated for raw mucus and plasma data received from Urvi Pajankar to ensure direct comparisons were made. This comparison was completed to ensure that there were no underlying differences in data transformations or analysis between the two sampling types (ie. lethal vs non-lethal sampling). Additionally, this process was repeated for the control using previous liver and kidney proteomic data from Nancy Tannouri MSc thesis's pertaining to rainbow trout. This comparison was completed to ensure that there were no underlying changes between the generations of rainbow trout, the condition of the fish, the annotated gene ontology from Uniprot, or the quality of proteins identified from the LC-HR-MS/MS.

Chapter 3. Results

3.0 Nickel Burden

A previous study by Urvi Pajankar, the different experimental treatments were measured for nickel burden in the blood plasma. This concluded that the accumulation of nickel was the highest in the fish exposed to the highest Ni treatment (45.7 ppb), followed by the fish exposed to the medium Ni treatment (4.5 ppb), then by the lowest Ni treatment (0.45 ppb). The mean of nickel burden accumulated in the fish exposed to 45.7 ppb of Ni was approximately x6.7 fold the mean of Ni accumulated in the control fish. Urvi Pajankar determined that fish exposed to the highest Ni treatment (45.7 ppb) were significantly different from the Ni burden of fish exposed to control and the low waterborne Ni (0.45 ppb) using Dunn's multiple comparison (adjusted p-value < 0.01).

3.1 Sex-Specific Differences

Sex difference analysis was conducted for the proteins measured in each individual tissue type (kidney and liver) and no sex specific differences were apparent (Two-way ANOVA ($p > 0.05$)). No clustering distinction in the PCA plot appeared when related to sex in either kidney and liver (Figure 3 and Figure 4, respectively). Thus, with no significant differences in variance and abundance for any proteins due to biological sex, we pooled the data from males and females together for the remaining analyses in the following sections.

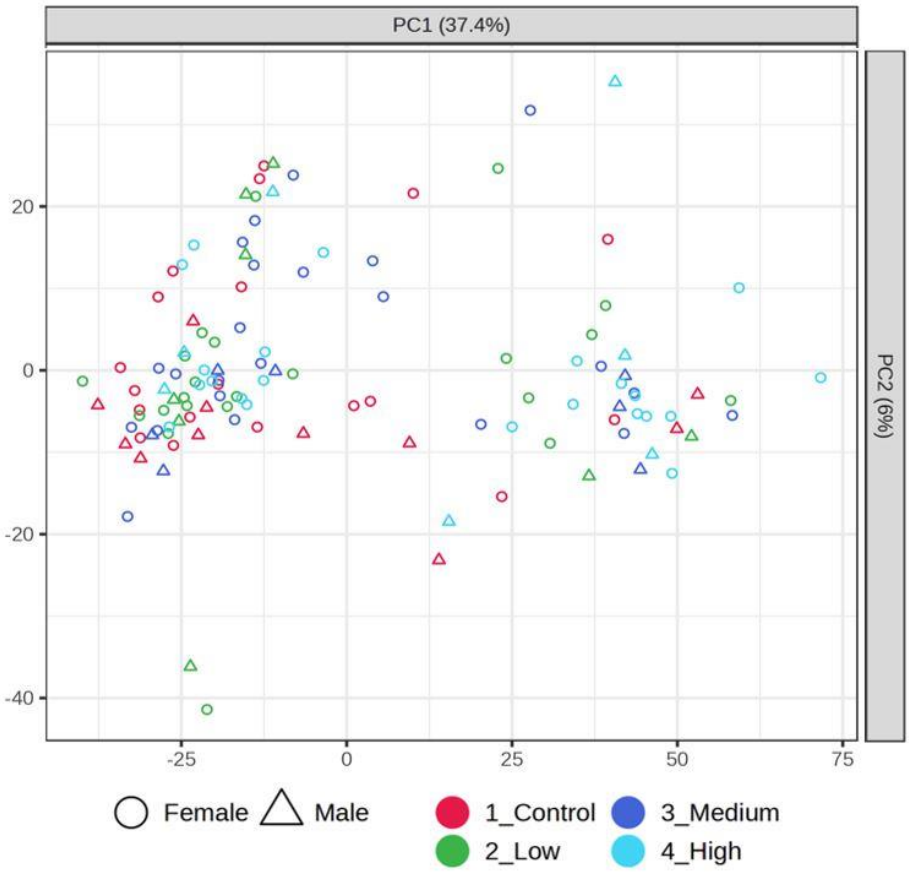

Figure 3. Two-way analysis PCA plots of kidney samples from the different treatment groups compared to male and female metadata, representing the top 2 PCA plots. Each data point is one fish (n = 30, per treatment), treatment is indicated by colour, and sex is indicated by shape. Principle Component 1 (PC1) and 2 (PC2) explains 43.4% of variance. No clear clusters formed in regards to sex in kidney proteomes. Plots were made using Metaboanalyst 5.0.

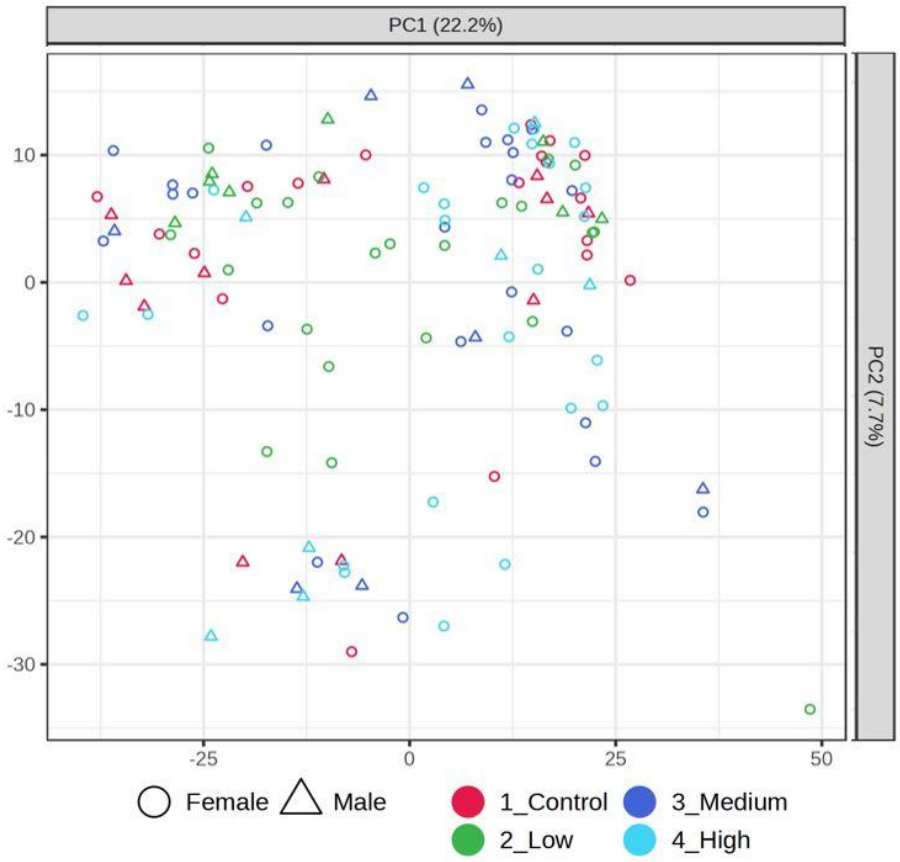

Figure 4. Two-way analysis PCA plots of liver samples from the different treatment groups compared to male and female metadata, representing the top 2 PCA plots. Each data point is one fish (n = 30, per treatment), treatment is indicated by colour, and sex is indicated by shape. Principle Component 1 (PC1) and 2 (PC2) explain 30% of variance. No clear clusters formed in regards to sex in liver proteomes. Plots were made using Metaboanalyst 5.0.

3.2 Hepatosomatic Index

Descriptive statistics for the HSI assay and Fulton's condition factor can be found in Table 2. The HSI data did not pass for normality ($\alpha = 0.05$) with raw or transformed data. There were no significant differences in HSI between the two lower nickel treatments (0.45 ppb and 4.5 ppb Ni^{2+}) and the control (One-way ANOVA, Dunnett's post-hoc test ($p > 0.05$)). There was a significant difference in HSI between the highest nickel treatment (45 ppb Ni^{2+}) and the control (One-way ANOVA, Dunnett's post-hoc test ($p > 0.05$)). No

significant effect in the Fulton's condition factor was observed with a Kruskal-Wallis test with a Dunn's multiple comparison test ($p > 0.05$). The results are displayed as a box plot in Figure 5.

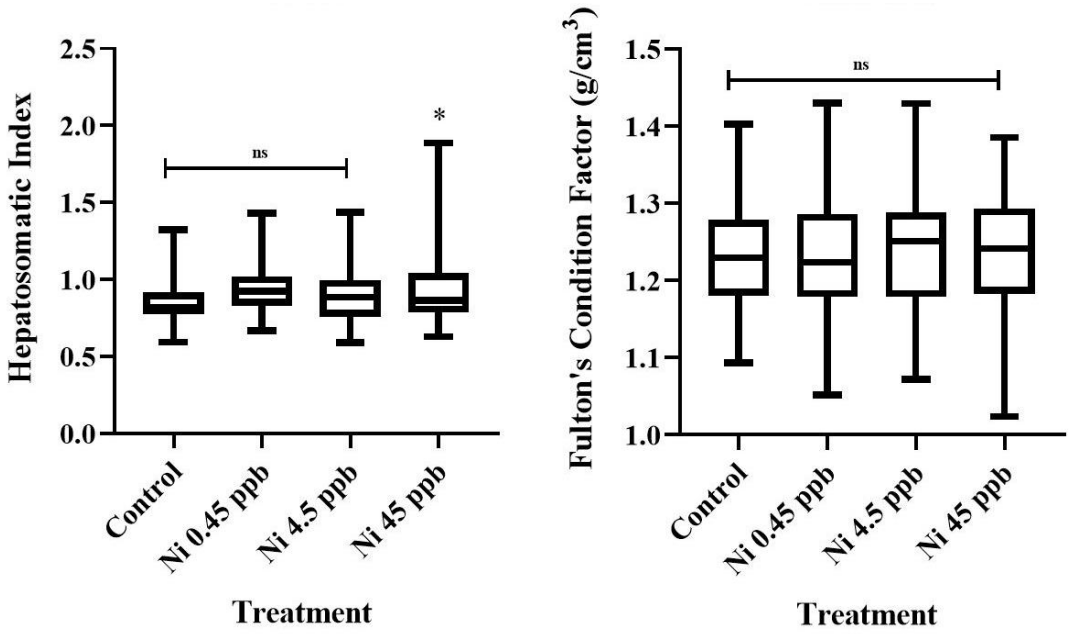

Figure 5. a) Hepatosomatic index and b) Fulton's condition factor of rainbow trout exposed to aquatic nickel. Box plot represents the 25th, 50th (median), and 75th quartiles with outliers, n = 30 for all exposure groups. No significant effect was observed with a Dunnett's post-hoc test ($p > 0.05$) or with a Kruskal-Wallis test with a Dunn's multiple comparison test ($p > 0.05$). Plots were created using GraphPad 8.0.2.

Table 2. Descriptive statistics for the HST and Fulton's condition factor of rainbow trout exposed to different concentrations of aquatic nickel. No significant effect was observed with a Dunnett's post-hoc test ($p > 0.05$) or with a Kruskal-Wallis test with a Dunn's multiple comparison test ($p > 0.05$), n = 30 for all exposure groups.

		Exposure			
		Control	Ni^{2+} 0.45 ppb	Ni^{2+} 4.5 ppb	Ni^{2+} 45 ppb
HSI	Mean	0.856	0.943	0.889	0.984*
	Standard Deviation	0.15	0.17	0.16	0.30
Fulton's Condition Factor	Mean	1.234	1.237	1.243	1.232
	Standard Deviation	0.069	0.080	0.084	0.093

* significant difference found

3.3 Liver Proteomics

3.3.1 Protein Abundance

Data-dependent acquisition using liquid chromatography high resolution tandem mass-spectrometry analysis (DDA LC-HR-MS/MS) was able to identify a total of 8097 proteins in the liver proteome of rainbow trout. Duplicate proteins were consolidated and missing values were replaced with ⅕ the lowest ion abundance detected, leaving a total of 4497 proteins before statistical analysis. Statistical analysis revealed that 9 proteins (Atp2a2; Dhrs2; Dicer1; Kif20b; Rpl8; Sfmbt1; Slc35e1; Tnks1bp1; Tpx2) were significantly affected by the nickel treatments (FDR < 0.25, Tukey's HSD post-hoc p-value < 0.05). When a more stringent correction for the false discovery (FDR < 0.05, Tukey's HSD post-hoc p-value < 0.05) was applied, the abundance of only 1 protein (Dicer1) was significantly affected. Whereas, with a less stringent false discovery rate (FDR < 0.50, Tukey's HSD post-hoc p-value < 0.05), it revealed that 26 liver proteins were significantly altered by the nickel treatments.

A heatmap was plotted to visualize the abundance of the 26 liver proteins significant for nickel treatment effect in rainbow trout (Figure 6). The majority of these proteins are thought to be widely expressed in humans (Table 3). There were 2 clusters formed based on the expression profiles of the abundance of proteins in all 4 treatments. Cluster 1 contained 15 proteins while cluster 2 contained 11 proteins. The proteins in cluster 1 had low abundances in the control and low nickel treatment groups and increasing higher abundances towards the highest nickel treatment (45 ppb Ni^{2+}). In cluster 2, protein abundances were highest in the controls with a decreasing trend towards the highest nickel

treatment. The function and expression annotations of the preceding significant liver proteins are summarized in Table 3.

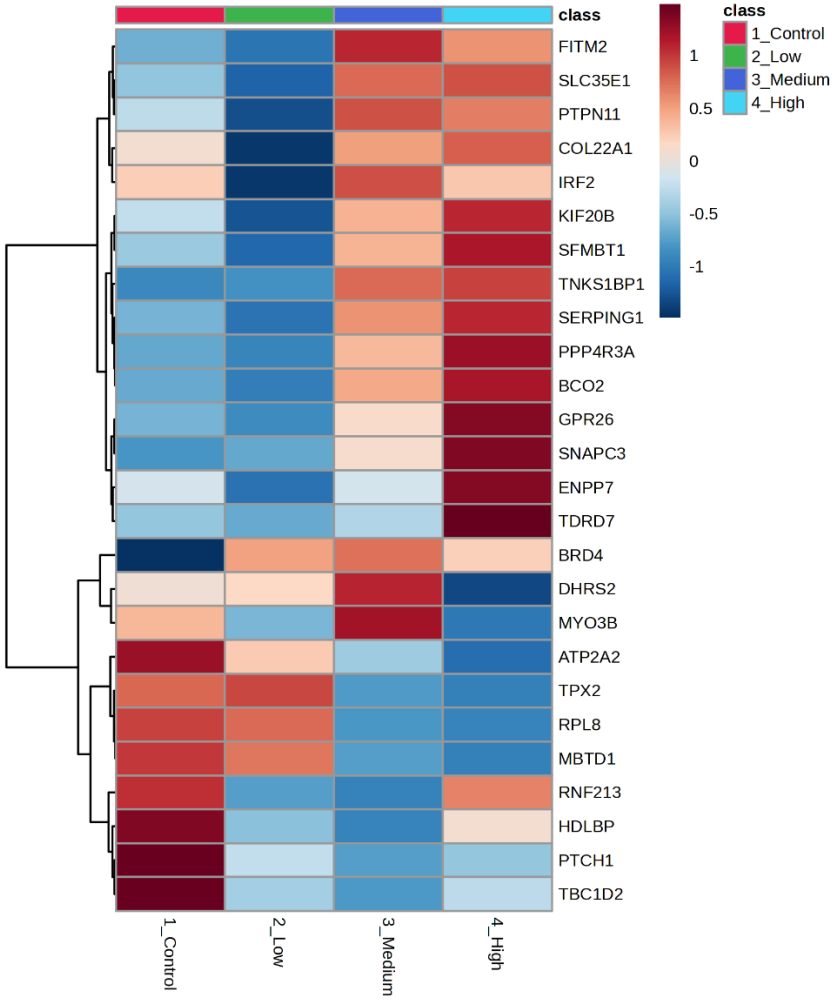

Figure 6. Heatmap of the abundance of the proteins significantly affected by nickel treatment in the liver proteome of rainbow trout. 26 proteins were affected by nickel treatment (main effect of treatment) using Metaboanalyst 5.0 (FDR < 0.50, Tukey's HSD post-hoc p-value < 0.05). Abundances are represented by standard scaling, while clustered rows represent the different expression profiles among the 26 proteins; clusters were obtained using Euclidean distance calculations. Each column is an average of the samples (n = 30, per treatment) and labelled by the nickel treatment group.

Table 3. Function and expression of proteins uniquely detected in the liver proteome of rainbow trout when exposed to nickel treatment. Protein list based on proteins that were significantly increased (red) or decreased (blue) in the presence of nickel treatment compared to the control. Top 10 proteins for each category is presented below.

Gene Symbol	Function	Expression	Biological Process	Molecular Function
Kif20b	Kinesin family member 20B, microtubule binding motor protein	Broad expression in tissues	Cellular process	ATP-dependent activity, binding, catalytic activity, cytoskeletal motor activity
Slc35e1	Solute carrier family 35 member, secondary carrier transporter	Ubiquitous expression in tissues, low tissue specificity		Transporter activity
Tnks1bp1	Tankyrase 1 binding protein	Ubiquitous expression in tissues	Cellular process, metabolic process, response to stimuli	
Ppp4r3a	Serine/threonine-protein phosphatase 4 regulatory subunit, ATP synthase	Ubiquitous expression in tissues, low tissue specificity	Cellular process, metabolic process, response to stimuli	Binding, catalytic activity, molecular function regulator
Serping1	Plasma protease C1 inhibitor, protease inhibitor	Expression in liver tissue	Biological regulation, cellular process, metabolic process	Binding, catalytic activity, molecular function regulator
Enpp7	Ectonucleotide pyrophosphatase/ phosphodiesterase, hydrolase	Ubiquitous expression in tissues (liver, duodenum, jejunum, ileum, esophagus, stomach)	Biological regulation, metabolic process	
Fitm2	Acyl-coenzyme A diphosphatase, hydrolase	Ubiquitous expression in tissues (heart and other tissues)	Cellular process, localization, metabolic process	
Bco2	Carotenoid-cleaving dioxygenase, oxygenase	Ubiquitous expression in tissues (liver, kidney, small intestine, heart, stomach)	Cellular process, metabolic process	Catalytic activity
Gpr26	G-protein coupled receptor	Broad expression in tissues	Biological regulation, cellular process, response to stimuli, signaling	Molecular transducer activity
Tdrd7	Tudor domain-containing protein, scaffold/adaptor protein	Ubiquitous expression in tissues	Cellular process, developmental process, multicellular organismal process, reproduction, reproductive process,	
Rpl8	Component of the large ribosomal subunit, ribosomal protein	Ubiquitous expression in tissues	Cellular process, metabolic process	Binding, structural molecule activity
Tpx2*	Non-motor microtubule binding potein	Broad expression in tissues, expressed in carcinoma cell lines	Biological regulation, cellular process	Binding
Dhrs2	Dehydrogenase/reductase	Biased expression in urinary bladder and liver	Biological regulation	Catalytic activity
Dicer1*	Double-stranded RNA (dsRNA) endoribonuclease	Ubiquitous expression in tissues, low tissue specificity	Developmental process, metabolic process, multicellular organismal process	ATP-dependent activity, binding

Atp2a2	ATPase sarcoplasmic/endoplasmic reticulum Ca2+, primary active transporter	Broad expression in tissues	Biological regulation, cellular process, localization	ATP-dependent activity, catalytic activity, transporter activity
Hdlbp	Vigilin, RNA metabolism protein	Ubiquitous expression in tissues, low tissue specificity	Metabolic process	
Ptch1	Protein patched homolog	Expressed in brain, lung, liver, heart, skeletal muscle, pancreas, and kidney	Biological regulation, cellular process, response to stimuli, signaling	Binding, molecular transducer activity
Tbc1d2	TBC1 domain family member, GTPase activating protein	Broad expression in tissues (kidney, liver, lung)	Biological regulation	Binding, catalytic activity, molecular function regulator
Myo3b	Myosin-IIIb	Ubiquitous expression in tissues (epididymis, kidney, retina)	Response to stimuli	ATP-dependent activity
Mbtd1	MBT domain-containing protein	Ubiquitous expression in tissues, low tissue specificity	Cellular process	Binding

* found to be a significant liver protein in all variations of initial analysis.

Additionally, an over-representation analysis of the 26 liver proteins from the nickel treatment was conducted using Cytoscape 3.9.1 software to determine the over-represented pathways and GO biological processes ($p < 0.10$). In total, 200 distinct pathways were over-represented among all of the liver proteins from the nickel exposure. Ultimately, the comparative toxicogenomics database (CTDbase) was used to complete an over-representation analysis on the 26 liver proteins significantly affected by nickel treatment, revealing hemostasis as the only biological network that was significant ($p < 0.01$), found in Table 4. The 5 proteins (Atp2a2; Irf2; Kif20b; Ptpn11; Serping1) represent different biological processes and molecular functions while maintaining the hemostasis pathway.

Table 4. Over-represented pathway of proteins from liver proteome of rainbow trout exposed to nickel. The list of 26 proteins significantly affected by nickel treatment were searched against the gene set analyzer for enriched pathways on CTDbase to find biological pathway associations in response to nickel exposure ($p < 0.05$). The list here only includes manually selected terms from all over-represented pathways that best represent the networks of interest.

Pathway	Pathway ID	P-value	Proteins from Input List	Genomic Frequency
Hemostasis	R-HSA-109582	0.00814	Atp2a2|Irf2|Kif20b|Ptpn11|Serping1	1.41%

3.3.2 Toxicological Effects on Liver

The associated disease function of the 26 liver proteins include neoplasms and liver disease, summarized in Table 5. GO analysis of the 26 proteins associated with the liver contain many biological processes specific to cellular process, metabolic process, biological regulation, and response to stimuli were affected by aquatic nickel (Figure 7a). The GO analysis also revealed molecular functions specific to binding, catalytic activity, and molecular function regulators were affected by aquatic nickel (Figure 7b).

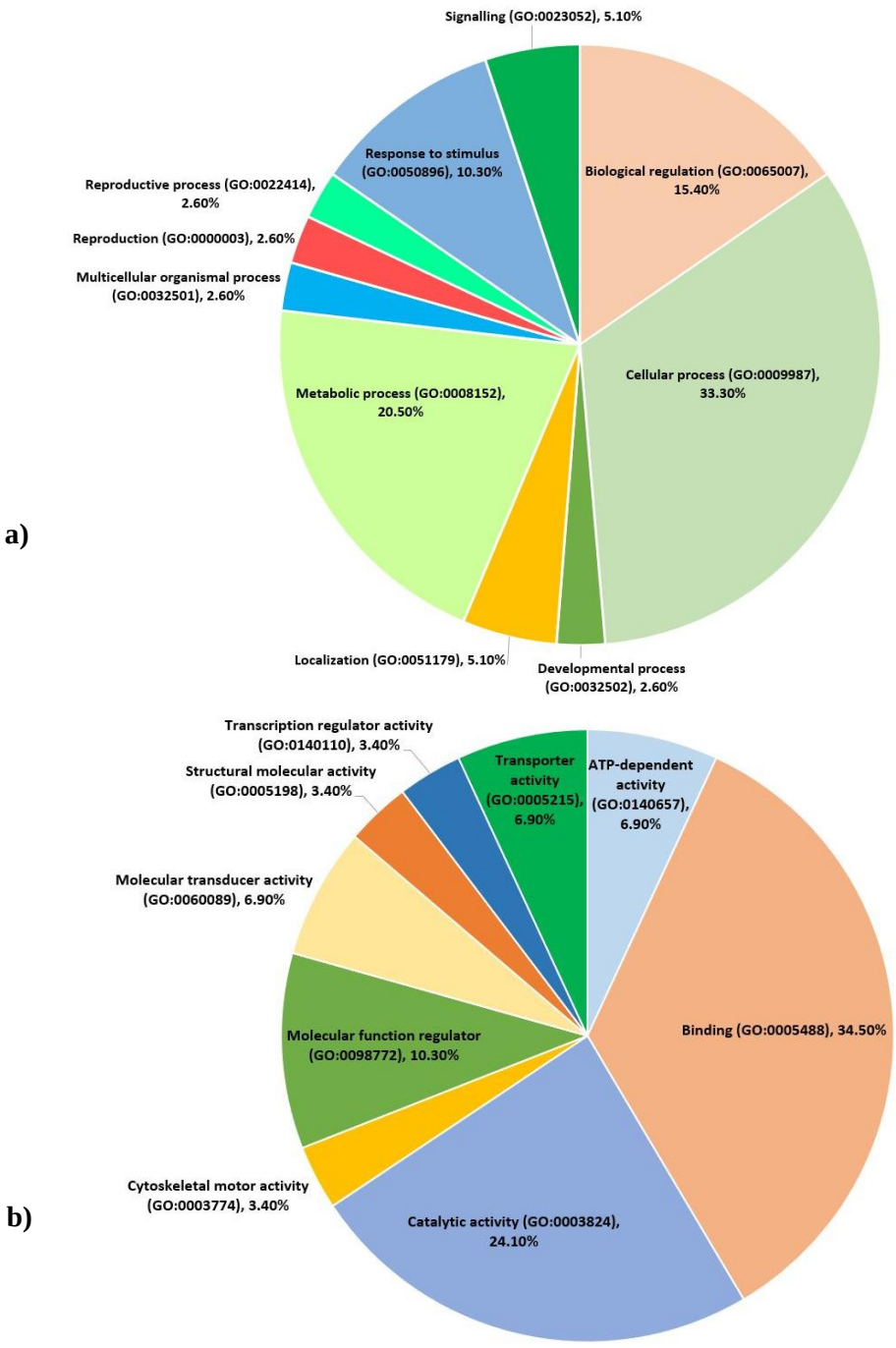

Figure 7. Genomic percentage of a) biological processes and b) molecular functions in liver proteome of rainbow trout affected by aquatic nickel treatment. The list of 26 liver proteins significantly affected by nickel treatment were searched against the GO Enrichment Analysis powered by Panther to find the over-represented lists of proteins involved in the biological processes and molecular functions involved in response to nickel exposure ($p < 0.01$). Each section of the pie charts represents the function, GO term, and percentage of genes found for that purpose. All proteins were searched in regards to Homo sapiens. A background protein list was not used.

Table 5. Disease association of GO in liver proteins of rainbow trout significantly affected by nickel treatment. The list of 26 proteins significantly affected by nickel treatment were searched against the gene set analyzer for enriched diseases on CTDbase to find disease associations in response to nickel exposure ($p < 0.05$). The list here only includes manually selected terms from all over-represented pathways that best represent the networks of interest.

Disease Category	Disease Name	p-value	Disease ID	Proteins from Input List
Cancer	Neoplasms	0.005	MESH:D009369 MESH:D018204 MESH:D009371 MESH:D009386 MESH:D009372	Bco2|Brd4|Col22a1|Dicer1|Dync1h1|Hdlbp|Irf2|Larp4|Ptch1|Ptpn11|Serping1|Tbc1d2|Tpx2
	Neuroectodermal Tumours	0.040	MESH:D018242	Brd4|Ptch1|Ptpn11
	Sarcoma	0.049	MESH:D012509 MESH:D009217 MESH:D012208	Brd4|Dicer1|Ptch1
Digestive System Disease	Liver Diseases	0.079	MESH:D008107	Bco2|Brd4|Dicer1|Gna14|Irf2|Pan2|Serping1|Tpx2
Connective Tissue Disease	Neoplasms	0.077	MESH:D009372	Brd4|Ptch1|Ptpn11

3.3.3 Comparison to Standard Liver

In a previous study by Nancy Tannouri MSc, investigating the entire proteome of rainbow trout, DDA LC-HR-MS/MS identified 1692 proteins in the liver proteome. Statistical analysis identified 138 liver proteins that were significantly different between male and female rainbow trout (FDR < 0.25) and in total, 372 liver enriched proteins, indicating the significant proteins distinct to the liver tissue (compared to blood plasma). As stated previously, DDA LC-HR-MS/MS identified 4497 liver proteins in the liver proteome of rainbow trout exposed to aquatic nickel treatment. There were no evident changes in standard liver proteome between the liver in my control group and the liver of Nancy Tannouri's research. Due to changes in the comparative database, this is not a clear indication of more protein abundance due to nickel exposure. There were 845 proteins

found in both lists of liver proteins. There were no significant differences between male and female rainbow trout exposed to aquatic nickel treatments.

3.4 Kidney Proteomics

3.4.1 Protein Abundance

Data-dependent acquisition using liquid chromatography high resolution tandem mass-spectrometry analysis (DDA LC-HR-MS/MS) was able to identify a total of 6449 proteins in the kidney proteome of rainbow trout. Duplicate proteins were consolidated and missing values were placed with ⅕ of the lowest ion abundance value, leaving a total of 5556 proteins before statistical analysis. Statistical analysis revealed that 275 proteins were significant for nickel treatment (FDR < 0.25, Tukey's HSD post-hoc p-value < 0.05).

A heatmap was created to visualize the abundance of the top 100 of the 275 kidney proteins significantly affected by nickel treatment in the kidney of rainbow trout (Figure 8). The majority of these proteins are thought to be widely expressed in humans (Table 6). There were 5 clusters formed based on the expression profiles of the abundance of proteins in all 4 treatments. Cluster 3 is the largest cluster, containing 48 displayed proteins, while the other 4 clusters contain an average of 13 ±3 proteins. The proteins in cluster 1 had low abundances in the control and highest (45 ppb Ni^{2+}) treatment group, with an increased abundance in the low (0.45 ppb Ni^{2+}) and medium (4.5 ppb Ni^{2+}) treatment groups. In cluster 2, protein abundances favoured the treatment groups as compared to the control. The proteins in cluster 3 were highest in the control with a decreasing trend towards the highest nickel treatment. Cluster 4 had the highest protein abundance in the lowest treatment group, followed by the control, and the lowest protein abundance in the highest treatment group. The proteins in cluster 5 had high abundance in the control and low

treatment groups with a decreasing trend towards the highest treatment group. The function and expression annotations of the preceding significant kidney proteins are summarized in Table 6.

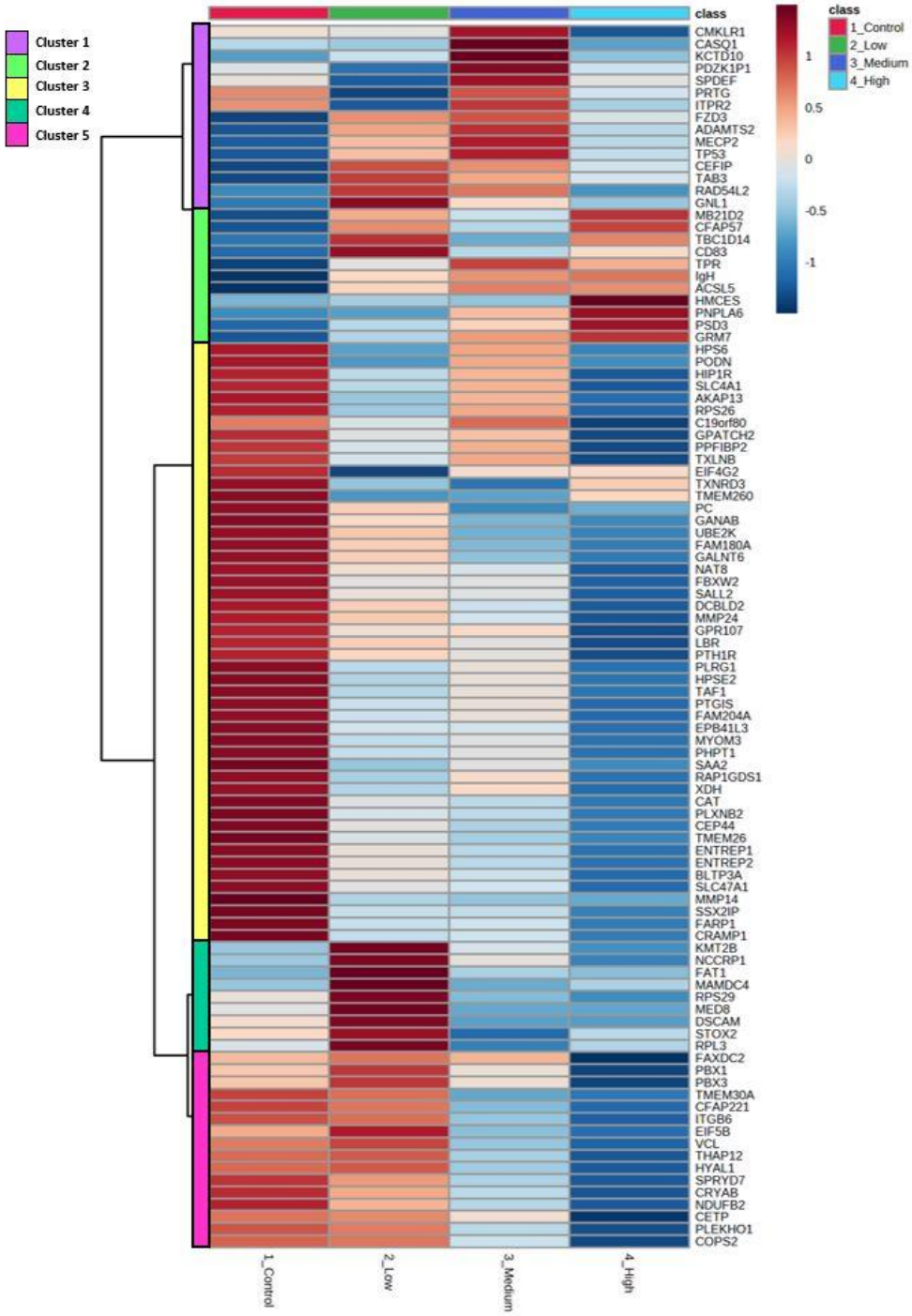

Figure 8. Heatmap of the abundance of the proteins significantly affect by nickel treatment in the kidney proteome of rainbow trout. The top 100 proteins out of the 275 proteins significantly affected by nickel treatment were displayed using Metaboanalyst 5.0 (FDR > 0.05, Tukey's HSD post-hoc p-value < 0.05). Abundances are represented by standard scaling, while clustered rows represent the different expression profiles among the displayed 100 proteins; clusters were obtained using Euclidean distance calculations. Each column is an average of the samples (n = 30, per treatment) and labelled by the nickel treatment group.

Table 6. Function and expression of proteins uniquely detected in the kidney proteome of rainbow trout when exposed to nickel treatment. Protein list based on proteins that were significantly increased (red) or decreased (blue) in the presence of nickel treatment compared to the control. Top 5 proteins for each cluster is presented below, except cluster 3 as 10 proteins are presented.

Cluster	Gene Symbol	Function	Expression	Biological Process	Molecular Function
1	Cmklr1	Chemokine-like receptor, G-protein coupled receptor	Broad expression in tissues, cardiovascular system, kidney, gastrointestinal tissues	Biological regulation, cellular process, immune system process, localization, locomotion, response to stimuli, signaling	Binding, molecular transducer activity
1	Pdzk1p1	Na/H exchange regulatory cofactor, scaffold/adaptor protein		Cellular process, localization	Binding, molecular adaptor activity
1	Itpr2	Inosital trisphosphate receptor type, ligand-gated ion channel	Broad expression in tissues, skeletal muscle and heart	Cellular process	Binding, transporter activity
1	Tp53	Cellular tumour antigen p53, p53-like transcription factor	Ubiquitous expression in tissues, low tissue specificity	Biological regulation, cellular process, metabolic process	Binding, transcription regulator activity
1	Rad54l2	Helicase	Ubiquitous expression in tissues, low tissue specificity		Binding, ATP-dependent activity
2	**Mb21d2**	Nucleotidyltranserase	Ubiquitous expression in tissues, low tissue specificity		Binding, ATP-dependent activity
2	**Cd83**	CD83 antigen	Expressed by activated lymphocytes, ubiquitous expression in tissues, low tissue specificity	Biological regulation, response to stimuli, signaling	
2	**Tpr**	Nucleoprotein, primary active transporter	Broad expression in tissues, esophagus, liver, smooth muscle, kidney, lung, spleen	Cellular process, localization, metabolic process	Structural molecule activity
2	**Hmces**	Abasic site processing protein	Ubiquitous expression in tissues, low tissue specificity	Cellular process, metabolic process	
2	**Grm7**	Metabotrophic glutamate receptor, G-protein coupled receptor	Broad expression in tissues (brain)	Biological regulation, cellular process, response to stimuli, signaling	Binding, catalytic activity, molecular transducer activity
3	**Podn**	Podocan	Ubiquitous expression in tissues, kidney, liver, heart, pancreas, smooth muscle	Biological regulation, cellular process, metabolic process	Binding
3	**Akap13**	A-kinase anchor protein	Ubiquitous expression in tissues (heart, testis), low tissue specificity	Biological regulation, cellular process, metabolic process, response to stimuli, signaling	Binding, molecular adaptor activity

3	**Gpatch2**	G patch domain containing protein, RNA metabolism protein	Ubiquitous expression in tissues, low tissue specificity		Binding
3	**Ganab**	Neutral alpha-glucosidase AB, glucosidase	Expressed in liver and kidney	Cellular process, metabolic process	Binding, catalytic activity
3	**Nat8**	Acetyltransferase	Expressed in liver and kidney	Cellular process	Catalytic activity
3	**Plrg1**	Pleiotrophic regulator	Ubiquitous expression in tissues, low tissue specificity	Cellular process, localization, metabolic process	
3	**Fam204a**		Ubiquitous expression in tissues, low tissue specificity		
3	**Saa2**	Serum amyloid A2 protein	Expressed by liver into plasma	Biological phase	
3	**Cep44**	Centrosomal protein	Ubiquitous expression in tissues, low tissue specificity	Cellular process	Binding
3	**Entrep1**	Ubiquitin protein ligase	Expressed in muscle	Cellular process, signaling	
4	Kmt2b	Histone-lysine N-methyltransferase, histone modifying enzyme	Broad expression in tissues (testis, brain, kidney, colon), low tissue specificity	Biological regulation, cellular process, metabolic process	Catalytic activity
4	Fat1	Protoccadherin, cadherin	Broad expression in tissues, epithelial and smooth muscle	Biological adhesion, biological regulation, biological phase, cellular process	Binding
4	Rps29	Component of the large ribosomal subunit, ribosomal protein	Ubiquitous expression in tissues, low tissue specificity		Binding, structural molecule activity
4	Stox2	Storkhead-box protein	Ubiquitous expression in tissues, low tissue specificity	Biological regulation, cellular process, metabolic process	Binding, transcription regulator activity
4	Rpl3	Component of the large ribosomal subunit, ribosomal protein	Ubiquitous expression in tissues, low tissue specificity	Cellular process	Binding, structural molecule activity
5	Pbx3	Pre-B-cell leukemia transcription factor, homeodomain transcription factor	Ubiquitous expression in tissues, low tissue specificity	Biological regulation, cellular process, developmental process, metabolic process, multicellular organismal process	Binding, transcription regulator activity
5	Cfap221	Cilia-and-flagella associated protein, structural protein	Ubiquitous expression in tissues (testis)		Binding
5	Eif5b	Eukaryotic translation initiation factor	Ubiquitous expression in tissues, low tissue specificity		Binding, translation regulator activity
5	Spryd7	SPRY domain containing protein	Ubiquitous expression in tissues, low tissue specificity		
5	Cetp	Cholesteryl ester transfer protein	Broad expression in tissues (liver and plasma)	Biological regulation, cellular process, localization, metabolic process, multicellular organismal process	Binding, transporter activity

An initial over-representation analysis of all identified proteins affected by nickel treatment was conducted using Cytoscape 3.9.1 software to determine the over-represented pathways and GO biological processes involved in the response to nickel exposure ($p < 0.10$). In total, 290 distinct pathways were over-represented to be involved in the response to nickel exposure (Appendix C1). The 275 significantly affected proteins identified previously were compared against the over-represented pathways, leaving 221 over-represented pathways and GO biological processes involved in the response to nickel exposure. These networks include regulation of cellular process, pyruvate metabolic process, regulation of biological process, regulation of cell communication, positive regulation of axon extension, and positive regulation of axonogenesis (Figure 9). Comparatively, CTDbase was used to complete an over-representation analysis on the 275 kidney proteins significantly affected by nickel treatment, revealing 12 biological networks that were significant ($p < 0.05$), found in Table 7. The 275 proteins represent many various biological processes and molecular functions while maintaining the many pathways.

Table 7. Over-represented pathways of proteins from kidney proteome of rainbow trout exposed to nickel. The list of 275 proteins significantly affected by nickel treatment was searched against the gene set analyzer for enriched pathways on CTD to find biological pathway associations in response to nickel exposure ($p < 0.05$). The list here only includes manually selected terms from all over-represented pathways that best represent the networks of interest.

Pathway	Pathway ID	P-value	Proteins from Input List	Genomic Frequency
Metabolism	R-HSA-1430728	4.05E-05	Acsl5|Bcan|Cat|Cetp|Clock|Eno2|Ggt5|Gpd2|Hpse2|Hyal1|Ip6k2|Itpr2|Lbr|Lyve1|Med8|Ndufa5|Ndufb2|Pc|Pgam2|Pla2g4f|Pnpla6|Por|Prkg2|Ptgis|Rora|Rpl3|Rps26|Rps29|Slc25a21|Slc4a1|Sqor|Sult1a3|Tpr|Uck1|Uqcrb|Xdh	4.81%
Signal Transduction	R-HSA-162582	0.0407	Akap13|Akt2|Arhgap15|Arhgef19|Cd28|Cdh5|Cdon|Cilp|Cxcr2|Dab2ip|Fgg|Fzd3|Gab1|Grm7|Hgs|Igf1r|Inhbb|Itpr2|Mapk13|Mylk|Ngf|Nmbr|Porcn|Prkg2|Ptch1|Pth1r|Rapgef1|Rgs12|Smad5|Tab3|Tp53|Usp34|Vcl	5.73%

Pathway	Pathway ID	P-value	Proteins from Input List	Genomic Frequency
Immune System	R-HSA-168256	0.00502	Akt2|Asb12|Cat|Cd28|Cd40|Ceacam6|Cxcr2|Dab2ip|Eif4g2|Fbxw2|Fgg|Gab1|Ip6k2|Itgam|Itpr2|Kif26a|Mapk13|Muc5ac|Nlrp1|Pa2g4|Rapgef1|Rora|Sarm1|Tab3|Tmem30a|Tp53|Tpr|Ube2k|Ube4a|Vcl|Xdh	4.69%
Disease	R-HSA-1643685	0.00547	Adamts2|Akt2|Bcan|Cd28|Dab2ip|Fgg|Gab1|Hgs|Muc5ac|Pc|Porcn|Rpl3|Rps26|Rps29|Taf1|Taf5|Tpr|Vcl	1.90%
Signaling by NGF	R-HSA-166520	0.00741	Akap13|Akt2|Arhgef19|Cd28|Dab2ip|Fgg|Gab1|Itpr2|Mapk13|Ngf|Rapgef1|Tp53|Vcl	1.06%
Extracellular Matrix Organization	R-HSA-1474244	0.00212	Adamts2|Bcan|Ceacam6|Col20a1|Dspp|Fgg|Itgam|Itgb6|Ltbp2|Mmp14|Mmp24	0.66%
NGF Signaling via TRKA from Plasma Membrane	R-HSA-187037	0.02536	Akt2|Cd28|Dab2ip|Fgg|Gab1|Itpr2|Mapk13|Ngf|Rapgef1|Tp53|Vcl	0.86%
Proteoglycans in Cancer	hsa05205	0.00423	Akt2|Fzd3|Gab1|Hpse2|Igf1r|Itpr2|Mapk13|Ptch1|Tp53	0.45%
Transcriptional Misregulation in Cancer	hsa05202	0.01363	Atm|Cd40|Igf1r|Itgam|Pbx1|Pbx3|Prom1|Tp53	0.40%
Neurotrophin Signaling Pathway*	hsa04722	0.00797	Akt2|Gab1|Mapk13|Ngf|Ntrk3|Rapgef1|Tp53	0.26%
Platelet Activation	hsa04611	0.00991	Akt2|Fgg|Itpr2|Mapk13|Mylk|Pla2g4f|Prkg2	0.27%
Apoptosis	hsa04210	0.02093	Aifm1|Akt2|Atm|Dab2ip|Itpr2|Ngf|Tp53	0.31%

***** found only in kidney proteome, not found in mucus or plasma proteome

3.4.2 Toxicological Effects on Kidney

The associated disease function of the 275 kidney proteins include a number of cancers, metabolic diseases, musculoskeletal diseases, nervous system diseases, urogenital diseases, among other pathological processes, summarized in Table 8. GO analysis of the 275 proteins associated with the kidney contain many biological processes specific to biological regulation, cellular process, metabolic process, response to stimuli, signaling, among others, were affected by aquatic nickel (Figure 9a). The GO analysis also revealed molecular functions specific to binding, catalytic activity, molecular transducer activity, transcription regulator activity, among others, were affected by aquatic nickel (Figure 9b).

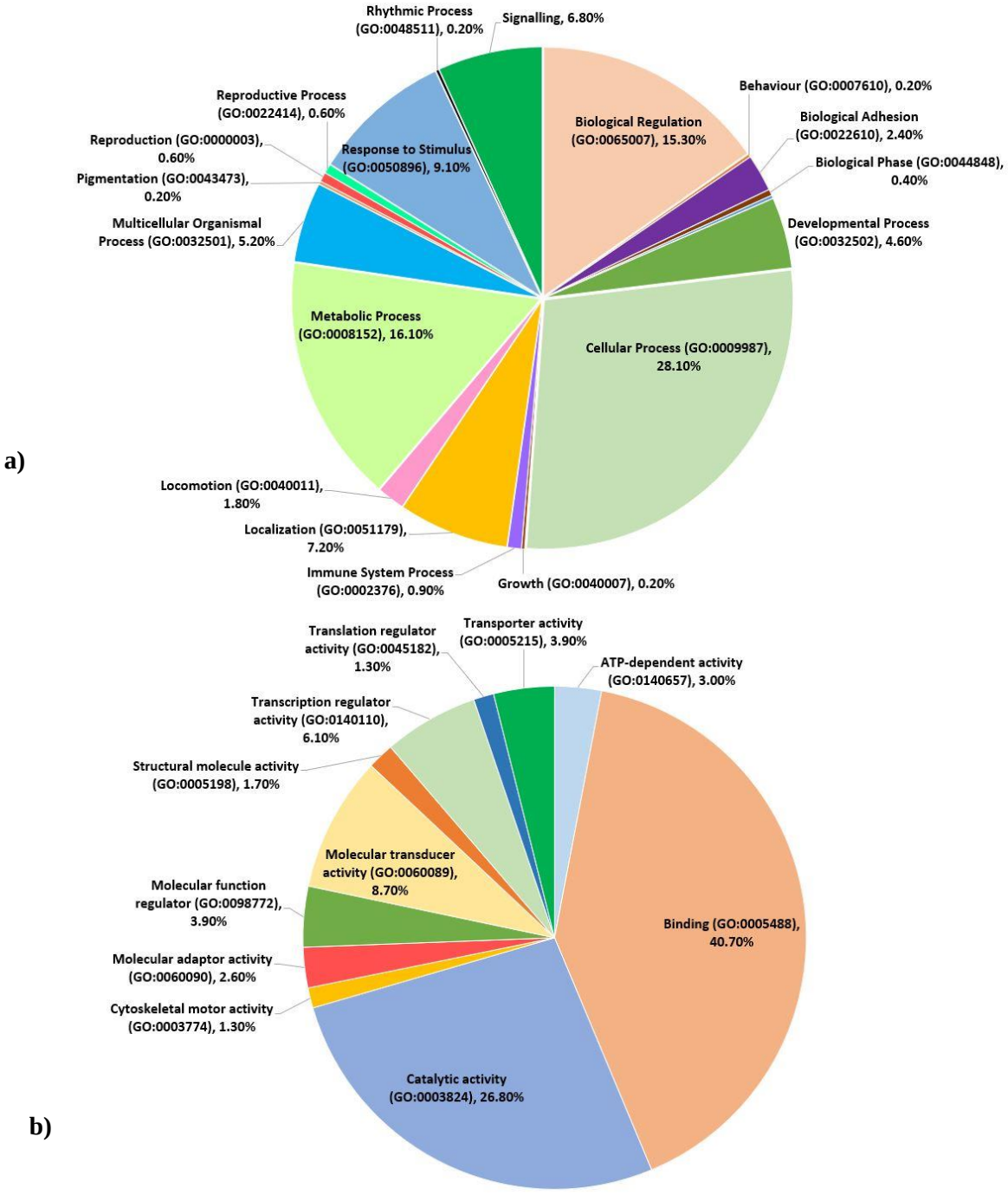

Figure 9. Genomic percentage of a) biological processes and b) molecular functions in kidney proteome of rainbow trout affected by aquatic nickel treatment. The list of 275 kidney proteins significantly affect by nickel treatment were searched against the GO Enrichment Analysis powered by Panther to find the over-represented list of proteins involved in the biological processes and molecular functions involved in response to nickel exposure ($p < 0.01$). Each section of the pie chart represents the function, GO term, and percentage of genes found for that purpose. All proteins were searched in regards to Homo sapiens. A background protein list was not used.

Table 8. Disease association of GO in kidney proteins of rainbow trout significantly affected by nickel treatment. The list of 275 proteins significantly affected by nickel treatment were searched against the gene set analyzer for enriched diseases on CTDbase to find disease associations in response to nickel exposure ($p < 0.05$). The list here only includes manually selected terms from all over-represented pathways that best represent the networks of interest.

Disease Category	Disease Name	p-value	Disease ID	Proteins from Input List
Blood Disease	Hematologic Diseases	2.22E-05	MESH:D006402 MESH:D001855	Adamts2|Ahi1|Atrx|Cd40|Dnmt1|Ercc4|Fgg|Hps6|Igf1r|Lbr|Rps26|Rps29|Samd9l|Slc4a1|Slx4|Tp53|Xdh
Cancer	Neoplasms	2.14E-17	MESH:D009369 MESH:D009370 MESH:D009371 MESH:D009373 MESH:D009375 MESH:D018302	Adamts2|Akap13|Akt2|Asap1|Atm|Atrx|Baz2a|Bcorl1|Bltp3a|Bptf|Cat|Cd28|Cd40|Cdh5|Cdon|Cetp|Chd1|Chrna9|Cmklr1|Cpeb1|Cryab|Csmd1|Dab2ip|Dcbld2|Dhdh|Dnmt1|Dspp|Ehd3|Emx2|Eno2|Epb41l3|Ercc4|Fam180a|Fat1|Fgg|Gab1|Igf1r|Itgam|Kdm6b|Kmt2b|Lyve1|Mecp2|Mmp14|Mmp24|Mrpl9|Mylk|Myo5b|Ngf|Nlrp1|Nmbr|Ntrk3|Pa2g4|Pbx1|Pc|Pgam2|Pggt1b|Por|Ppfibp2|Prom1|Psd3|Ptch1|Ptgis|Pth1r|Rbm38|Rora|Rpl3|Rps26|Septin9|Slc66a3|Spdef|Srr|Syne1|Tp53|Tpr|Xdh
	Digestive System Neoplasms	1.42E-07	MESH:D004067	Akap13|Atm|Atrx|Cat|Cdh5|Cdon|Cetp|Chd1|Cryab|Csmd1|Dcbld2|Dnmt1|Ehd3|Eno2|Fam180a|Fat1|Fgg|Igf1r|Kmt2b|Lyve1|Mecp2|Mmp14|Myo5b|Pa2g4|Prom1|Ptch1|Pth1r|Rbm38|Rora|Rps26|Slc66a3|Syne1|Tp53
	Gastrointestinal Neoplasms	0.00105	MESH:D005770	Akap13|Atm|Cdh5|Cdon|Chd1|Cryab|Dcbld2|Dnmt1|Fat1|Fgg|Mmp14|Pa2g4|Prom1|Ptch1|Rbm38|Rora|Rps26|Syne1|Tp53
	Genital Neoplasms	0.00123	MESH:D005834 (male) MESH:D014565	Akap13|Atm|Cdh5|Cdon|Chd1|Cryab|Dcbld2|Dnmt1|Fat1|Fgg|Mmp14|Pa2g4|Prom1|Ptch1|Rbm38|Rora|Rps26|Syne1|Tp53 Akap13|Akt2|Asap1|Atm|Baz2a|Bcorl1|Bltp3a|Bptf|Cat|Chd1|Cmklr1|Cryab|Dab2ip|Dhdh|Dnmt1|Eno2|Ercc4|Igf1r|Mmp14|Pgam2|Por|Ppfibp2|Prom1|Spdef|Tp53
	Liver Neoplasms	0.00854	MESH:D008113	Atm|Cat|Cetp|Csmd1|Ehd3|Eno2|Fam180a|Igf1r|Kmt2b|Lyve1|Mecp2|Mmp14|Myo5b|Pth1r|Slc66a3|Tp53
	Neoplastic Cell Transformation	0.00525	MESH:D002471	Cat|Chrna9|Eno2|Igf1r|Mmp14|Por|Prom1|Tp53
	Urinary Bladder Neoplasms	0.00525	MESH:D001749 MESH:D014571	Akap13|Asap1|Atm|Bcorl1|Bptf|Cat|Cryab|Dnmt1|Eno2|Ercc4|Por|Tp53
	Carcinoma	4.37E-06	MESH:D002277 MESH:D063646 MESH:D003528 MESH:D006528 MESH:D005910	Akap13|Akt2|Atm|Atrx|Bcorl1|Cat|Cetp|Cryab|Csmd1|Dnmt1|Dspp|Ehd3|Fam180a|Fat1|Igf1r|Kdm6b|Kmt2b|Lyve1|Mecp2|Mmp14|Nlrp1|Prom1|Ptch1|Pth1r|Rpl3|Srr|Syne1|Tp53|Xdh
	Adenocarcinoma	4.25E-04	MESH:D000230	Akap13|Akt2|Atm|Atrx|Bcorl1|Cat|Cetp|Cryab|Csmd1|Dnmt1|Ehd3|Fam180a|Fat1|Igf1r|Kdm6b|Kmt2b|Lyve1|Mecp2|Mmp14|Pth1r|Srr|Tp53
Cardiovascular Disease	Cardiovascular Diseases	0.00571	MESH:D002318 MESH:D014652	Adamts2|Atm|Cat|Cd40|Cetp|Cobll1|Cryab|Cxcr2|Dab2ip|Hip1r|Igf1r|Itgam|Itpr2|Lbr|Mmp14|Mylk|Ngf|Plxnd1|Por|Ptgis|Sh3pxd2b|Tm6sf2|Tp53|Usp34|Vcl|Xdh

Disease Category	Disease Name	p-value	Disease ID	Proteins from Input List
Congenital Abnormalities	Abnormalities	1.72E-08	MESH:D000015 MESH:D000013 MESH:D009358	Adamts2|Aifm1|Atrx|Cat|Cdon|Chrnb1|Dnaaf11|Dnmt1|Dspp|Emx2|Ercc4|Ganab|Gjc2|Igf1r|Inf2|Itgb6|Ltbp2|Mcph1|Mecp2|Mmp14|Ngf|Nlrp1|Pnpla6|Por|Porcn|Ptch1|Ptgis|Pth1r|Sall2|Sh3pxd2b|Tp53|Tubgcp6|Vipas39|Znf469
Connective Tissue Disease	Connective Tissue Diseases	1.46E-04	MESH:D003240	Adamts2|Asap1|Bltp3a|Cat|Cd28|Cd40|Cd83|Cxcr2|Faxdc2|Fgg|Hyal1|Igf1r|Itgam|Lbr|Ltbp2|Pcnx3
	Skin and Connective Tissue Diseases	2.11E-09	MESH:D017437	Adamts2|Akt2|Apcdd1|Asap1|Atm|Bltp3a|Cat|Cd28|Cd40|Cd83|Cdh5|Csmd1|Cxcr2|Dnmt1|Epb41l3|Ercc4|Faxdc2|Fgg|Hps6|Hyal1|Igf1r|Itgam|Itpr2|Lbr|Ltbp2|Mmp14|Mrpl9|Ngf|Nlrp1|Nmbr|Pcnx3|Pnpla6|Porcn|Ptch1|Ptgis|Syne1|Tp53|Znf469
Digestive System Disease	Gastrointestinal Diseases	4.04E-06	MESH:D005767 MESH:D004066	Aifm1|Akap13|Arhgap15|Atm|Atrx|Cat|Cd83|Cdh5|Cdon|Cetp|Chd1|Cobll1|Cryab|Csmd1|Cxcr2|Dcbld2|Dnmt1|Dscam|Ehd3|Eno2|Fam180a|Fat1|Fgg|Ganab|Igf1r|Itgam|Itgb6|Kmt2b|Lbr|Lyve1|Mapk13|Mecp2|Mmp14|Mylk|Myo5b|Nat8|Pa2g4|Pc|Prom1|Prtg|Ptch1|Pth1r|Rbm38|Rora|Rps26|Slc26a9|Slc66a3|Srr|Syne1|Tm6sf2|Tp53|Vipas39
	Liver Diseases	0.00159	MESH:D008107	Aifm1|Atm|Cat|Cd83|Cdh5|Cetp|Cobll1|Cryab|Csmd1|Dscam|Ehd3|Eno2|Fam180a|Fat1|Ganab|Igf1r|Itgb6|Kmt2b|Lbr|Lyve1|Mecp2|Mmp14|Myo5b|Nat8|Pc|Prtg|Pth1r|Slc66a3|Srr|Tm6sf2|Tp53
Ear-Nose-Throat Disease	Otorhinolaryngologic Diseases	5.77E-04	MESH:D010038	Aifm1|Akt2|Atrx|Cat|Dnaaf11|Dnmt1|Dspp|Gab1|Ripor2|Sh3pxd2b|Syne1|Tp53|Triobp
Endocrine System Disease	Endocrine System Disease	0.01379	MESH:D004700	Aifm1|Akt2|Atm|Atrx|Cat|Cmklr1|Dcbld2|Dnmt1|Ercc4|Gab1|Gpd2|Igf1r|Inhbb|Pnpla6|Por|Ptch1|Pth1r|Smad5|Spdef|Tp53|Tpr
Eye Disease	Eye Disease	4.27E-05	MESH:D005128 MESH:D003316	Ahi1|Aifm1|Atm|Cat|Cryab|Gjd2|Hps6|Ltbp2|Mmp14|Mylk|Ngf|Nlrp1|Pnpla6|Prom1|Rp1|Rp1l1|Sall2|Sh3pxd2b|Tubgcp6|Znf469
Hemic and Lymphatic Disease	Hemic and Lymphatic Diseases	1.43E-07	MESH:D006425	Adamts2|Ahi1|Atm|Atrx|Cat|Cd28|Cd40|Cpeb1|Dnmt1|Ercc4|Fgg|Gjc2|Hps6|Igf1r|Lbr|Pbx1|Pc|Rps26|Rps29|Samd9l|Slc4a1|Slx4|Tp53|Xdh
Immune System Disease	Immune System Diseases	3.57E-05	MESH:D007154 MESH:D001327	Ahi1|Aifm1|Asap1|Atm|Bltp3a|Cat|Cd28|Cd40|Cd83|Cpeb1|Cxcr2|Dnmt1|Faxdc2|Igf1r|Itgam|Itgb6|Lbr|Mylk|Nlrp1|Pbx1|Pc|Pcnx3|Pnpla6|Ptch1|Ptgis|Tp53
Mental Disorders	Neurodevelopment Disorder	1.03E-07	MESH:D065886 MESH:D001523	Ahi1|Aifm1|Camta1|Cat|Cd2ap|Chd2|Csmd1|Dnmt1|Dscam|Eno2|Farp1|Grm7|Igf1r|Ip6k2|Kdm6b|Mecp2|Myo1d|Myo5b|Ngf|Plxnb2|Pbx1|Pc|Plekho1|Pnpla6|Por|Psd3|Ptgis|Rgs12|Rora|Sh3pxd2b|Smad5|Snx14|Syne1|Tp53|Vcl|Xdh
Metabolic Disease	Metabolic Diseases	2.68E-04	MESH:D008659	Aifm1|Akt2|Atm|Casq1|Cat|Cd40|Cetp|Cog2|Ercc4|Gjc2|Gpd2|Hps6|Hyal1|Itgam|Lbr|Mmp14|Mylk|Myo5b|Pc|Por|Pth1r|Slc4a1|Slx4|Smad5|Tp53|Uqcrb|Vcl|Xdh
	Nutritional and Metabolic Diseases	3.35E-04	MESH:D009750	Aifm1|Akt2|Apcdd1|Atm|Casq1|Cat|Cd40|Cetp|Cog2|Ercc4|Gjc2|Gpd2|Hps6|Hyal1|Itgam|Lbr|Mmp14|Mylk|Myo5b|Pc|Por|Pth1r|Slc4a1|Slx4|Smad5|Tp53|Uqcrb|Vcl|Xdh

Disease Category	Disease Name	p-value	Disease ID	Proteins from Input List
Musculoskeletal Disease	Bone Diseases	2.69E-05	MESH:D001847 MESH:D001848 MESH:D001851	Aifm1|Cat|Cilp|Ercc4|Gpd2|Lbr|Ltbp2|Mmp14|Myo5b|Pnpla6|Por|Porcn|Ptch1|Pth1r|Sh3pxd2b|Tp53|Vcl
	Joint Diseases	1.89E-04	MESH:D007592 MESH:D001168	Acsl5|Asap1|Cat|Cd28|Cd40|Cd83|Chadl|Cxcr2|Dnmt1|Faxdc2|Igf1r|Mmp14|Nlrp1|Vipas39|Xdh|Znf469
	Musculoskeletal Diseases	1.46E-12	MESH:D009140	Acsl5|Aifm1|Asap1|Atrx|Casq1|Cat|Cd28|Cd40|Cd83|Cdon|Chadl|Chrnb1|Cilp|Cryab|Cxcr2|Dnmt1|Ercc4|Faxdc2|Gpd2|Igf1r|Lbr|Ltbp2|Mcph1|Mecp2|Mmp14|Myo5b|Nlrp1|Pgam2|Pnpla6|Por|Porcn|Ptch1|Pth1r|Sh3pxd2b|Syne1|Tp53|Tubgcp6|Vcl|Vipas39|Xdh|Znf469
Nervous System Disease	Ataxia	6.05E-05	MESH:D001259 MESH:D002524	Atm|Camta1|Dnmt1|Hyou1|Pnpla6|Samd9l|Snx14|Syne1
	Brain Diseases	1.94E-09	MESH:D001927	Ahi1|Aifm1|Atm|Camta1|Cat|Cd2ap|Ceacam6|Chd2|Cxcr2|Dnmt1|Eno2|Gjc2|Hyou1|Igf1r|Ip6k2|Itgam|Itpr2|Marchf6|Mecp2|Mylk|Myo5b|Ncapg2|Ngf|Pc|Pnpla6|Ptch1|Samd9l|Snx14|Syne1|Szt2|Tp53|Xdh
	Central Nervous System Diseases	1.62E-09	MESH:D002493	Ahi1|Aifm1|Atm|Camta1|Cat|Cd2ap|Ceacam6|Chd2|Cxcr2|Dnmt1|Eno2|Gjc2|Hyou1|Igf1r|Ip6k2|Itgam|Itpr2|Kmt2b|Marchf6|Mecp2|Mylk|Myo5b|Ncapg2|Ngf|Pc|Pnpla6|Ptch1|Samd9l|Snx14|Syne1|Szt2|Taf1|Tp53|Xdh
	Cerebellar Diseases	1.47E-04	MESH:D002526	Ahi1|Atm|Camta1|Dnmt1|Hyou1|Pnpla6|Samd9l|Snx14|Syne1
	Dyskinesias	5.72E-07	MESH:D020820	Aifm1|Atm|Camta1|Cat|Dnmt1|Hyou1|Ip6k2|Kmt2b|Mecp2|Ngf|Pnpla6|Samd9l|Snx14|Syne1
	Movement Disorders	0.00549	MESH:D009069	Aifm1|Cat|Ceacam6|Eno2|Igf1r|Ip6k2|Kmt2b|Ncapg2|Ngf|Taf1
	Nervous System Diseases	7.71E-14	MESH:D009422	Ahi1|Aifm1|Atm|Atrx|Camta1|Casq1|Cat|Cd2ap|Cd40|Cd83|Cdon|Ceacam6|Chd1|Chd2|Chrnb1|Cryab|Cxcr2|Dnmt1|Dspp|Emx2|Eno2|Ercc4|Gab1|Gjc2|Hyou1|Igf1r|Inf2|Ip6k2|Itgam|Itpr2|Kdm6b|Kmt2b|Marchf6|Mcph1|Mecp2|Mylk|Myo5b|Ncapg2|Ngf|Ntrk3|Pc|Pgam2|Pnpla6|Por|Ptch1|Ripor2|Samd9l|Septin9|Sh3pxd2b|Snx14|Syne1|Szt2|Taf1|Tp53|Triobp|Tubgcp6|Xdh
	Neurodegenerative Diseases	2.26E-04	MESH:D019636	Aifm1|Cd2ap|Ceacam6|Cryab|Dnmt1|Eno2|Ercc4|Gjc2|Hyou1|Igf1r|Inf2|Ip6k2|Ncapg2|Ngf|Pnpla6|Snx14|Syne1|Tp53
	Neuromuscular Diseases	1.89E-04	MESH:D009468	Aifm1|Casq1|Cat|Chrnb1|Cryab|Cxcr2|Dnmt1|Ercc4|Gjc2|Igf1r|Inf2|Ngf|Pgam2|Pnpla6|Septin9|Syne1|Tp53
	Peripheral Nervous System Diseases	4.48E-04	MESH:D010523	Aifm1|Cat|Cxcr2|Dnmt1|Ercc4|Gjc2|Igf1r|Inf2|Ngf|Pnpla6|Septin9
Pathologic Process	Infarction	0.02418	MESH:D007238	Atm|Cat|Cxcr2|Dab2ip|Ngf|Tm6sf2|Xdh
	Infections	0.03194	MESH:D007239	Asap1|Cd28|Cxcr2|Itgam|Itgb6|Mylk|Ngf|Pbx1|Pc|Ptch1|Sarm1|Slc4a1|Tp53
	Ischemia	5.60E-04	MESH:D007511	Atm|Cat|Cdh5|Cxcr2|Dab2ip|Ngf|Tm6sf2|Tp53|Xdh
	Necrosis	0.01965	MESH:D009336	Aifm1|Atm|Cat|Cxcr2|Dab2ip|Ngf|Tm6sf2|Xdh

Disease Category	Disease Name	p-value	Disease ID	Proteins from Input List
	Pathologic Processes	2.46E-08	MESH:D010335 MESH:D013568	Aifm1|Akt2|Atm|Atrx|Cat|Cd83|Cdh5|Chrna9|Cobll1|Cpeb1|Cryab|Cxcr2|Dab2ip|Dnmt1|Eno2|Ercc4|Fat1|Fgg|Hip1r|Hpse2|Igf1r|Itgam|Itgb6|Lbr|Mecp2|Mmp14|Mmp24|Mylk|Nat8|Ngf|Nlrp1|Pa2g4|Pc|Por|Prom1|Prtg|Rbm38|Rps26|Septin9|Sh3pxd2b|Slc66a3|Srr|Tm6sf2|Tp53|Usp34|Xdh
Respiratory Tract Disease (Gills)	Gill Diseases	8.21E-06	MESH:D008171 MESH:D012140	Adamts2|Asap1|Atrx|Cat|Cd28|Cdh5|Cxcr2|Dab2ip|Dnaaf11|Dnmt1|Emx2|Eno2|Fat1|Igf1r|Itgb6|Mecp2|Mmp14|Mylk|Ngf|Pggt1b|Por|Ptgis|Pth1r|Slc26a9|Tp53|Xdh
Skin Diseases	Skin Diseases	2.40E-07	MESH:D012871	Adamts2|Akt2|Apcdd1|Atm|Cat|Cd28|Cd40|Cd83|Cdh5|Csmd1|Cxcr2|Dnmt1|Epb41l3|Ercc4|Hps6|Igf1r|Itgam|Itpr2|Lbr|Mmp14|Mrpl9|Ngf|Nlrp1|Nmbr|Pnpla6|Porcn|Ptch1|Ptgis|Syne1|Tp53|Znf469
Urogenital Disease	Female Urogenital Diseases	6.71E-07	MESH:D052776	Akap13|Asap1|Atm|Bcorl1|Bptf|Cat|Cd2ap|Cmklr1|Cops2|Cryab|Dcbld2|Dnmt1|Emx2|Eno2|Ercc4|Fam180a|Gab1|Ganab|Hpse2|Igf1r|Inf2|Ngf|Ntrk3|Pgam2|Por|Prom1|Slc47a1|Slc4a1|Spdef|Tp53|Vipas39
	Urogenital Diseases	9.30E-05	MESH:D000091642 MESH:D014570 MESH:D001745 MESH:D000091662	Akap13|Akt2|Asap1|Atm|Atrx|Baz2a|Bcorl1|Bltp3a|Bptf|Cat|Cd28|Cd2ap|Ceacam6|Chd1|Cmklr1|Cops2|Cryab|Cxcr2|Dab2ip|Dcbld2|Dhdh|Dnmt1|Ecm2|Emx2|Eno2|Ercc4|Fam180a|Fetub|Gab1|Ganab|Hpse2|Igf1r|Inf2|Itgb6|Lbr|Mmp14|Ngf|Ntrk3|Pgam2|Por|Ppfibp2|Prom1|Ptch1|Ptgis|Slc47a1|Slc4a1|Spdef|Tp53|Vipas39
	Male Urogenital Diseases	1.99E-05	MESH:D052801 MESH:D005832	Akap13|Akt2|Asap1|Atm|Atrx|Baz2a|Bcorl1|Bltp3a|Bptf|Cat|Cd2ap|Chd1|Cryab|Dab2ip|Dhdh|Dnmt1|Eno2|Ercc4|Ganab|Hpse2|Inf2|Mmp14|Ngf|Pgam2|Por|Ppfibp2|Slc47a1|Slc4a1|Tp53|Vipas39

3.4.3 Comparison to Standard Kidney

In the previous study by Nancy Tannouri MSc, DDA LC-HR-MS/MS identified 1454 proteins in the kidney proteome. Statistical analysis identified 138 proteins were significant different between male and female rainbow trout (FDR < 0.25) and in total, 275 kidney enriched proteins, indicating the significant proteins distinct to the kidney tissue (compared to blood plasma). As stated previously, DDA LC-HR-MS/MS identified 5556 kidney proteins in the kidney proteome of rainbow trout exposed to aquatic nickel treatment. There were no evident changes in standard kidney proteome between the kidney in my control group and the kidney of Nancy Tannouri's research. Due to changes in the

comparative database, this is not a clear indication of more protein abundance due to nickel exposure. There were 679 proteins found in both lists of kidney proteins. There were no significant differences between male and female rainbow trout exposed to aquatic nickel treatments.

3.5 Comparison to Mucus and Blood Plasma

3.5.1 Main and Interaction Effects

DDA LC-HR-MS/MS identified a total of 2840 proteins in the blood plasma proteome and 6934 proteins in the mucus proteome of rainbow trout, after missing and duplicate values were removed. Furthermore, 1336 duplicated values between the overall liver proteome and the blood plasma proteome were removed, leaving a combined 5330 unique proteins determined between the liver and plasma. Similarly, 2748 duplicated values between the overall liver proteome and the mucus proteome were removed, leaving a combined 8212 unique proteins determined between the liver and the mucus proteome. In the same analysis, 1396 duplicated values between the overall kidney proteome and the blood plasma proteome were removed, leaving a combined 5948 unique proteins determined between the kidney and plasma. Likewise, 2896 duplicated values between the overall kidney proteome and the mucus proteome were removed, leaving a combined 8542 unique proteins determined between the kidney and the mucus proteome.

1828 plasma proteins and 1424 mucus proteins were significant in each proteome for rainbow trout exposed to nickel treatment (One-way ANOVA, FDR < 0.05, Tukey's HSD post-hoc p-value < 0.05), compared to the significant 26 liver proteins and 275 kidney proteins (Figure 10). This indicates a significantly higher proportion of plasma and mucus proteins were affected by nickel treatment compared to the proteome of liver or kidney

tissue. There are 21 shared proteins amongst the kidney, mucus, and plasma proteomes, 37 shared proteins between the kidney and plasma proteome, and 40 shared proteins amid the kidney and mucus proteome. There are less commonly shared proteins between the liver proteome and the biofluids (ie. mucus and plasma).

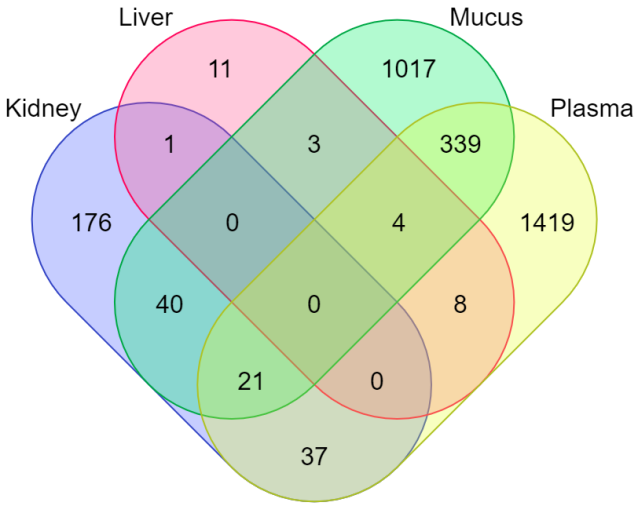

Figure 10. Go enrichment analysis of the significant proteins in kidney, liver, mucus, and plasma proteome in rainbow trout exposed to nickel treatment. Venn diagram of the number of proteins commonly shared between the four groups and all combinations of the four groups.

There was significant overlap in the biological functions affected between the organs and biofluid proteomes in response to nickel exposure, like biological regulation (GO:0065007;15.5% ±0.5), cellular process (GO:0009987; 29.4% ±0.7), metabolic process (GO:0008152; 16.5% ±0.3), response to stimulus (GO:0050896; 8.4% ±0.5), and signaling (GO:0023052; 6.7% ±0.1). The overall representation of each category from both biological processes and molecular functions were statistically similar for kidney, mucus, and plasma. There were no significant differences in overall proportion of biological processes between the tissues (kidney and liver) and biofluids (mucus and plasma) proteomes (Two-way ANOVA, Tukey's HSD post-hoc test ($p < 0.01$)). The biological process of pigmentation only appears in the affected proteome of kidney and plasma, by

comparison, rhythmic process and behaviour only appear in the affected proteome of kidney and mucus. Likewise, there was significant overlap in the molecular functions, such as binding (GO:0005488; 37.3% ±1.5), catalytic activity (GO:0003824; 29.8% ±1.5), molecular function regulator (GO:0098772; 4.9% ±0.7), molecular transducer activity (GO:0060089; 6.7% ±0.9), transcription regulator activity (GO:0140110; 6.7% ±0.4), and transporter activity (GO:0005215; 5.7% ±0.9). Similarly, there were no significant differences in overall proportion of molecular functions between the tissues (kidney and liver) and biofluids (mucus and plasma) proteomes (Two-way ANOVA, Tukey's HSD post-hoc test ($p < 0.01$)). The molecular function of low-density lipoprotein in particle receptor activity is only found in the affected proteome of mucus. The results are displayed as a bar graph in Figure 11a and Figure 11b.

The proportion of proteins represented in each pathway affected due to nickel exposure for kidney, mucus, and plasma were relatively equal in number (Figure 12d), with 4 exceptions. The over-representation pathways affected by nickel established that almost all of the pathways established in the kidney (11/12) or liver (1/1) proteome are found in the biofluid proteomes. The transcriptional misregulation-in-cancer pathway was not found to be affected in plasma and the apoptosis pathway was not found to be affected in mucus, although each pathway was found to be affected in the kidney. A pathway that was only found to be affected in the kidney was the neurotrophin signaling in cancer pathway. Separately, the hemostasis pathway was found to be affected in the liver, and in the mucus and plasma to a smaller extent, and not in the kidney. Both mucus and plasma had a larger amount of significant proteins identified in their proteomes compared to either the kidney

or liver proteome. There were 66 pathways identified in mucus, 77 identified pathways in plasma, and 138 pathways identified in both mucus and plasma (Figure 12b).

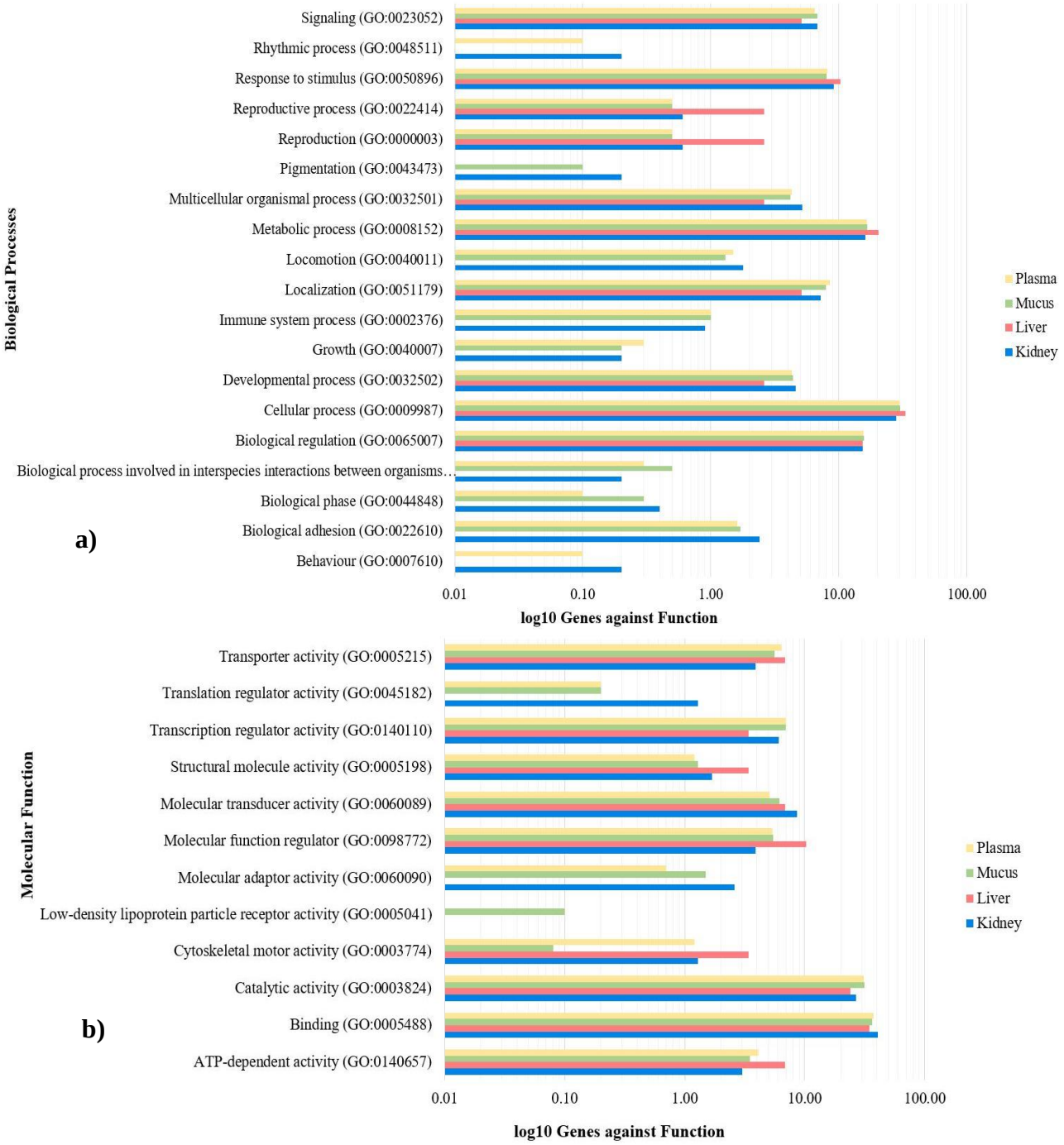

Figure 11. GO enrichment analysis of kidney, mucus, and plasma proteins that experienced a change in abundance in rainbow trout exposed to nickel treatment compared to the control. The lists of 26 liver, 275 kidney, 1424 mucus, and 1828 plasma proteins significantly affected by nickel treatment were searched against the GO Enrichment Analysis powered by Panther to find the over-represented lists of proteins involved in the biological processes and molecular functions involved in response to nickel exposure ($p < 0.01$). Bar plot representing the number and percentage of proteins affected by nickel in comparison to the control treatment (pairwise comparison, $p < 0.01$) for a) biological processes and b) molecular functions.

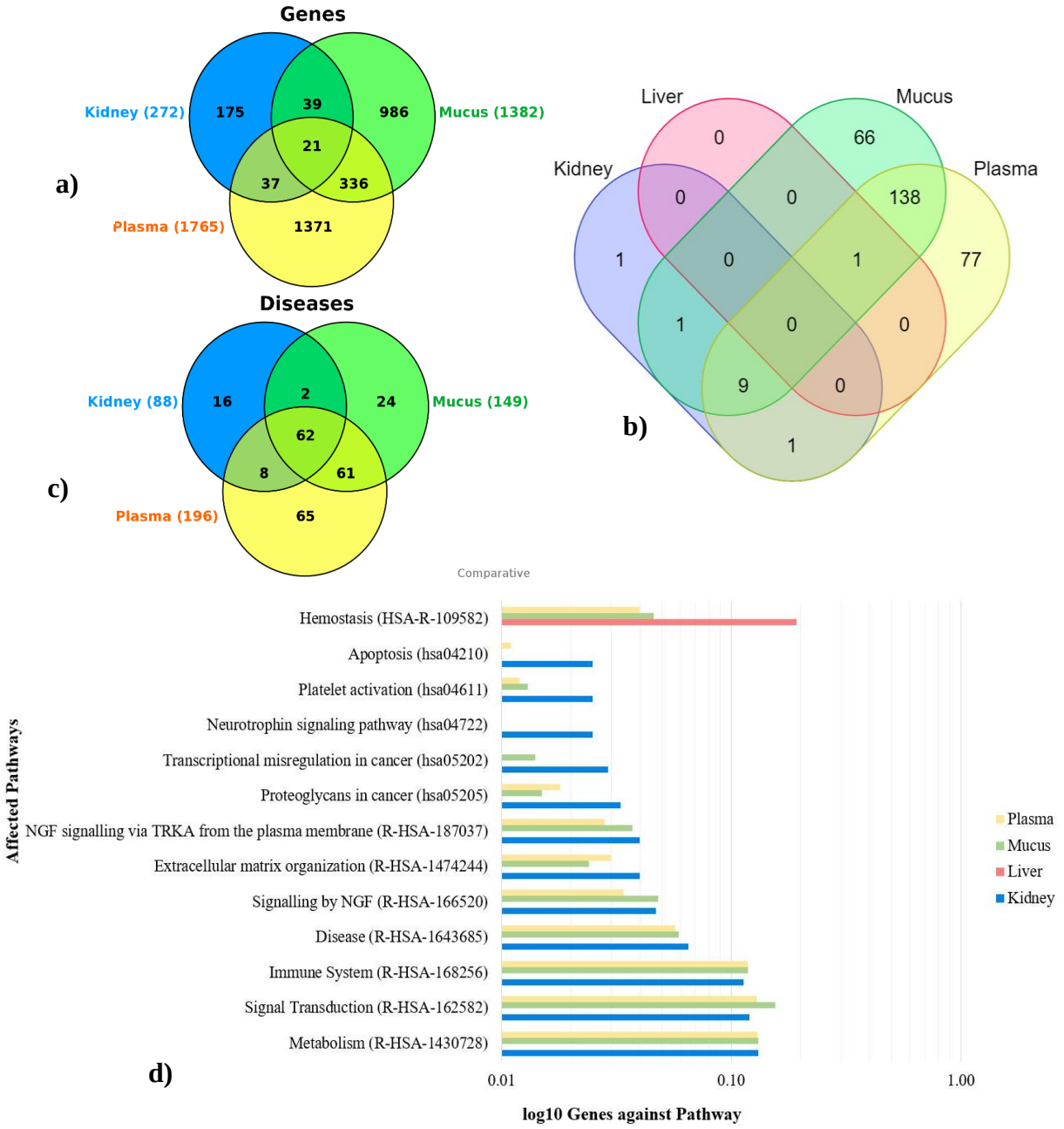

Figure 12. GO enrichment analysis of kidney, mucus, and plasma proteins that experienced a change in abundance in rainbow trout exposed to nickel treatment compared to the control. The lists of 26 liver, 275 kidney, 1424 mucus, and 1828 plasma proteins significantly affected by nickel treatment were searched against the CTDbase. a) Venn diagram representing the number of proteins shared between the kidney proteome and the biofluids' proteomes from CTDbase ; b) Venn diagram illustrating the number of shared pathways between both tissues (kidney and liver) and biofluids (mucus and plasma) proteomes; c) Venn diagram representing the number of associated diseases caused by the change in protein abundance shared between the kidney proteome and the biofluids' proteomes from CTDbase; d) Bar graph of GO enrichment analysis displaying the affected pathways of the 275 kidney proteins in comparison to liver, mucus, and plasma. GO terms manually selected based on uniqueness and p-value < 0.05.

Chapter 4. Discussion

4.0 Nickel water chemistry

Urvi Pajankar determined that baseline nickel concentrations were consistent at 0.5 μg/L for the water supply in the lab in Oshawa, Ontario. This Ni concentration is 40x below the drinking water guideline for nickel set by the World Health Organization (WHO; Organization 2021). The concentration of Ni in the lab is 50x below the lowest end of the threshold for the Canadian Water Quality Guideline for aquatic life (CCME; SQGHH and Provisional 2015). The current measured Ni concentrations in the rivers surrounding the OROF are 0.2 μg/L, which is statistically similar to the baseline Ni concentration from the lab. Therefore, our control group with no additional Ni represents the current state of the OROF watershed region. The first treatment of 0.45 μg/L Ni (low) had a mean dissolved concentration of 1.52 ±2.4 μg/L Ni (Pajankar 2022), which is 16x below the lowest end of the threshold for the CWQG. The second treatment of 4.5 μg/L Ni (medium) was 5.5x below the lowest end of the threshold for the CWQG. Finally, the third treatment of 45 μg/L Ni (high) was 1.8x above the lowest end of the threshold for the CWQG.

4.1 Protein – Exposure group comparison

All three of the Ni treatment groups shared many of the significantly different proteins identified in rainbow trout organs (kidney: 274/275; liver: 25/26). Similarly, all three of the Ni treatment groups shared many of the significantly different proteins identified in biofluids (mucus: 1424/1424; plasma: 1828/1828). More proteins were identified to be significantly affected by the three nickel treatments in rainbow trout biofluids than the organs. Many of these proteins decreased in abundance in comparison to

the control. This shows that the response to nickel by the fish was nearly identical for the Ni concentration gradient used.

4.2 Accumulation of nickel

Nickel is known to accumulate in organ tissues in multiple species of fish, based on previous studies on Tarpon prochilodus (*Prochilodus lineatus*), goldfish, and lake whitefish (Palermo et al. 2015; Kubrak et al. 2012; Ptashynski et al. 2002). Based upon these other studies, we expected to see evidence of genotoxicity in rainbow trout, specifically at the highest Ni concentration of 45.7 ppb, which resulted in the accumulation of significant levels of Ni within the plasma. Since Ni accumulates in the organs in different proportions, biochemical analysis of the kidney and liver tissue would be required to confirm the differential bioaccumulation. Palermo et al. (2015) observed Ni bioaccumulation was highest in the kidney, followed by the liver, gills, and muscle when exposed to concentrations of 0.025, 0.25, and 2.5 mg/L (Ni) after 96 hours. Concentrations of Ni used by Palermo et al. (2015) were much higher than in our study. A similar observation was concluded by Kubrak et al. (2012) with goldfish, as the kidney experienced concentration-dependent accumulation of nickel. In contrast, the study by Ptashynski et al. (2002) examined lake whitefish exposed to dietary Ni at 0.01, 0.1, and 1.0 mg/g for 10, 30, and 104 days, and there were no significant differences in Ni accumulation in the kidney, liver, or gills of the treated groups compared to the control group. In that study, there were significant qualitative pathological differences among the organ's tissues observed, indicating that the livers were structurally altered with both dose and duration. Thus, longer exposure durations may also be required for lower exposure concentrations to impact organ tissue in rainbow trout.

4.3 Hepatosomatic Index

No significant differences were identified for HSI between the control and treatment groups exposed to the three nickel concentrations. This indicated that there was no change in the energy reserves of the fish due to nickel exposure at the measured concentrations. Therefore, at the concentrations in our experiment, the nickel exposure was not a significant enough stressor for the fish to disrupt metabolic function or feeding behaviour. Additionally, this indicates that heavy metal-induced fatty liver disease did not develop within the 30-day exposure period. Analysis of the liver tissue confirmed that the low levels of nickel used in this experiment did not affect the proteome (0 significantly affected proteins, One-way ANOVA, FDR < 0.05). It is possible that at higher concentrations, we would have observed an effect on HSI, as has been observed in previous studies (Pandit and Gupta 2019; Agrawal, Srivastava, and Chaudhry 1979). The study performed by Pandit, Priyanka, and Gupta (2019) had an exposure concentration ranging from 10 to 30 mg/L ($NiCl_2$), which is much greater than what was used in our study. They observed a very high correlation between the dose of nickel toxicant and HSI, along with major changes to liver tissue structure. The study by Agrawal, Srivastava, and Chaudhry (1979) used an exposure concentration of 45 ppm ($NiSO_4$), approximately 45 mg/L, which is 1000x the concentrations used in our study. They observed no difference in HSI between the control and treated banded Gourami fish (*Colisa fasciatius*) after 90 hours of exposure. While our exposure period was longer and our concentrations were lower, we expected to observe no significant changes in the HSI of the rainbow trout, because we were aiming to use sub-lethal concentrations that are more representative of environmental safety guidelines and therefore more realistic of an environmental exposure scenario.

4.4 Genotoxicity of nickel

Nickel is a known genotoxic, immunotoxic, and carcinogenic agent in humans, and it also appears to have similar effects on aquatic wildlife. The effects on freshwater fish include ionoregulatory impairment, inhibition of respiration, and promotion of oxidative stress (Blewett and Leonard 2017). The majority of these effects were observed at extremely high concentrations that would not necessarily be environmentally relevant. Studies often utilize acute toxicity tests using a 96-hour median lethal concentration (LC_{50}) as the basis for the exposure concentrations. The lowest concentrations in these studies are often much higher than the highest concentration we used in our study (Hunt et al. 2002; Kubrak et al. 2012; Zheng et al. 2014). For example, the lowest acute concentration used by Hunt et al. (2009) on topsmelt silverside (*Atherinops affinis*) was 2650 mg/L (~ 2650 ppm), which is approximately 50,000x higher than the nominal 45.7 ppb concentration used in our study. An example of a more environmentally relevant nickel value is the lowest concentration used by Kubrak et al. (2012) on goldfish, being 10 mg/L (~ 10 ppm), which is still over 200x higher than the highest Ni concentration used in our study. Similarly, the study by Zheng et al. (2014) on goldfish used the same lowest concentration but also examined the high concentration of 100 mg/L (~ 100 ppm). High-concentration studies are valuable to understand the true worst-case scenario of exposure to these metals. However, these concentrations are only environmentally relevant in extreme cases of negligence. Therefore, it is unreasonable to expect the same worst-case scenario of adverse effects to occur.

The study by Kubrak et al. (2012) observed concentration-dependent Ni accumulation in the kidney, along with a mild increase in iron accumulation and increased

lipid peroxide levels caused by oxidative stress. During exposure to nickel in the kidney, they observed exacerbated oxidative stress induced damage to lipids proportional to the level of iron accumulation. This was not observed during our study, potentially due to the nominal concentrations of Ni used for exposure. However, in the kidney proteome, we observed an increase in abundance in DNA repair (Hmces) and activation of NADPH oxidases (Lbr) and a decrease in abundance in tumour suppression (Epb41l3), wound healing (Dcbld2), and cell proliferation (Podn). This indicates we may have observed the molecular initiating events of the previously noted adverse outcomes of nickel in the kidney. Furthermore, because we kept our concentrations environmentally relevant to the OROF region, the immunotoxic potential of nickel was not fully reached, and toxicity to the fish was low. Recovery to baseline protein abundance levels may even be possible with a depuration period post-exposure, although further studies are required.

In both the kidney and liver, we observed the over-representation of disease pathways involved in neoplasms as an abnormal and excessive growth of tissue. As stated previously, we determined many proteins that indicate the beginning of the known adverse outcomes of nickel occurring in the kidney. In a similar manner to the kidney, these changes are beginning to occur in the liver of rainbow trout, according to our study. Neoplasia occurring in the liver in response to the exposure of nickel was observed in English sole (*Parophrys vetulus*) and winter flounder (*Pleuronectes americanus*) (Malins et al. 1987; Chang, Zdanowicz, and Murchelano 1998). The field study by Malins et al. (1987) on English sole observed the formation of hepatic neoplasms due to various metals, including nickel, found naturally occurring in the sediment. The study by Chang, Zdanowicz, and Murchelano (1998) on winter flounder observed a weak positive

correlation between nickel and liver neoplasms, indicating the carcinogenic property of nickel. Their study showed that the pre-neoplastic liver lesions consisted of small, non-compressive, spherical lesions containing hepatocytes with minimal atypia and pronounced basophilia (Chang, Zdanowicz, and Murchelano 1998). In the liver proteome of rainbow trout from our study, we noted an increase in abundance in blood coagulation (Serping1) and regulation of reactive oxygen species processes (Bco2) and a decrease in abundance in apoptosis (Tpx2) and tumour suppression (Ptch1), along with over-represented disease pathways involved in neoplasms (Disease ID: MESH:D009369; MESH:D018204; MESH:D009371; MESH:D009386; MESH:D009372). This outlines the commencement of the deleterious effects of nickel occurring in the liver and corresponds with the negative effects of nickel recognized in the above studies. Additionally, we think that because we kept our concentrations environmentally relevant to the OROF region, the carcinogenic potential of nickel was not fully reached after the 30-day exposure, but that carcinogenesis could be realized if a more chronic exposure (months to years) were to occur.

4.5 Axial and neuron regulation in the kidney proteome

There are many studies that have demonstrated that damaged kidneys can have detrimental effects on the central nervous system in mammalian species (Tanaka and Okusa 2020; Beltran, Bixby, and Masters 2003; Liu et al. 2008), but the connection between the two has not been thoroughly investigated in fish (Stuermer et al. 1992; Cacialli et al. 2019). Nerve growth factor (NGF) is an active mediator in many essential functions in the central nervous system. A study of mice by Liu et al. (2008) demonstrated that brain changes (neuronal pyknosis and astrocyte activation) were specific to kidney injury and not observed during liver injury. It is possible that a similar effect occurred in our study,

as the kidney proteins significantly affected by the nickel treatment were related to many nervous system diseases, such as ataxia, brain diseases, central nervous system diseases, cerebellar diseases, dyskinesias, movement disorders, neurodegenerative diseases, and peripheral nervous system diseases. However, neurological effects were not observed during our study. Previous work by MSc Pajankar with the same fish did reveal a large number of proteins that were altered in abundance within the blood plasma and epidermal mucus were linked to neurological functions. A study on goldfish by Stuermer et al. (1992) indicated that the central nervous system is capable of regenerating axons due to the special properties of the neurons. Neurons in a fish's axial pathway contribute to successful axonal regeneration (Stuermer et al. 1992). Additionally, a study of mice by Beltran et al. (2003) measured mRNA expression in neuron populations with increased high-affinity nerve growth factor receptor (TrkA), indicating the involvement in differentiation and axonogenesis of central and peripheral nervous system neurons. NGF is the first neurotrophic factor implicated in acting as a target-derived signal from organs to promote terminal branching of sensory axons in the peripheral tissue of fish (Stuermer et al. 1992; Gibson and Ma 2011). In our current study, pathways affected by nickel treatment in the kidney were signaling by NGF (R-HSA-166520), NGF signaling via TrkA from plasma membrane (R-HSA-187037), and the neutrophin signaling pathway (hsa04722). Interestingly, the first two pathways mentioned are also found in the epidermal mucus and blood plasma proteomes of rainbow trout exposed to nickel.

4.5.1 Stress, behavioural changes, and the kidney proteome

Plexin-B2 (Plxnb2) was identified as a significantly affected protein in the kidney of our study, and it appears to be integral to the previously described pathways. Plexins are

a family of cell surface receptors with the biological function of binding to ligands in multiple organs and are known to modulate the brain and behaviour (Xuan et al. 2022; Jongbloets and Pasterkamp 2014; Simonetti et al. 2021). In the study by Xuan et al. (2022) on mice, Plxnb2 was identified as a key regulator in brain development processes including angiogenesis, axonal growth, differentiation of neurons, and synaptic formation. They showed that reducing Plxnb2 expression in the amygdala induced anxiety. Additionally, the study by Paldy et al. (2021) used *Plxnb2*-deficient mice to identify the protective role of Plxnb2 in stress regulation, as abnormal fear behaviour is a core-stress related symptom in many psychiatric disorders. A study by Perälä et al. (2010) on zebrafish with deleted *Plnxb2* indicated that there were no significant behavioural locomotion changes between the affected fish and the control fish containing *Plnxb2*. They concluded that due to a fundamental difference in the mechanisms of primary neurulation in mammal and teleost lineages, the molecular networks involved in neural tube formation in mice and zebrafish are not identical (Perälä et al. 2010). In comparison, a study by Lamont et al. (2009) on zebrafish determined that *PlxnB2* acts cell autonomously to control the timing of angioblast sprouting. The rainbow trout in our study exhibited a dose-dependent decrease in Plxnb2 abundance in the kidney, skin mucus, and blood plasma proteomes. There are obviously differences between mammals and teleosts, and there is a lack of information pertaining to plexins in fish behaviour studies. Extrapolating the information from all studies suggests that, while there may not be a change in aspects of brain formation, Plxnb2 has the potential to affect behaviours regarding stress. This is indicated in the various disease pathways explored in the kidney proteome, such as neurodegenerative diseases and neurodevelopmental disorders.

Additionally, the Gmr7 protein was identified as a significantly affected protein in the kidney of our study. Grm7 is a G-protein coupled receptor activated by glutamate that regulates axon outgrowth during neuronal development. Typically, the eight subtypes of metabotropic glutamate receptors are classified into three groups: group I, 1 and 5; group II, 2 and 3; and group III, 4, 6, 7, and 8 (Haug et al. 2013). Group III mGluR (also known as Grm), which contains Grm7, is negatively linked to adenyl cyclase and downregulates cyclic nucleotide synthesis in fish (Haug et al. 2013). In mammalian species, Grm7 is abundant in the hippocampus, amygdala, and locus coeruleus regions of the brain (Masugi et al. 1999; Mitsukawa et al. 2006). In a study by Masugi et al. (1999) on mice lacking Grm7, mice displayed a lack of fear response and conditioned taste aversions, although there were no alterations in locomotion or pain sensitivity. They indicated that due to these two distinct behavioural paradigms, Grm7 is critical to the amygdala function of mice (Masugi et al. 1999). This is confirmed in the study by Mitsukawa et al. (2006), as they demonstrated that Grm7 is integral to the stress response of mice to aversive stimuli. This study identified an altered corticosteroid level and feedback regulation in mice lacking Grm7, suggesting Grm7 may modulate an increase in stress hormones (Mitsukawa et al. 2006). Furthermore, a study on zebrafish by Haug et al. (2012) determined functional conservation of the metabotropic glutamate receptors (Grm or mGluR) between zebrafish and mammals and that the equivalent genes in zebrafish are known to be expressed in corresponding brain regions of mammals. The rainbow trout in our study exhibited a dose-dependent increase in Grm7 abundance in the kidney and an increase in Grm4 and Grm8 in skin mucus and blood plasma proteomes. While the proteins themselves represent a different subtype of metabotropic glutamate receptors, all three Grm (or mGluR) are

classified together in group III. There are obviously differences between mammals and teleosts, and there is a lack of information pertaining to metabotropic glutamate receptors in fish behaviour studies. Combining the information from the presented studies suggests that the protein Gmr7 may have the potential to affect behaviour regarding stress. This is indicated in various diseases explored in the kidney proteome, such as neurodegenerative diseases and neurodevelopmental disorders. Taking a snapshot of these two proteins that changed abundance in rainbow trout due to nickel exposure shows how stress is beginning to affect the fish, potentially indicating behavioural changes. At higher concentrations of waterborne nickel, Plxnb2 decreases and Grm7 increases in abundance in the kidney proteome. Further studies observing any changes in behaviour and targeted proteomic analysis of brain tissue of rainbow trout exposed to nickel would be required to confirm these observations from the kidney, mucus, and plasma. rainbow trout exposed to nickel

4.6 Kidney and associated diseases

As previously stated in the genotoxicity of nickel section, we observed the over-representation of disease pathways involved in neoplasms in both the kidney and liver. We also observed many diseases specific to the kidney organ itself and the overall health of the fish. For instance, we observed the over-representation of the disease pathway involved in kidney disease (MESH:D014570) and kidney cancer (MESH:D014571) in addition to liver disease (MESH:D008107) and liver cancer (MESH:D008113), all within the kidney proteome. In the kidney proteome, we observed an increased abundance in DNA repair and cell growth (Atm), tumour transformations and survival of malignant cells (Igf1r), T-cell proliferation and survival (Cd28), and tumour suppression through induction of growth arrest or apoptosis (Tp53). In the study by Borja et al. (2023) on human participants, they

determined the shared functional pathway between ATM and TP53 and showed that DNA damage creates selection pressure for the inactivation of the gene (*p53*) responsible for controlling cell division and cell death, which can be lost through the loss of serine-protein kinase (ATM). Therefore, in our study, the increased abundance of both Atm and Tp53 indicates the potential for the same functional pathway outlined in humans as seen in our rainbow trout. In our study, the increase in abundance in DNA repair and cell growth (Atm) would also indicate an increase in tumour suppression through the induction of growth arrest or apoptosis (Tp53) (Borja et al. 2023). In a study by Gonzalez-Fernandez et al. (2021) on European seabass (*Dicentrarchus labrax*), Cd28 was significantly decreased in the kidney after infection with nodavirus. They determined that Cd28 modulates the metabolic process, which regulates specific pro-inflammatory T-cell responses in fish (González-Fernández, Esteban, and Cuesta 2021). Thus, infection causes decreased transcription of Cd28 as the infection progresses, resulting in T-cell stimulation, followed by an inhibitory state to control and limit the immune response and homeostasis in fish upon infection (González-Fernández, Esteban, and Cuesta 2021). While we cannot draw exact parallels to our study as we investigated metal contamination, it is interesting to observe an increase in Cd28 in response to nickel. Simultaneously, we observed a decrease in the abundance of the antioxidant enzyme (Cat), inhibition of apoptosis (Cryab), quality-control assessment of glycoprotein folding (Ganab), ATP-dependent carboxylation of pyruvate (Pc), and a solute transporter that mediates electroneutral anion exchange (Slc4a1). A study by Hfaiedh et al. (2008) on rats injected with $NiCl_2$ demonstrated that low concentrations of Ni induced adverse effects as it rapidly diffused in all organs and induced oxidative stress. They determined that catalase (Cat) activity was transiently

increased at the beginning of exposure in the kidney and liver, suggesting that Ni leads to H_2O_2 accumulation in those organs (Hfaiedh et al. 2008). However, they observed a decrease in Cat activity in those organs throughout their 10-day experiment, indicating the inhibition of Cat activity is due to H_2O_2 accumulation and lipoperoxidation (Hfaiedh et al. 2008). These results were confirmed in the study by Topal et al. (2017), as rainbow trout exposed to 2 to 5.7 mg/L Ni (~ 2000-5700 ppb) experienced a significant decrease in Cat activity and tubular degeneration in kidney tissues. In our study using environmental Ni concentrations, we observed a decrease in Cat abundance in the kidney tissue. Research has indicated that the protein CRYAB is highly expressed in breast cancer, neck cancer, and kidney cancer in humans (Shi et al. 2017). The study by Shi et al. (2017) showed that Cryab in mice regulated cell cycle transition and proliferation and regulated tumour angiogenesis, invasion, and metastasis via vascular endothelial growth factor. The downregulation of Cryab expression induced apoptosis and increased the expression of the epithelial marker E-cadherin (Shi et al. 2017). As our study saw a decrease in Cryab abundance in the kidney proteome, this could indicate increased apoptosis as well as an increase in expression of cadherin, as shown in the increased abundance of Cdh5 in the kidney proteome and Cdhr1, Cdhr5, and Cdh18 in the plasma proteome. Research suggests that in mammals, there are two variants of the anion exchanger Slc4a1, each expressed in the red blood cells and in the kidney, respectively. Research by Treppiccione et al. (2017) using knockout mice determined that the lack of Slc4a1 caused impairment of renal function and hemolytic anemia. As our study saw the commencement of decreased kidney Slc4a1 abundance, we propose that high concentrations of nickel may cause renal impairment and hemolytic anemia with further decreased abundance in the protein

expression. Further targeted protein studies using higher concentrations of nickel are required to confirm this hypothesis. Extrapolating the information from these other studies suggests that the change in protein abundances are to be expected in rainbow trout when exposed to a metal contaminant. The beginning of the deleterious effects that we observed due to nickel corresponds to changes in protein abundances that have been proven to directly affect kidney and liver diseases. This is indicated by the various disease pathways explored in the kidney proteome that share key identified proteins.

Similarly, we observed hematologic diseases (MESH:D006402) and skin diseases (MESH:D012871) in the kidney proteome. In the kidney proteome, we observed an increase in abundance of the ability to process several types of procollagen proteins (Adamts2), receptor on antigen-presenting cells of the immune system (Cd40), DNA methylation (Dnmt1), DNA repair (Ercc4), and a decrease in abundance of biogenesis associated with melanosomes, platelet dense granules, and lysosomes (Hps6), and catalyzation leading to cholesterol biosynthesis (Lbr). A study by Dupont et al. (2018) on mice exemplified that the inhibition of Adamts2 activity leads to connective tissue disorders, inflammation, and angiogenesis as potential substrates of Adamts2, which are factors of innate immunity that contain a collagen domain. They demonstrated that Adamts2 participates in the regulation of the activation of the immune system and has a significant role in collagen maturation and matrix biology in mice (Dupont et al. 2018). In our study, the increased abundance of Adamts2 in the kidney proteome could indicate that Adamts2 reduces endothelial cell proliferation and has angiogenic and anti-tumour molecular functions. A study on humphead snapper (*Lutjanus sanguineus*) demonstrated that high expression levels of Cd40 in immune-related organs implied that Cd40 is involved

in various immune processes in response to infection (Cai et al. 2017). In our study, the increased abundance of Cd40 could suggest an increase in Cd40 signaling leading to the production of cytokines in the kidney as an immune response to Ni exposure. A study by Ji et al. (2006) on human bronchial epithelial cells exposed to Ni_3S_2 led to the upregulation of DNMT1 expression. Our study also saw a slightly increased abundance of Dnmt1 in the kidney proteome due to Ni exposure. This Ni-induced increase in DNA methylation is in support of the study by Lee, Broday, and Costa (1998) that demonstrates an increase in DNA methylation in chronic soluble ($NiCl_2$) and insoluble (Ni_3S_2) nickel experiments on mice. A study by Tsai et al. (2016) demonstrated that LBR is the major sterol reductase required for cholesterol synthesis in human cells. A study by Toman et al. (2013) demonstrated that the dose of 100 mg/L Ni in drinking water caused a decrease in blood cholesterol in rats, as Ni displayed dysregulation in pathways involving lipid and cholesterol metabolism. Additionally, this study also found that Ni has the capability to cause renal dysfunction and influence enzymatic activities to impact liver function (Toman et al. 2013). The significant decrease in Lbr abundance in our study could suggest that Ni is impacting the biosynthesis of cholesterol and that Ni is impacting renal function, as demonstrated by the studies described above. Further targeted protein studies using higher concentrations of nickel are required to confirm this observation. These results are interesting because the changes in the kidney proteome also reflect changes observed in blood and skin mucus, along with many other changes throughout the body, including neurological and hepatic function. This is indicated by the various disease pathways explored in the kidney proteome that share key identified proteins.

4.7 Organ proteome and biofluid proteome

Biofluid sampling offers a non-lethal and non-invasive method of collection, which is valuable for proteomics. In recent years, blood plasma and epidermal mucus have become more desirable sampling techniques compared to traditional methods that involved the sacrifice of fish to sample and study their organs. As the blood plasma is a dynamic matrix and transports proteins from the whole organism, it is highly informative and suitable for proteomic analysis. Skin mucus is a dynamic and semipermeable barrier on the external surface of fish skin that plays an important role as a protective barrier. Both blood plasma and skin mucus provide a wealth of information about the health status of fish. A comparison between the organ proteome and the biofluid proteome provided valuable information pertaining to the relevance of biofluid proteomes in relation to traditional sampling methods.

In the kidney and mucus proteomes, we observed the over-representation of transcriptional misregulation-in-cancer (hsa05202) as an affected pathway of nickel treatment. This pathway is described as the amplification, deletion, rearrangement via chromosomal translocation, and inversion of genes encoding transcription factors (TFs) or subjection to point mutations that result in a gain or loss of function (www.genome.jp/entry/hsa05202). Twenty-one over-represented cancer-related diseases that represent this misregulation-in-cancer pathway were found in the kidney proteome to be affected by nickel treatment. In comparison, nine over-represented cancer related diseases were found in the liver proteome, 38 over-represented cancer-related diseases were found in the mucus proteome, and 54 over-represented cancer-related diseases were found in the plasma proteome to be affected by nickel treatment. This prominently shows

that biofluids are more sensitive to overall health changes in fish when compared to organ tissue proteomes. The CTDbase has limitations in the representation of affected pathways, as the transcriptional misregulation-in-cancer pathway was not represented in the significantly affected proteins from the plasma proteome, although it contains many proteins and biological functions suggesting the depiction of this pathway. Comparably, non-lethal approaches in rainbow trout and other fish species reported useful protein identification results in blood plasma and skin mucus (Morro et al. 2020; Nynca et al. 2017). The findings of the previous student in our lab, Nancy Tannouri's MSc (2021) research, identified a reliable rainbow trout blood plasma proteome and recognized proteins from a variety of functions and target tissues, in furtherance of Morro et al. (2020). Additionally, a study by Nynca et al. (2017) determined a substantial overlap in the composition of major proteins in the blood plasma proteome of carp and rainbow trout, indicating the protective mechanisms in teleost fish are well conserved. Due to the integral role of blood in the transport of molecules to and from tissues, the use of non-lethal plasma collection is vital to future ecotoxicological studies. Biofluids are highly informative and can be used to obtain an overview of the overall physiological state of the fish.

In the kidney and plasma proteomes, we observed the over-representation of the pathway apoptosis (hsa04210) affected by our waterborne nickel treatment. Cell apoptosis is a normal process of programmed cell death to maintain tissue homeostasis. A large decrease in apoptosis can cause several diseases, such as cancer and autoimmune diseases; however, an excessive increase in apoptosis is responsible for various neurodegenerative diseases. The research by Zheng et al. (2014) on goldfish exposed to Ni identified increased expression levels of phosphorylated Jun N-terminal kinases (JNK) in the liver, which

activated pro-apoptotic signaling events. The study determined that JNK activation has an important role in stimulating apoptotic signaling pathways in fish through the stimulation of pro-apoptotic protein Bax activities and the inhibition of the anti-apoptotic protein Bcl2 to regulate the release of cytochrome c and apoptosis (Zheng et al. 2014). In our study, we observed an increase in the Bax protein in plasma, suggesting that an increase in apoptosis is possible. While we did not find an over-representation of the apoptosis pathway in the liver proteome, we did see an over-representation of the hemostasis pathway (R-HSA-109582). This lack of over-represented apoptosis pathway in the liver could be due to the low-level Ni concentrations used in our study. Our study identified hemostasis as an affected pathway of nickel treatment in the liver, mucus, and plasma proteome. Hemostasis is the process that causes the cessation of bleeding from a blood vessel. A downstream target for JNK signaling in apoptosis is the caspase pathway, as caspase-3 (Casp3) degrades key proteins in apoptosis (Shlevkov and Morata 2012). The study by Zheng et al. (2014) also identified activation of Casp3 due to Ni exposure. In our study, we did not identify Casp3 as a significantly affected protein but did identify Casp8, which activates Casp3 by proteolytic cleavage (Zeng et al. 2021). This suggests that the caspase pathway could possibly be activated within our study parameters with longer exposure times, but further studies would need to be completed. In goldfish, nickel exhibits cytotoxicity in fish livers by inducing apoptosis, and in addition, oxidative stress, Casp3, and Bcl2/Bax are confirmed to play important roles in Ni-induced apoptosis (Zheng et al. 2014). Our research supports the initiation of the adverse outcomes reported by Zheng et al. (2014), and thus these outcomes could also occur in rainbow trout at the lower concentrations of Ni used in our study and can be detected using the plasma proteome alone.

Chapter 5. Conclusion

Nickel is a common component of natural freshwater that may pose serious ecological risks to aquatic wildlife. Due to Canada's significant presence in exporting and producing nickel, the potential for more nickel contamination of aquatic watersheds is possible. Being the largest nickel producer, the province of Ontario has the most opportunity to negatively impact aquatic watersheds and the surrounding environment. Nickel is economically important due to its capability to resist corrosion, with increasing commercial demand for the production of rechargeable batteries and hybrid vehicle batteries. As large-scale mining production in the OROF region has yet to commence, it is vital to understand how nickel contamination affects the surrounding wildlife. In recent years, there has been strong evidence for the genotoxic, neurological, immunotoxic, and carcinogenic effects of nickel on freshwater fish.

In our study, we subjected adult rainbow trout to environmentally relevant concentrations of nickel that were much lower than those previously studied. We demonstrated that at these low concentrations, the rainbow trout kidney proteome is sensitive to nickel exposure; however, the skin mucus and blood plasma proteomes are significantly more sensitive to nickel exposure. A number of the differentially expressed proteins in the organ tissues were represented in the biofluids of the fish. Similarly, the affected biological processes and molecular functions were statistically consistent between the organs' proteomes and the biofluids' proteomes, indicating that the biofluids are capable of representing the affected processes within the fish tissues. Many of the specific responses identified do not necessarily indicate toxicity, as higher-level impacts like genotoxicity or carcinogenicity were not observed. However, the responses in the organs'

and biofluids' proteomes provide insight into the mechanisms involved in acclimating to low levels of waterborne nickel. Overall, the information provided by the organs' and biofluids' proteomes indicates early signs of nickel exposure at concentrations that begin to accumulate in the kidney tissue and blood plasma. The findings of our study, in furtherance of Urvi Pajankar's research, support what is known by expanding on current knowledge and suggesting new avenues of research to corroborate other findings. Targeted studies are required to confirm some of the observed protein changes and fill in the knowledge gaps surrounding the mechanism of nickel toxicity in fish.

We also demonstrated that the non-lethal and non-invasive biofluid sampling collection provides a wealth of information about the health status of fish, especially at environmentally relevant low concentrations of contaminants. The use of organ tissue collection is not necessary in biomonitoring as the proteins in blood plasma and skin mucus provide more information regarding the overall health of the fish. Given the non-lethal and non-invasive nature of blood and mucus sampling, environmental effects monitoring would greatly benefit from the use of blood plasma and epidermal mucus in place of lethal tissue sampling. Further environmental monitoring programs should continue to use the lower range of the Canadian Water Quality Guideline of 25 μg/L (~ 25 ppb) nickel, as it is likely a protective level to maintain the health of larger aquatic wildlife such as rainbow trout. Early detection and prediction of metal toxicity through the use of non-lethal sampling is an essential safeguard for protecting aquatic ecosystems, ensuring fish vitality, and guaranteeing public safety.

REFERENCES

Agrawal, Shanker J, Anil K Srivastava, and H S Chaudhry. 1979. “Haematological Effects of Nickel Toxicity on a Fresh Water Teleost, Colisa Fasciatus.” *Acta Pharmacologica et Toxicologica* 45 (3): 215–17.

Alsop, Derek, and Chris M Wood. 2011. “Metal Uptake and Acute Toxicity in Zebrafish: Common Mechanisms across Multiple Metals.” *Aquatic Toxicology* 105 (3–4): 385–93.

Apweiler, Rolf, Amos Bairoch, Cathy H Wu, Winona C Barker, Brigitte Boeckmann, Serenella Ferro, Elisabeth Gasteiger, Hongzhan Huang, Rodrigo Lopez, and Michele Magrane. 2004. “UniProt: The Universal Protein Knowledgebase.” *Nucleic Acids Research* 32 (suppl_1): D115–19.

Athikesavan, S, S Vincent, T Ambrose, and B Velmurugan. 2006. “Nickel Induced Histopathological Changes in the Different Tissues of Freshwater Fish, Hypophthalmichthys Molitrix(Valenciennes).” *Journal of Environmental Biology* 37 (2): 391–95.

Barceloux, Donald G, and Donald Barceloux. 1999. “Nickel.” *Journal of Toxicology: Clinical Toxicology* 37 (2): 239–58.

Basketter, David A, Gianni Angelini, Arieh Ingber, Petra S Kern, and Torkil Menné. 2003. “Nickel, Chromium and Cobalt in Consumer Products: Revisiting Safe Levels in the New Millennium.” *Contact Dermatitis* 49 (1): 1–7.

Beltran, Pedro J, John L Bixby, and Brian A Masters. 2003. “Expression of PTPRO during Mouse Development Suggests Involvement in Axonogenesis and Differentiation of NT-3 and NGF-dependent Neurons.” *Journal of Comparative Neurology* 456 (4): 384–95.

Binet, Monique T, Merrin S Adams, Francesca Gissi, Lisa A Golding, Christian E Schlekat, Emily R Garman, Graham Merrington, and Jennifer L Stauber. 2018. “Toxicity of Nickel to Tropical Freshwater and Sediment Biota: A Critical Literature Review and Gap Analysis.” *Environmental Toxicology and Chemistry* 37 (2): 293–317.

Blaylock, B G, and M L Frank. 1979. “Comparison of the Toxicity of Nickel to the Developing Eggs and Larvae of Carp (Cyprinus Carpio).” *Bull. Environ. Contam. Toxicol.;(United States)* 21.

Blewett, Tamzin A, and Erin M Leonard. 2017. “Mechanisms of Nickel Toxicity to Fish and Invertebrates in Marine and Estuarine Waters.” *Environmental Pollution* 223: 311–22.

Borja, Nicholas A, Rachel Silva-Smith, Marilyn Huang, Dipen J Parekh, Daniel Sussman, and Mustafa Tekin. 2023. “Atypical ATMs: Broadening the Phenotypic Spectrum of ATM-Associated Hereditary Cancer.” *Frontiers in Oncology* 13: 1068110.

Cacialli, Pietro, Claudia Gatta, Livia d'Angelo, Adele Leggieri, Antonio Palladino, Paolo de Girolamo, Elisabeth Pellegrini, and Carla Lucini. 2019. "Nerve Growth Factor Is Expressed and Stored in Central Neurons of Adult Zebrafish." *Journal of Anatomy* 235 (1): 167–79.

Cai, Jia, Yunxia Fan, Hongli Xia, Yishan Lu, Jichang Jian, and Zaohe Wu. 2017. "Identification and Characterization of CD40 from Humphead Snapper (Lutjanus Sanguineus)." *Fish & Shellfish Immunology* 70: 665–72.

Chang, Sukwoo, V S Zdanowicz, and R A Murchelano. 1998. "Associations between Liver Lesions in Winter Flounder (Pleuronectes Americanus) and Sediment Chemical Contaminants from North-East United States Estuaries." *ICES Journal of Marine Science* 55 (5): 954–69.

Chau, Y K, and O T R Kulikovsky-Cordeiro. 1995. "Occurrence of Nickel in the Canadian Environment." *Environmental Reviews* 3 (1): 95–120.

Chowdhury, M Jasim, Carol Bucking, and Chris M Wood. 2008. "Pre-Exposure to Waterborne Nickel Downregulates Gastrointestinal Nickel Uptake in Rainbow Trout: Indirect Evidence for Nickel Essentiality." *Environmental Science & Technology* 42 (4): 1359–64.

Consortium, UniProt. 2018. "UniProt: The Universal Protein Knowledgebase." *Nucleic Acids Research* 46 (5): 2699.

Couture, Patrice, and Greg Pyle. 2011. "Field Studies on Metal Accumulation and Effects in Fish." In *Fish Physiology*, 31:417–73. Elsevier.

Covey, Thomas R, Edgar D Lee, Andries P Bruins, and Jack D Henion. 1986. "Liquid Chromatography/Mass Spectrometry." *Analytical Chemistry* 58 (14): 1451A-1461A.

Dargie, Greta C, Simon L Lewis, Ian T Lawson, Edward T A Mitchard, Susan E Page, Yannick E Bocko, and Suspense A Ifo. 2017. "Age, Extent and Carbon Storage of the Central Congo Basin Peatland Complex." *Nature* 542 (7639): 86–90.

Dave, Göran, and Ruiqin Xiu. 1991. "Toxicity of Mercury, Copper, Nickel, Lead, and Cobalt to Embryos and Larvae of Zebrafish, Brachydanio Rerio." *Archives of Environmental Contamination and Toxicology* 21: 126–34.

Denkhaus, E, and K Salnikow. 2002. "Nickel Essentiality, Toxicity, and Carcinogenicity." *Critical Reviews in Oncology/Hematology* 42 (1): 35–56.

Dise, Nancy B. 2009. "Peatland Response to Global Change." *Science* 326 (5954): 810–11.

Dixit, Sushil S, Aruna S Dixit, and John P Smol. 1992. "Assessment of Changes in Lake Water Chemistry in Sudbury Area Lakes since Preindustrial Times." *Canadian Journal of Fisheries and Aquatic Sciences* 49 (S1): 8–16.

Driessnack, Melissa K, Ankur Jamwal, and Som Niyogi. 2017. "Effects of Chronic Exposure to Waterborne Copper and Nickel in Binary Mixture on Tissue-Specific Metal Accumulation and Reproduction in Fathead Minnow (Pimephales Promelas)."

Chemosphere 185: 964–74.

Dupont, Laura, Gregory Ehx, Mathilde Chantry, Christine Monseur, Cédric Leduc, Lauriane Janssen, Didier Cataldo, Marc Thiry, Christine Jerome, and J-M Thomassin. 2018. "Spontaneous Atopic Dermatitis Due to Immune Dysregulation in Mice Lacking Adamts2 and 14." *Matrix Biology* 70: 140–57.

Eisler, Ronald. 1998. *Nickel Hazards to Fish, Wildlife, and Invertebrates: A Synoptic Review*. US Department of the Interior, US Geological Survey, Patuxent Wildlife ….

Fraser, Jake, J Anderson, J Lazuen, Y Lu, O Heathman, N Brewster, J Bedder, and O Masson. 2021. "Study on Future Demand and Supply Security of Nickel for Electric Vehicle Batteries." *Publication Office of the European Union: Luxembourg*.

Gandar, Allison, Pascal Laffaille, Nathalie Marty-Gasset, Didier Viala, Caroline Molette, and Séverine Jean. 2017. "Proteome Response of Fish under Multiple Stress Exposure: Effects of Pesticide Mixtures and Temperature Increase." *Aquatic Toxicology* 184: 61–77.

Garai, P, P Banerjee, P Mondal, and N C Saha. 2021. "Effect of Heavy Metals on Fishes: Toxicity and Bioaccumulation." *J Clin Toxicol. S* 18.

Gibson, Daniel A, and Le Ma. 2011. "Developmental Regulation of Axon Branching in the Vertebrate Nervous System." *Development* 138 (2): 183–95.

González-Fernández, Carmen, María A Esteban, and Alberto Cuesta. 2021. "Molecular Characterization of the T Cell Costimulatory Receptors CD28 and CTLA4 in the European Sea Bass." *Fish & Shellfish Immunology* 109: 106–15.

Grande, M, and S Andersen. 1983. "Lethal Effects of Hexavalent Chromium, Lead and Nickel on Young Stages of Atlantic Salmon (Salmo Salar L.) in Soft Water." *Vatten (Sweden)*.

Hardy, Ronald W. 2002. "Rainbow Trout, Oncorhynchus Mykiss." *Nutrient Requirements and Feeding of Finfish for Aquaculture*, 184–202.

Haug, Marion F, Matthias Gesemann, Thomas Mueller, and Stephan C F Neuhauss. 2013. "Phylogeny and Expression Divergence of Metabotropic Glutamate Receptor Genes in the Brain of Zebrafish (Danio Rerio)." *Journal of Comparative Neurology* 521 (7): 1533–60.

Hausinger, Robert P. 2013. *Biochemistry of Nickel*. Vol. 12. Springer Science & Business Media.

Hfaiedh, N, M S Allagui, Serge Carreau, L Zourgui, A Feki, and F Croute. 2008. "Impact of Dietary Restriction on Peroxidative Effects of Nickel Chloride in Wistar Rats." *Toxicology Mechanisms and Methods* 18 (7): 597–603.

Hoang, Tham Chung, Joseph R Tomasso, and Stephen J Klaine. 2004. "Influence of Water Quality and Age on Nickel Toxicity to Fathead Minnows (Pimephales Promelas)." *Environmental Toxicology and Chemistry: An International Journal* 23

(1): 86–92.

Hunt, John W, Brian S Anderson, Bryn M Phillips, Ron S Tjeerdema, H Max Puckett, Mark Stephenson, David W Tucker, and Daniel Watson. 2002. “Acute and Chronic Toxicity of Nickel to Marine Organisms: Implications for Water Quality Criteria.” *Environmental Toxicology and Chemistry: An International Journal* 21 (11): 2423–30.

Javed, Muhammad. 2012. “Effects of Zinc and Lead Toxicity on the Growth and Their Bioaccumulation in Fish.” *Pak. Vet. J* 32 (3): 357–62.

———. 2013. “Chronic Effects of Nickel and Cobalt on Fish Growth.” *International Journal of Agriculture and Biology* 15 (3).

Jongbloets, Bart C, and R Jeroen Pasterkamp. 2014. “Semaphorin Signalling during Development.” *Development* 141 (17): 3292–97.

Kubrak, Olga I, Viktor V Husak, Bohdana M Rovenko, Harald Poigner, Maria A Mazepa, Michael Kriews, Doris Abele, and Volodymyr I Lushchak. 2012. “Tissue Specificity in Nickel Uptake and Induction of Oxidative Stress in Kidney and Spleen of Goldfish Carassius Auratus, Exposed to Waterborne Nickel.” *Aquatic Toxicology* 118: 88–96.

Kubrak, Olga I, Harald Poigner, Viktor V Husak, Bohdana M Rovenko, Stefanie Meyer, Doris Abele, and Volodymyr I Lushchak. 2014. “Goldfish Brain and Heart Are Well Protected from Ni2+-Induced Oxidative Stress.” *Comparative Biochemistry and Physiology Part C: Toxicology & Pharmacology* 162: 43–50.

Liang, Xuefang, Christopher J Martyniuk, and Denina B D Simmons. 2020. “Are We Forgetting the ‘Proteomics’ in Multi-Omics Ecotoxicology?” *Comparative Biochemistry and Physiology Part D: Genomics and Proteomics* 36: 100751.

Liu, Manchang, Yideng Liang, Srinivasulu Chigurupati, Justin D Lathia, Mikhail Pletnikov, Zhaoli Sun, Michael Crow, Christopher A Ross, Mark P Mattson, and Hamid Rabb. 2008. “Acute Kidney Injury Leads to Inflammation and Functional Changes in the Brain.” *Journal of the American Society of Nephrology* 19 (7): 1360–70.

Malins, Donald C, Bruce B McCain, Mark S Myers, Donald W Brown, Margaret M Krahn, W T Roubal, Michael H Schiewe, John T Landahl, and Sin Lam Chan. 1987. “Field and Laboratory Studies of the Etiology of Liver Neoplasms in Marine Fish from Puget Sound.” *Environmental Health Perspectives* 71: 5–16.

Masugi, Miwako, Mineto Yokoi, Ryuichi Shigemoto, Keiko Muguruma, Yasuyoshi Watanabe, Gilles Sansig, Herman Van Der Putten, and Shigetada Nakanishi. 1999. “Metabotropic Glutamate Receptor Subtype 7 Ablation Causes Deficit in Fear Response and Conditioned Taste Aversion.” *Journal of Neuroscience* 19 (3): 955–63.

McLaren, B A, E Keller, D J O’donnell, and C A Elvehjem. 1947. “The Nutrition of Rainbow Trout. 2. Further Studies with Purified Rations.” *Arch. Biochem.* 15: 179–

85.

Meyer, Joseph S, Robert C Santore, Joe P Bobbitt, Larry D Debrey, Connie J Boese, Paul R Paquin, Herbert E Allen, Harold L Bergman, and Dominic M Ditoro. 1999. "Binding of Nickel and Copper to Fish Gills Predicts Toxicity When Water Hardness Varies, but Free-Ion Activity Does Not." *Environmental Science & Technology* 33 (6): 913–16.

Min, Eun Young, Jun-Hwan Kim, Jung Sick Lee, and Ju-Chan Kang. 2021. "Nickel Bioaccumulation and the Antioxidant Response in Pacific Abalone Haliotis Discus Hannai, Ino 1953 Exposed to Waterborne Nickel during Thermal Stress." *Aquaculture Reports* 20: 100726.

Mitsukawa, Kayo, Cedric Mombereau, Erika Lötscher, Doncho P Uzunov, Herman van der Putten, Peter J Flor, and John F Cryan. 2006. "Metabotropic Glutamate Receptor Subtype 7 Ablation Causes Dysregulation of the HPA Axis and Increases Hippocampal BDNF Protein Levels: Implications for Stress-Related Psychiatric Disorders." *Neuropsychopharmacology* 31 (6): 1112–22.

Morro, Bernat, Mary K Doherty, Pablo Balseiro, Sigurd O Handeland, Simon MacKenzie, Harald Sveier, and Amaya Albalat. 2020. "Plasma Proteome Profiling of Freshwater and Seawater Life Stages of Rainbow Trout (Oncorhynchus Mykiss)." *Plos One* 15 (1): e0227003.

Mustafiz, Ananda, Ajit Ghosh, Amit K Tripathi, Charanpreet Kaur, Akshay K Ganguly, Neel S Bhavesh, Jayant K Tripathi, Ashwani Pareek, Sudhir K Sopory, and Sneh L Singla-Pareek. 2014. "A Unique N I2+-dependent and Methylglyoxal-inducible Rice Glyoxalase I Possesses a Single Active Site and Functions in Abiotic Stress Response." *The Plant Journal* 78 (6): 951–63.

Nash, Philip. 1986. "The Cr− Ni (Chromium-Nickel) System." *Bulletin of Alloy Phase Diagrams* 7 (5): 466–76.

Nynca, Joanna, Georg Arnold, Thomas Fröhlich, and Andrzej Ciereszko. 2017. "Proteomic Identification of Rainbow Trout Blood Plasma Proteins and Their Relationship to Seminal Plasma Proteins." *Proteomics* 17 (11): 1600460.

Oliveira-Filho, Eduardo Cyrino, Daphne Heloisa de Freitas Muniz, Maria Fernanda Nince Ferreira, and Cesar Koppe Grisolia. 2010. "Evaluation of Acute Toxicity, Cytotoxicity and Genotoxicity of a Nickel Mining Waste to Oreochromis Niloticus." *Bulletin of Environmental Contamination and Toxicology* 85: 467–71.

Organization, World Health. 2021. "Nickel in Drinking Water: Background Document for Development of WHO Guidelines for Drinking-Water Quality." World Health Organization.

Palermo, Francine F, Wagner E Risso, Juliana D Simonato, and Claudia B R Martinez. 2015. "Bioaccumulation of Nickel and Its Biochemical and Genotoxic Effects on Juveniles of the Neotropical Fish Prochilodus Lineatus." *Ecotoxicology and Environmental Safety* 116: 19–28.

Pandit, Dina Nath, and M L Gupta. 2019. “Heapto-Somatic Index, Gonado-Somatic Index and Condition Factor of Anabas Testudineus as Bio-Monitoring Tools of Nickel and Chromium Toxicity.” *International Journal of Innovations in Engineering and Technology* 12 (3): 25–28.

Pane, E F, J G Richards, and C M Wood. 2003. “Acute Waterborne Nickel Toxicity in the Rainbow Trout (Oncorhynchus Mykiss) Occurs by a Respiratory Rather than Ionoregulatory Mechanism.” *Aquatic Toxicology* 63 (1): 65–82.

Pane, Eric F, Carol Bucking, Monika Patel, and Chris M Wood. 2005. “Renal Function in the Freshwater Rainbow Trout (Oncorhynchus Mykiss) Following Acute and Prolonged Exposure to Waterborne Nickel.” *Aquatic Toxicology* 72 (1–2): 119–33.

Pane, Eric F, Aziz Haque, and Chris M Wood. 2004. “Mechanistic Analysis of Acute, Ni-Induced Respiratory Toxicity in the Rainbow Trout (Oncorhynchus Mykiss): An Exclusively Branchial Phenomenon.” *Aquatic Toxicology* 69 (1): 11–24.

Paul, Nilantika, Samujjwal Chakraborty, and Mahuya Sengupta. 2014. “Lead Toxicity on Non-Specific Immune Mechanisms of Freshwater Fish Channa Punctatus.” *Aquatic Toxicology* 152: 105–12.

Perälä, Nina, Nina Peitsaro, Maria Sundvik, Henri Koivula, Kirsi Sainio, Hannu Sariola, Pertti Panula, and Tiina Immonen. 2010. “Conservation, Expression, and Knockdown of Zebrafish Plxnb2a and Plxnb2b.” *Developmental Dynamics* 239 (10): 2722–34.

Pickering, Quentin H. 1974. “Chronic Toxicity of Nickel to the Fathead Minnow.” *Journal (Water Pollution Control Federation)*, 760–65.

Pino, Lindsay K, Brian C Searle, James G Bollinger, Brook Nunn, Brendan MacLean, and Michael J MacCoss. 2020. “The Skyline Ecosystem: Informatics for Quantitative Mass Spectrometry Proteomics.” *Mass Spectrometry Reviews* 39 (3): 229–44.

Poonkothai, MVBS, and B Shyamala Vijayavathi. 2012. “Nickel as an Essential Element and a Toxicant.” *International Journal of Environmental Sciences* 1 (4): 285–88.

Preston, Michael D, Kurt A Smemo, James W McLaughlin, and Nathan Basiliko. 2012. “Peatland Microbial Communities and Decomposition Processes in the James Bay Lowlands, Canada.” *Frontiers in Microbiology* 3: 70.

Ptashynski, M D, and J F Klaverkamp. 2002. “Accumulation and Distribution of Dietary Nickel in Lake Whitefish (Coregonus Clupeaformis).” *Aquatic Toxicology* 58 (3–4): 249–64.

Ptashynski, M D, R M Pedlar, R E Evans, C L Baron, and J F Klaverkamp. 2002. “Toxicology of Dietary Nickel in Lake Whitefish (Coregonus Clupeaformis).” *Aquatic Toxicology* 58 (3–4): 229–47.

Ptashynski, M D, R M Pedlar, R E Evans, K G Wautier, C L Baron, and J F Klaverkamp. 2001. “Accumulation, Distribution and Toxicology of Dietary Nickel in Lake Whitefish (Coregonus Clupeaformis) and Lake Trout (Salvelinus Namaycush).”

Comparative Biochemistry and Physiology Part C: Toxicology & Pharmacology 130 (2): 145–62.

Rogers, J T, J G Richards, and C M Wood. 2003. "Ionoregulatory Disruption as the Acute Toxic Mechanism for Lead in the Rainbow Trout (Oncorhynchus Mykiss)." *Aquatic Toxicology* 64 (2): 215–34.

Seregin, IVy, and A D Kozhevnikova. 2006. "Physiological Role of Nickel and Its Toxic Effects on Higher Plants." *Russian Journal of Plant Physiology* 53 (2): 257–77.

Shahzad, Babar, Mohsin Tanveer, Abdul Rehman, Sardar Alam Cheema, Shah Fahad, Shamsur Rehman, and Anket Sharma. 2018. "Nickel; Whether Toxic or Essential for Plants and Environment-A Review." *Plant Physiology and Biochemistry* 132: 641–51.

Shi, Chuanbing, Xiaojun Yang, Xiaodong Bu, Ning Hou, and Pingsheng Chen. 2017. "Alpha B-Crystallin Promotes the Invasion and Metastasis of Colorectal Cancer via Epithelial-Mesenchymal Transition." *Biochemical and Biophysical Research Communications* 489 (4): 369–74.

Shlevkov, Evgeny, and Ginés Morata. 2012. "A Dp53/JNK-Dependant Feedback Amplification Loop Is Essential for the Apoptotic Response to Stress in Drosophila." *Cell Death & Differentiation* 19 (3): 451–60.

Simonetti, Manuela, Eszter Paldy, Christian Njoo, Kiran Kumar Bali, Thomas Worzfeld, Claudia Pitzer, Thomas Kuner, Stefan Offermanns, Daniela Mauceri, and Rohini Kuner. 2021. "The Impact of Semaphorin 4C/Plexin-B2 Signaling on Fear Memory via Remodeling of Neuronal and Synaptic Morphology." *Molecular Psychiatry* 26 (4): 1376–98.

SQGHH, Provisional, and SQGE Provisional. 2015. "Nickel - Canadian Soil Quality Guidelines for the Protection of Environmental and Human Health." https://ccme.ca/en/res/nickel-canadian-soil-quality-guidelines-for-the-protection-of-environmental-and-human-health-en.pdf.

Sreedevi, P, B Sivaramakrishna, A Suresh, and K Radhakrishnaiah. 1992. "Effect of Nickel on Some Aspects of Protein Metabolism in the Gill and Kidney of the Freshwater Fish, Cyprinus Carpio L." *Environmental Pollution* 77 (1): 59–63.

Stuermer, Claudia A O, Martin Bastmeyer, Matthias Bähr, Gabriele Strobel, and Katja Paschke. 1992. "Trying to Understand Axonal Regeneration in the CNS of Fish." *Journal of Neurobiology* 23 (5): 537–50.

Svecevičius, Gintaras. 2010. "Acute Toxicity of Nickel to Five Species of Freshwater Fish." *Polish Journal of Environmental Studies* 19 (2): 453–56.

Tallkvist, Jonas, Christopher L Bowlus, and Bo Lönnerdal. 2003. "Effect of Iron Treatment on Nickel Absorption and Gene Expression of the Divalent Metal Transporter (DMT1) by Human Intestinal Caco-2 Cells." *Pharmacology & Toxicology* 92 (3): 121–24.

Tanaka, Shinji, and Mark D Okusa. 2020. "Crosstalk between the Nervous System and

the Kidney." *Kidney International* 97 (3): 466–76.

Templeton, Doug. 1994. "Nickel." In *Techniques and Instrumentation in Analytical Chemistry,* 15:469–87. Elsevier.

Tjälve, Hans, James Gottofrey, and Kathleen Borg. 1988. "Bioaccumulation, Distribution and Retention of 63Ni2+ in the Brown Trout (Salmo Trutta)." *Water Research* 22 (9): 1129–36.

Toman, R, N Lukáč, P Massanyi, and Z Hajkova. 2013. "Changes of Blood Parameters Associated with Nickel Administration in Rats." *Animal Welfare, Ethology and Housing Systems* 9 (3, Suppl. 2): 604–11.

Tomei, Francesco, Maria Valeria Rosati, Manuela Ciarrocca, Maria Rosaria Marchetti, Tiziana Paola Baccolo, Vincenza Anzelmo, and Enrico Tomao. 2004. "Urban Pollution and Nickel Concentration in Serum." *International Journal of Environmental Health Research* 14 (1): 65–74.

Topal, Ahmet, Muhammed Atamanalp, Ertan Oruç, Mesut Bünyami Halıcı, Melda Şişecioğlu, Hüseyin Serkan Erol, Arzu Gergit, and Bahar Yılmaz. 2015. "Neurotoxic Effects of Nickel Chloride in the Rainbow Trout Brain: Assessment of c-Fos Activity, Antioxidant Responses, Acetylcholinesterase Activity, and Histopathological Changes." *Fish Physiology and Biochemistry* 41: 625–34.

Ubaid-ullah, M, M Javed, and S Abdullah. 2004. "Impact of Waste Disposal on the Uptake and Accumulation of Heavy Metals in the Planktonic Biomass of the River Ravi." *Int. J. Agric. Biol* 6: 629–32.

Wasinger, Valerie C, Stuart J Cordwell, Anne Cerpa-Poljak, Jun X Yan, Andrew A Gooley, Marc R Wilkins, Mark W Duncan, Ray Harris, Keith L Williams, and Ian Humphery-Smith. 1995. "Progress with Gene-product Mapping of the Mollicutes: Mycoplasma Genitalium." *Electrophoresis* 16 (1): 1090–94.

Wintz, H, T Fox, and C Vulpe. 2002. "Functional Genomics and Gene Regulation in Biometals Research." *Biochem. Soc. Transactions* 30 (1): 166–68.

Xuan, Fang-Ling, Ling Yan, Yanli Li, Fengmei Fan, Hu Deng, Mengzhuang Gou, Keerthana Chithanathan, Indrek Heinla, Liang Yuan, and Kadri Seppa. 2022. "Glial Receptor PLXNB2 Regulates Schizophrenia-Related Stress Perception via the Amygdala." *Frontiers in Immunology* 13: 1005067.

Zeng, Chu, Zhi-Shuai Hou, Hong-Kui Zhao, Yuan-Ru Xin, Meng-Qun Liu, Xiao-Dong Yang, Hai-Shen Wen, and Ji-Fang Li. 2021. "Identification and Characterization of Caspases Genes in Rainbow Trout (Oncorhynchus Mykiss) and Their Expression Profiles after Aeromonas Salmonicida and Vibrio Anguillarum Infection." *Developmental & Comparative Immunology* 118: 103987.

Zheng, Gui-Hong, Chan-Min Liu, Jian-Mei Sun, Zhao-Jun Feng, and Chao Cheng. 2014. "Nickel-Induced Oxidative Stress and Apoptosis in Carassius Auratus Liver by JNK Pathway." *Aquatic Toxicology* 147: 105–11.

APPENDIX A. Over-represented biological processes and GO terms in CPDB networks

Table A1. Over-represented GO biological processes in kidney proteins of rainbow trout significantly affected by nickel treatment. The list of 275 significantly affected by nickel treatment was search against the Consensus Pathway database (CPDB) to find over-represented gene ontology (GO) biological processes involved in response to nickel exposure (p-value < 0.05). The list here only includes manually selected terms from all the over-represented pathways that best represent the networks of interest.

P-value	GO Term ID	GO Term	Proteins from Input List
1.27E-06	GO:0048856	anatomical structure development	Bptf; Lyve1; Akt2; Rapgef1; Atrx; Apcdd1; Lbr; Adamts2; Dnmt1; Rora; Ntrk3; Inhbb; Plxnd1; Cdh5; Igf1r; Spef2; Arhgef19; Prom1; Eif4g2; Hyal1; Mylk; Rbm38; Cdon; Arhgap15; Mmp14; Ngf; Ncapg2; Gjc2; Kif26a; Gab1; Faxdc2; Hip1r; Plxnb2; Chd2; Fat1; Xdh; Spo11; Txnrd3; Odf2; Hmces; Farp1; Hgs; Sarm1; Bcan; Tp53; Taf1; Hlx; Camsap2; Ripor2; Spdef; Safb2; Mef2b; Itgam; Mcph1; Clock; Smad5; Myo1d; Ahi1; Slc4a1; Akap13; Inf2; Fzd3; Chrnb1; Cd83; Dnaaf11; Kdm6b; Tmem30a; Adgrb1; Szt2; Epb41l3; Mecp2; Stox2; Dab2ip; Zfp36l1; Srr; Prtg; Sall2; Syne1; Chrna9; Mapk8ip2; Rp1l1; Triobp; Emx2; Sh3pxd2b; Asap1; Pth1r; Cryab; Cat; Cd28; Dscam; P2rx5; Casq1; Atm; Slc9a3r1; Cnot1; Rp1; Kmt2b; Cramp1; Itgb6; Nolc1; Vcl; Cd40; Ptgis; Chadl; Mmp24; Plekho1; Pbx3; Pbx1; Dspp; Ptch1; Cmklr1
5.95E-05	GO:0009653	anatomical structure morphogenesis	Mmp14; Ngf; Lyve1; Smad5; Atm; Cryab; Ahi1; Chrna9; Gab1; Akap13; Arhgef19; Dscam; Inf2; Plxnb2; Fzd3; Casq1; Slc9a3r1; Farp1; Cdon; Rora; Xdh; Arhgap15; Kdm6b; Plxnd1; Cnot1; Fgg; Cdh5; Adgrb1; Rp1; Szt2; Epb41l3; Spef2; Itgb6; Dab2ip; Mecp2; Vcl; Cd40; Ptgis; Zfp36l1; Prom1; Atrx; Hgs; Plekho1; Pbx3; Mapk8ip2; Pbx1; Sarm1; Tp53; Triobp; Hlx; Eif4g2; Hyal1; Emx2; Mylk; Fat1; Dspp; Nolc1; Ptch1; Ripor2
1.24E-06	GO:0048513	animal organ development	Bptf; Mmp14; Pth1r; Ncapg2; Clock; Smad5; Myo1d; Cryab; Ahi1; Chrna9; Cat; Fzd3; Akt2; Spef2; Slc4a1; Akap13; Faxdc2; Apcdd1; Dscam; Xdh; Plxnb2; Lbr; Casq1; Adamts2; Atm; Cd83; Dnaaf11; Rora; Ntrk3; Inhbb; Spo11; Szt2; Kdm6b; Plxnd1; Rp1l1; Adgrb1; Mcph1; Rp1; Kmt2b; Cd28; Gjc2; Itgb6; Arhgef19; Mecp2; Stox2; Dab2ip; Zfp36l1; Chadl; Srr; Chd2; Prom1; Sall2; Atrx; Ripor2; Pbx3; Pbx1; Bcan; Tp53; Triobp; Taf1; Hlx; Eif4g2; Hyal1; Spdef; Emx2; Mylk; Safb2; Mef2b; Cdon; Dspp; Itgam; Sh3pxd2b; Nolc1; Ptch1; Slc9a3r1
2.66E-05	GO:0007420	brain development	Bptf; Mcph1; Gjc2; Atm; Ahi1; Plxnb2; Fzd3; Rora; Kdm6b; Szt2; Spef2; Mecp2; Dab2ip; Srr; Atrx; Pbx3; Pbx1; Bcan; Tp53; Taf1; Emx2; Cdon; Itgam; Myo1d; Ptch1
5.73E-06	GO:0048468	cell development	Pth1r; Ngf; Clock; Smad5; Atm; Ahi1; Gab1; Akt2; Slc4a1; Rapgef1; Dscam; Plxnb2; Fzd3; Casq1; Chrnb1; Slc9a3r1; Szt2; Ntrk3; Inhbb; Tmem30a; Plxnd1; Cdh5; Adgrb1; Rp1; Odf2; Epb41l3; Spef2; Farp1; Dab2ip; Mecp2; Vcl; Prtg; Atrx; Pbx3; Mapk8ip2; Pbx1; Sarm1; Rp1l1; Tp53; Triobp; Camsap2; Eif4g2; Ripor2; Spdef; Gjc2; Cdon; Spo11; Nolc1; Ptch1; Asap1; Akap13
8.53E-08	GO:0030154	cell differentiation	Akt2; Hps6; Rapgef1; Atrx; Lbr; Dnmt1; Rora; Ntrk3; Inhbb; Plxnd1; Fgg; Cdh5; Cd28; Cetp; Prom1; Pa2g4; Eif4g2; Txnrd3; Cdon; Spo11; Mmp14; Ngf; Ncapg2; Emx2; Gab1; Faxdc2; Plxnb2; Xdh; Rbm38; Odf2; Farp1; Sarm1; Tp53; Hlx; Camsap2; Ripor2; Spdef; Safb2; Mef2b; Itgam; Clock; Smad5; Atm; Ahi1; Slc4a1; Akap13; Fzd3; Chrnb1; Cd83;

			Kdm6b; Tmem30a; Adgrb1; Szt2; Epb41l3; Mecp2; Dab2ip; Zfp36l1; Prtg; Syne1; Mapk8ip2; Rp1l1; Triobp; Vipas39; Gjc2; Sh3pxd2b; Asap1; Pth1r; Cat; Spef2; Dscam; Casq1; Slc9a3r1; Cnot1; Rp1; Kmt2b; Itgb6; Nolc1; Vcl; Chadl; Mmp24; Plekho1; Pbx3; Pbx1; Dspp; Ptch1; Cmklr1
3.52E-05	GO:0030030	cell projection organization	Ngf; Ehd3; Szt2; Epb41l3; Gab1; Rapgef1; Dscam; Plxnb2; Fzd3; Slc9a3r1; Dnaaf11; Ntrk3; Tmem30a; Plxnd1; Rp1l1; Adgrb1; Rp1; Odf2; Igf1r; Spef2; Farp1; Dab2ip; Mecp2; Vcl; Ssx2ip; Ahi1; Prom2; Plekho1; Sarm1; Mapk8ip2; Triobp; Camsap2; Eif4g2; Ripor2; Mylk; Cd2ap; Tbc1d14; Septin9; Ptch1; Asap1; Cfap221
8.20E-06	GO:0016043	cellular component organization	Bptf; Lyve1; Akt2; Rapgef1; Atrx; Apcdd1; Lbr; Adamts2; Dnmt1; Rora; Ntrk3; Inhbb; Plxnd1; Fgg; Cdh5; Igf1r; Spef2; Arhgef19; Prom1; Eif4g2; Hyal1; Mylk; Rbm38; Cdon; Arhgap15; Mmp14; Ngf; Ncapg2; Gjc2; Kif26a; Gab1; Faxdc2; Hip1r; Plxnb2; Chd2; Fat1; Xdh; Spo11; Txnrd3; Odf2; Hmces; Farp1; Hgs; Sarm1; Bcan; Tp53; Taf1; Hlx; Camsap2; Ripor2; Spdef; Safb2; Mef2b; Itgam; Mcph1; Clock; Smad5; Myo1d; Ahi1; Slc4a1; Akap13; Inf2; Fzd3; Chrnb1; Cd83; Dnaaf11; Kdm6b; Tmem30a; Adgrb1; Szt2; Epb41l3; Mecp2; Stox2; Dab2ip; Zfp36l1; Srr; Prtg; Sall2; Syne1; Chrna9; Mapk8ip2; Rp1l1; Triobp; Emx2; Sh3pxd2b; Asap1; Pth1r; Cryab; Cat; Cd28; Dscam; P2rx5; Casq1; Atm; Slc9a3r1; Cnot1; Rp1; Kmt2b; Cramp1; Itgb6; Nolc1; Vcl; Cd40; Ptgis; Chadl; Mmp24; Plekho1; Pbx3; Pbx1; Dspp; Ptch1; Cmklr1
7.64E-06	GO:0071840	cellular component organization or biogenesis	Ripor2; Slx4; Snx14; Hpse2; Ttll11; Rad54l2; Ngf; Ube2k; Cd2ap; Szt2; Epb41l3; Taf5; Nfat5; Mmp24; Rap1gds1; Phpt1; Fat1; Casq1; Ncapg2; Tpr; Ahi1; Mcph1; Fgg; Tubgcp6; Nat8; Rp1l1; Camsap2; Gemin2; Plxnb2; Ecm2; Slc9a3r1; Kmt2b; Dab2ip; Mmp14; Fzd3; Atrx; Cetp; Grm7; Myo5b; Chd2; Mapk8ip2; Myo1d; Adamts2; Plxnd1; Dnaaf11; Prtg; Tmem30a; Tie; Ltbp2; Ndufb2; Kif9; Pa2g4; Ap3m2; Trappc8; Baz2a; Cfap221; Cdh5; Cog2; Igf1r; Ntrk3; Cryab; Triobp; Spo11; Wdr3; Adgrb1; Ppfibp2; Mylk; Itgam; Bcan; Cep44; Ercc4; Clock; Nlrp1; Bptf; Dnmt1; Asap1; Ehd3; Inf2; Tp53; Bcorl1; Syne1; Ccdc51; Farsa; Kctd10; Nolc1; Urb2; Plekho1; Rp1; Slc4a1; Vcl; Med8; Cd40; Ndufa5; Vipas39; Akt2; Farp1; DscamChd2; Aifm1; Xdh; Chrnb1; Mecp2; Taf1; Ptch1; Atm; Hgs; Kdm6b; Rp1; Fzd3; Spef2; Sh3pxd2b; Odf2; Hps6; Ssx2ip; Hip1r; Chd1
9.76E-08	GO:0048869	cellular developmental process	Akt2; Hps6; Rapgef1; Atrx; Lbr; Dnmt1; Rora; Ntrk3; Inhbb; Plxnd1; Fgg; Cdh5; Cd28; Cetp; Prom1; Pa2g4; Eif4g2; Txnrd3; Cdon; Arhgap15; Mmp14; Ngf; Ncapg2; Emx2; Gab1; Faxdc2; Plxnb2; Xdh; Spo11; Rbm38; Odf2; Farp1; Sarm1; Tp53; Hlx; Camsap2; Ripor2; Spdef; Safb2; Mef2b; Itgam; Clock; Smad5; Atm; Ahi1; Slc4a1; Akap13; Fzd3; Chrnb1; Cd83; Kdm6b; Tmem30a; Adgrb1; Szt2; Epb41l3; Mecp2; Dab2ip; Zfp36l1; Prtg; Syne1; Mapk8ip2; Rp1l1; Triobp; Vipas39; Gjc2; Sh3pxd2b; Asap1; Pth1r; Cat; Spef2; Dscam; Casq1; Slc9a3r1; Cnot1; Rp1; Kmt2b; Itgb6; Nolc1; Vcl; Chadl; Mmp24; Plekho1; Pbx3; Pbx1; Dspp; Ptch1; Cmklr1
3.74E-06	GO:0071214	cellular response to abiotic stimulus	Rp1; Atm; Tp53; Taf1; Itgb6; Cryab; Hyal1; Mylk; Ercc4; Zfp36l1; Cd40; Clock; Akt2; Mapk13; Ripor2
3.74E-06	GO:0104004	cellular response to environmental stimulus	Rp1; Atm; Tp53; Taf1; Itgb6; Cryab; Hyal1; Mylk; Ercc4; Zfp36l1; Cd40; Clock; Akt2; Mapk13; Ripor2
9.14E-05	GO:0071347	cellular response to interleukin-1	Mepk13; Fgg; Hyal1; Dab21p; Inhbb; Ptgis; Rora; Cd40

5.70E-05	GO:0071478	cellular response to radiation	Rp1; Tp53; Taf1; Itgb6; Cryab; Hyal1; Atm; Ercc4; Clock; Akt2; Mapk13
2.68E-06	GO:0032502	developmental process	Ripor2; Prom1; Ngf; Cdon; Pc; Txnrd3; Rapgef1; Safb2; Szt2; Cmklr1; Epb41l3; Cd83; Akap13; Mmp24; Emx2; Fat1; Casq1; Ncapg2; Smad5; Chrna9; Stox2; Ahi1; Mcph1; Fgg; Rp1l1;Camsap2; Hyal1; Plxnb2; Srr; Slc9a3r1; Dab2ip; Mmp14; Fzd3; Atrx; Orc3; Grm7; Cnot1; Chd2; Mapk8ip2; Sarm1; Cxcr2; Inhbb; Adamts2; Plxnd1; Dnaaf11; Prtg; Tie; Pbx3; Pbx1; Lbr; Gab1; Csmd1; C19orf80; Cramp1; Shisa6; Cd28; Pth1r; Cfap221; Apcdd1; Cdh5; Igf1r; Ntrk3; P2rx5; Cryab; Triobp; Spo11; Sall2; Hlx; Adgrb1; Spdef; Itgb6; Cops2; Mylk; Itgam; Bcan; Clock; Bptf; Rora; Pgam2; Lyve1; Tp53; Syne1; Nolc1; Plekho1; Dspp; Slc4a1; Cat; Vcl; Vipas39; Akt2; Mef2b; Farp1; Zar1l; Dscam,Chd2; Aifm1; Zfp36l1; Xdh; Chrnb1; Mecp2; Taf1; Ptch1; Atm; Kdm6b; Rbm38; Rp1; Fzd3; Spef2; Sh3pxd2b; Odf2; Kif26a; Gjc2; Hip1r
1.06E-04	GO:0060429	epithelium development	Mmp14; Clock; Smad5; Atm; Ahi1; Cat; Akt2; Rapgef1; Apcdd1; Plxnb2; Fzd3; Slc9a3r1; Xdh; Kdm6b; Plxnd1; Cdh5; Arhgef19; Vcl; Zfp36l1; Prom1; Sall2; Atrx; Pbx1; Tp53; Triobp; Ripor2; Spdef; Safb2; Dspp; Ptch1
7.77E-06	GO:0048699	generation of neurons	Ngf; Gjc2; Ahi1; Gab1; Rapgef1; Dscam; Plxnb2; Fzd3; Slc9a3r1; Rora; Ntrk3; Tmem30a; Plxnd1; Rp1l1; Adgrb1; Rp1; Szt2; Epb41l3; Farp1; Dab2ip; Mecp2; Vcl; Prtg; Prom1; Pbx3; Mapk8ip2; Pbx1; Sarm1; Tp53; Triobp; Camsap2; Eif4g2; Ripor2; Emx2; Cdon; Ptch1; Asap1
3.62E-05	GO:0060322	head development	Bptf; Mmp14; Gjc2; Atm; Ahi1; Plxnb2; Fzd3; Rora; Kdm6b; Mcph1; Szt2; Spef2; Mecp2; Dab2ip; Srr; Atrx; Pbx3; Pbx1; Bcan; Tp53; Taf1; Emx2; Cdon; Itgam; Myo1d; Ptch1
2.87E-07	GO:0007275	multicellular organism development	Bptf; Akt2; Rapgef1; Apcdd1; Lbr; Adamts2; Dnmt1; Rora; Ntrk3; Inhbb; Plxnd1; Rp1l1; Cdh5; Igf1r; Spef2; Arhgef19; Prom1; Eif4g2; Hyal1; Mylk; Cdon; Spo11; Mmp14; Ngf; Ncapg2; Gjc2; Kif26a; Gab1; Faxdc2; Hip1r; Plxnb2; Chd2; Xdh; Txnrd3; Odf2; Hmces; Farp1; Hgs; Sarm1; Bcan; Tp53; Taf1; Hlx; Camsap2; Ripor2; Spdef; Safb2; Mef2b; Itgam; Mcph1; Clock; Smad5; Myo1d; Ahi1; Slc4a1; Akap13; Fzd3; Cd83; Dnaaf11; Kdm6b; Tmem30a; Adgrb1; Szt2; Epb41l3; Mecp2; Stox2; Dab2ip; Zfp36l1; Srr; Prtg; Sall2; Atrx; Chrna9; Mapk8ip2; Triobp; Emx2; Sh3pxd2b; Asap1; Pth1r; Cryab; Cat; Cd28; Dscam; P2rx5; Casq1; Atm; Slc9a3r1; Cnot1; Rp1; Kmt2b; Cramp1; Itgb6; Nolc1; Vcl; Cd40; Ptgis; Chadl; Mmp24; Pbx3; Pbx1; Dspp; Ptch1; Cmklr1
1.36E-05	GO:0006734	NADH metabolic process	Tp53; Ptgis; Mdh1b; Eno2; Slc4a1; Tpr; Gpd2; Pgam2; Sarm1
3.34E-06	GO:0048519	negative regulation of biological process	Bptf; Akt2; Rapgef1; Apcdd1; Hyou1; Dnmt1; Rora; Ntrk3; Inhbb; Plxnd1; Fgg; Cdh5; Igf1r; Atm; Cetp; Prkg2; Tpr; Gpatch2; Pa2g4; Ip6k2; Kctd10; Eif4g2; Hyal1; Zar1l; Cd2ap; Pggt1b; Cpeb1; Mmp14; Ngf; Ncapg2; Rpl3; Thap12; Baz2a; Hip1r; Plxnb2; Xdh; Pc; Ceacam6; Grm7; Farp1; Itpr2; Sarm1; Tp53; Taf1; Hlx; Camsap2; Ripor2; Spdef; Shisa6; Itgam; Mcph1; Phpt1; Clock; Smad5; Myo1d; Ahi1; Slc4a1; Podn; Fzd3; Slx4; Cd83; Adgrb1; Rps26; Szt2; Nat8; Cryab; Mecp2; Dab2ip; Zfp36l1; Sult1a3; Kif26a; Prtg; Sall2; Atrx; Chrna9; Mapk8ip2; Rgs12; Triobp; Gjc2; Asap1; Tbc1d14; Pth1r; Znf318; Ercc4; Cat; Cd28; Dscam; Casq1; Slc9a3r1; Cnot1; Fetub; Vcl; Hgs; Ptgis; Chadl; Rps29; Pbx1; Dcbld2; Tab3; Cilp; Ptch1; Cmklr1; Prom2

1.86E-06	GO:0048523	negative regulation of cellular process	Bptf; Akt2; Rapgef1; Apcdd1; Hyou1; Dnmt1; Rora; Ntrk3; Inhbb; Plxnd1; Fgg; Cdh5; Igf1r; Atm; Cetp; Tpr; Gpatch2; Pa2g4; Ip6k2; Kctd10; Eif4g2; Hyal1; Cd2ap; Cpeb1; Mmp14; Ngf; Ncapg2; Kif26a; Thap12; Baz2a; Hip1r; Plxnb2; Xdh; Ceacam6; Grm7; Farp1; Itpr2; Sarm1; Tp53; Taf1; Hlx; Camsap2; Ripor2; Spdef; Shisa6; Itgam; Mcph1; Phpt1; Clock; Smad5; Myo1d; Ahi1; Slc4a1; Podn; Fzd3; Slx4; Adgrb1; Rps26; Szt2; Nat8; Cryab; Mecp2; Dab2ip; Zfp36l1; Sult1a3; Prtg; Sall2; Atrx; Chrna9; Mapk8ip2; Rgs12; Triobp; Gjc2; Asap1; Tbc1d14; Pth1r; Znf318; Ercc4; Cat; Cd28; Dscam; Casq1; Slc9a3r1; Cnot1; Fetub; Vcl; Hgs; Ptgis; Chadl; Pbx1; Dcbld2; Tab3; Cilp; Ptch1; Prom2
2.62E-07	GO:0007399	nervous system development	Bptf; Mmp14; Ngf; Gjc2; Atm; Kif26a; Gab1; Akt2; Spef2; Rapgef1; Mmp24; Dscam; P2rx5; Plxnb2; Fzd3; Slc9a3r1; Rora; Ntrk3; Kdm6b; Tmem30a; Plxnd1; Rp1l1; Adgrb1; Mcph1; Rp1; Szt2; Epb41l3; Myo1d; Farp1; Dab2ip; Mecp2; Vcl; Zfp36l1; Ahi1; Srr; Prtg; Prom1; Sall2; Atrx; Pbx3; Mapk8ip2; Pbx1; Bcan; Sarm1; Tp53; Triobp; Taf1; Hlx; Camsap2; Eif4g2; Ripor2; Emx2; Cdon; Itgam; Ptch1; Asap1
1.51E-05	GO:0061351	neural precursor cell proliferation	Plxnb2; Fzd3; Tp53; Gjc2; Emx2; Orc3; Rora; Cdon; Rapgef1
1.27E-06	GO:0022008	neurogenesis	Mmp14; Ngf; Gjc2; Ahi1; Gab1; Akt2; Rapgef1; Dscam; Plxnb2; Fzd3; Slc9a3r1; Rora; Ntrk3; Tmem30a; Plxnd1; Rp1l1; Adgrb1; Rp1; Szt2; Epb41l3; Farp1; Dab2ip; Mecp2; Vcl; Prtg; Prom1; Mmp24; Pbx3; Mapk8ip2; Pbx1; Sarm1; Tp53; Triobp; Camsap2; Eif4g2; Ripor2; Emx2; Cdon; Ptch1; Asap1
1.09E-04	GO:0048666	neuron development	Ngf; Ahi1; Gab1; Rapgef1; Dscam; Plxnb2; Fzd3; Slc9a3r1; Ntrk3; Tmem30a; Plxnd1; Rp1l1; Adgrb1; Rp1; Szt2; Epb41l3; Farp1; Vcl; Mecp2; Dab2ip; Pbx3; Mapk8ip2; Pbx1; Sarm1; Triobp; Camsap2; Eif4g2; Ripor2; Ptch1; Asap1
1.51E-05	GO:0030182	neuron differentiation	Ngf; Ahi1; Gab1; Rapgef1; Dscam; Plxnb2; Fzd3; Slc9a3r1; Rora; Ntrk3; Tmem30a; Plxnd1; Rp1l1; Adgrb1; Rp1; Szt2; Epb41l3; Farp1; Dab2ip; Mecp2; Vcl; Prom1; Pbx3; Mapk8ip2; Pbx1; Sarm1; Triobp; Camsap2; Eif4g2; Ripor2; Emx2; Cdon; Ptch1; Asap1
1.28E-05	GO:0120036	plasma membrane bounded cell projection organization	Ngf; Ehd3; Szt2; Epb41l3; Gab1; Rapgef1; Dscam; Plxnb2; Fzd3; Slc9a3r1; Dnaaf11; Ntrk3; Tmem30a; Plxnd1; Rp1l1; Adgrb1; Rp1; Odf2; Igf1r; Spef2; Farp1; Dab2ip; Mecp2; Vcl; Ssx2ip; Ahi1; Plekho1; Sarm1; Mapk8ip2; Triobp; Camsap2; Eif4g2; Ripor2; Mylk; Cd2ap; Tbc1d14; Septin9; Ptch1; Asap1; Cfap221
1.85E-05	GO:0048518	positive regulation of biological process	Bptf; Akt2; Rapgef1; Hpse2; Dnmt1; Rora; Ntrk3; Inhbb; Plxnd1; Fgg; Cdh5; Igf1r; Cd28; Cetp; Arhgef19; Camta1; Prom2; Prom1; Usp34; Pa2g4; Ip6k2; Nfat5; Eif4g2; Hyal1; Mylk; Acsl5; Pggt1b; Cdon; Plxnb2; Mmp14; Ngf; Ncapg2; Gab1; Faxdc2; Znf850; Cd2ap; Hip1r; Chd1; Xdh; Pc; Ceacam6; Ermap; Hmces; Hgs; Slc26a9; Znf658b; Sarm1; Ube2k; Tp53; Taf1; Hlx; Ripor2; Spdef; Mef2b; Itgam; Aifm1; Phpt1; Ehd3; Clock; Smad5; Atm; Ahi1; Akap13; Mapk13; Mios; Fzd3; Nlrp1; Slx4; Cd83; Plrg1; Ccpg1; Kdm6b; Tmem30a; Adgrb1; Nat8; Cpeb1; Mecp2; Dab2ip; Zfp36l1; Sall2; Muc5ac; Atrx; Mapk8ip2; Triobp; Gjc2; Septin9; Asap1; Pth1r; Stim2; Znf318; Ercc4; Ecm2; Cat; Sgms1; Dscam; P2rx5; Casq1; Slc9a3r1; Por; Cxcr2; Cnot1; Rp1; Kmt2b; Nolc1; Cd40; Ptgis; Nccrp1; Pbx1; Tab3; Edrf1; Ptch1; Cmklr1; Tpr
7.41E-06	GO:0048522	positive regulation of cellular process	Bptf; Akt2; Rapgef1; Hpse2; Pa2g4; Dnmt1; Rora; Ntrk3; Inhbb; Plxnd1; Fgg; Cdh5; Igf1r; Cd28; Arhgef19; Camta1; Prom2; Prom1; Usp34; Ip6k2; Nfat5; Eif4g2; Hyal1; Mylk; Cd2ap; Pggt1b; Cdon; Mmp14; Ngf; Ncapg2; Gab1; Faxdc2; Znf850; Hip1r; Plxnb2; Xdh; Ceacam6; Hmces; Hgs; Znf658b; Sarm1; Ube2k; Tp53; Taf1; Hlx; Ripor2; Spdef; Mef2b;

			Itgam; Aifm1; Phpt1; Clock; Smad5; Atm; Ahi1; Akap13; Mios; Fzd3; Nlrp1; Slx4; Cd83; Plrg1; Ccpg1; Kdm6b; Tmem30a; Adgrb1; Cpeb1; Mecp2; Dab2ip; Zfp36l1; Sall2; Atrx; Mapk8ip2; Triobp; Gjc2; Septin9; Asap1; Pth1r; Znf318; Ercc4; Cat; Dscam; P2rx5; Casq1; Slc9a3r1; Cxcr2; Cnot1; Rp1; Kmt2b; Nolc1; Cd40; Ptgis; Nccrp1; Pbx1; Tab3; Edrf1; Ptch1; Cmklr1; Tpr
4.19E-05	GO:0051094	positive regulation of developmental process	Mmp14; Ngf; Smad5; Ahi1; Gab1; Rapgef1; Faxdc2; Dscam; Plxnb2; Fzd3; Cd83; Ntrk3; Tmem30a; Plxnd1; Fgg; Cdh5; Adgrb1; Cd28; Hmces; Dab2ip; Cd40; Ptgis; Zfp36l1; Prom1; Pa2g4; Tp53; Triobp; Hlx; Eif4g2; Hyal1; Spdef; Gjc2; Cdon; Ptch1; Cmklr1; Ripor2
1.43E-04	GO:0040017	positive regulation of locomotion	Mmp14; Phpt1; Igf1r; Atm; Cdh5; Hyal1; Mylk; Dab2ip; Cd40; Gab1; Pc; Akt2; Ceacam6; Dscam; Ntrk3; Cmklr1; Ripor2
6.19E-05	GO:0045595	regulation of cell differentiation	Mmp14; Ngf; Ncapg2; Clock; Smad5; Ahi1; Rapgef1; Faxdc2; Dscam; Xdh; Plxnb2; Fzd3; Cd83; Dnmt1; Rora; Ntrk3; Tmem30a; Plxnd1; Fgg; Cdh5; Adgrb1; Kmt2b; Sarm1; Cd28; Cetp; Dab2ip; Mecp2; Vcl; Zfp36l1; Chadl; Prtg; Prom1; Pa2g4; Pbx1; Tp53; Triobp; Hlx; Camsap2; Eif4g2; Ripor2; Spdef; Gjc2; Rbm38; Cdon; Dspp; Ptch1; Cmklr1; Asap1; Akap13
1.09E-04	GO:2000145	regulation of cell motility	Mmp14; Phpt1; Atm; Gab1; Akt2; Plxnb2; Podn; Slc9a3r1; Ntrk3; Ceacam6; Plxnd1; Cdh5; Adgrb1; Igf1r; Vcl; Mecp2; Dab2ip; Ssx2ip; Cd40; Ripor2; Mylk; Cmklr1; Hyal1
2.09E-05	GO:0044087	regulation of cellular component biogenesis	Mmp14; Ripor2; Atm; Ercc4; Akap13; Hip1r; Slx4; Cnot1; Cdh5; Adgrb1; Rp1; Kif9; Cryab; Mecp2; Dab2ip; Hgs; Tpr; Tp53; Triobp; Camsap2; Hyal1; Asap1; Septin9; Vcl; Tbc1d14; Rapgef1
6.67E-07	GO:0051128	regulation of cellular component organization	Mmp14; Mcph1; Ngf; Ahi1; Ehd3; Ripor2; Atm; Ercc4; Epb41l3; Prom2; Akt2; Rapgef1; Dscam; Inf2; Hip1r; Plxnb2; Slx4; Slc9a3r1; Dnmt1; Ntrk3; Kif26a; Phpt1; Arhgef19; Tmem30a; Plxnd1; Cnot1; Fgg; Cdh5; Adgrb1; Ogfr; Rp1; Igf1r; Cd28; Sarm1; Kif9; Dab2ip; Cryab; Mecp2; Vcl; Chadl; Eno2; Tpr; Atrx; Plekho1; Ip6k2; Dcbld2; Tp53; Triobp; Camsap2; Eif4g2; Hyal1; Cd2ap; Shisa6; Arhgap15; Septin9; Asap1; Tbc1d14; Akap13
1.08E-06	GO:0050793	regulation of developmental process	Mmp14; Ngf; Ncapg2; Clock; Smad5; Ahi1; Gab1; Rapgef1; Faxdc2; Dscam; Xdh; Inf2; Plxnb2; Fzd3; Cd83; Dnmt1; Rora; Ntrk3; Arhgap15; Arhgef19; Tmem30a; Plxnd1; Cnot1; Fgg; Cdh5; Adgrb1; Kmt2b; Epb41l3; Cd28; Cetp; Hmces; Dab2ip; Mecp2; Vcl; Cd40; Ptgis; Zfp36l1; Rbm38; Prtg; Prom1; Hgs; Plekho1; Ripor2; Pa2g4; Pbx1; Sarm1; Tp53; Triobp; Hlx; Camsap2; Eif4g2; Hyal1; Spdef; Gjc2; Asap1; Cdon; Dspp; Chadl; Ptch1; Cmklr1; Slc9a3r1; Akap13
2.35E-05	GO:0043087	regulation of GTPase activity	Plxnb2; Rgs12; Arhgef19; Dab2ip; Cd40; Ntrk3; Akt2; Arhgap15; Rapgef1; Rap1gds1; Plxnd1; Asap1; Tbc1d14; Prom2
9.34E-05	GO:0040012	regulation of locomotion	Mmp14; Phpt1; Atm; Gab1; Akt2; Dscam; Plxnb2; Podn; Slc9a3r1; Ntrk3; Pc; Ceacam6; Plxnd1; Cdh5; Adgrb1; Igf1r; Vcl; Mecp2; Dab2ip; Ssx2ip; Cd40; Ripor2; Mylk; Cmklr1; Hyal1

1.37E-04	GO:0033043	regulation of organelle organization	Mcph1; Phpt1; Ehd3; Atm; Ercc4; Akt2; Akap13; Inf2; Hip1r; Slx4; Dnmt1; Ntrk3; Cnot1; Cdh5; Rp1; Cd28; Kif9; Arhgef19; Mecp2; Eno2; Tpr; Atrx; Tp53; Triobp; Camsap2; Cd2ap; Septin9; Asap1; Tbc1d14
1.38E-05	GO:0009628	response to abiotic stimulus	Mmp14; Clock; Atm; Ercc4; Cat; Akt2; Mapk13; Fzd3; Casq1; Hyou1; Rora; Nolc1; Rp1; Itgb6; Cryab; Mecp2; Cd40; Ptgis; Zfp36l1; Tpr; Itpr2; Mmp24; Chrna9; Nfat5; Tp53; Taf1; Hyal1; Mylk; Cpeb1; Ptch1; Ripor2
1.37E-04	GO:0006970	response to osmotic stress	Nfat5; Tp53; Nolc1; Zfp36l1; Mylk; Mapk13
2.34E-07	GO:0048731	system development	Bptf; Akt2; Rapgef1; Apcdd1; Lbr; Adamts2; Dnmt1; Rora; Ntrk3; Inhbb; Plxnd1; Rp1l1; Cdh5; Spef2; Arhgef19; Prom1; Eif4g2; Hyal1; Mylk; Cdon; Spo11; Mmp14; Ngf; Ncapg2; Gjc2; Kif26a; Gab1; Faxdc2; Hip1r; Plxnb2; Chd2; Xdh; Hmces; Farp1; Hgs; Sarm1; Bcan; Tp53; Taf1; Hlx; Camsap2; Ripor2; Spdef; Safb2; Mef2b; Itgam; Mcph1; Clock; Smad5; Myo1d; Ahi1; Slc4a1; Akap13; Fzd3; Cd83; Dnaaf11; Kdm6b; Tmem30a; Adgrb1; Szt2; Epb41l3; Mecp2; Stox2; Dab2ip; Zfp36l1; Srr; Prtg; Sall2; Atrx; Chrna9; Mapk8ip2; Triobp; Emx2; Sh3pxd2b; Asap1; Pth1r; Cryab; Cat; Cd28; Dscam; P2rx5; Casq1; Atm; Slc9a3r1; Rp1; Kmt2b; Itgb6; Nolc1; Vcl; Cd40; Ptgis; Chadl; Mmp24; Pbx3; Pbx1; Dspp; Ptch1; Cmklr1
4.77E-05	GO:0009888	tissue development	Bptf; Mmp14; Pth1r; Clock; Smad5; Atm; Ahi1; Cat; Akt2; Rapgef1; Arhgef19; Apcdd1; Plxnb2; Fzd3; Casq1; Slc9a3r1; Xdh; Kdm6b; Plxnd1; Cdh5; Itgb6; Dab2ip; Nolc1; Vcl; Zfp36l1; Chadl; Prom1; Sall2; Atrx; Pbx1; Tp53; Triobp; Hlx; Hyal1; Spdef; Mylk; Safb2; Cdon; Dspp; Itgam; Sh3pxd2b; Ptch1; Ripor2; Akap13

Table A2. Over-represented GO biological processes in liver proteins of rainbow trout significantly affected by nickel treatment. The list of 26 significantly affected by nickel treatment was search against the Consensus Pathway database (CPDB) to find over-represented gene ontology (GO) biological processes involved in response to nickel exposure (p-value < 0.05). The list here only includes manually selected terms from all the over-represented pathways that best represent the networks of interest.

P-value	GO Term ID	GO Term	Proteins from Input List
4.77E-02	GO:0009056	catabolic process	Fitm2; Atp2a2; Dicer1; Bco2; Rnf213; Tnks1bp1
3.37E-02	GO:0048468	cell development	Tdrd7; Atp2a2; Ptpn11; Dicer1; Dhrs2; Kif20b; Ptch1
1.00E-02	GO:0030154	cell differentiation	Tdrd7; Atp2a2; Ptpn11; Dicer1; Sfmbt1; Dhrs2; Kif20b; Ptch1
2.88E-02	GO:0044248	cellular catabolic process	Fitm2; Atp2a2; Dicer1; Bco2; Rnf213; Tnks1bp1
1.44E-02	GO:0016043	cellular component organization	Fitm2; Tdrd7; Atp2a2; Mbtd1; Ptpn11; Dicer1; Sfmbt1; Col22a1; Brd4; Tpx2; Myo3b; Kif20b; Rnf213; Ptch1; Tnks1bp1
1.73E-02	GO:0071840	cellular component organization or biogenesis	Fitm2; Tdrd7; Atp2a2; Mbtd1; Ptpn11; Dicer1; Sfmbt1; Col22a1; Brd4; Tpx2; Myo3b; Kif20b; Rnf213; Ptch1; Tnks1bp1
1.03E-02	GO:0048869	cellular developmental process	Tdrd7; Atp2a2; Ptpn11; Dicer1; Sfmbt1; Dhrs2; Kif20b; Ptch1
2.76E-02	GO:0033554	cellular response to stress	Atp2a2; Mbtd1; Ptpn11; Ppp4r3a; Brd4; Dhrs2; Tnks1bp1
4.48E-02	GO:0006259	DNA metabolic process	Mbtd1; Dicer1; Tnks1bp1
4.64E-02	GO:0007017	microtubule-based process	Tpx2; Kif20b
1.18E-02	GO:0048519	negative regulation of biological process	Tdrd7; Atp2a2; Mbtd1; Ptpn11; Serping1; Dicer1; Sfmbt1; Enpp7; Brd4; Tpx2; Irf2; Rnf213; Ptch1; Tnks1bp1
2.88E-02	GO:0009890	negative regulation of biosynthetic process	Mbtd1; Dicer1; Sfmbt1; Irf2; Ptch1; Tnks1bp1
2.74E-02	GO:0031327	negative regulation of cellular biosynthetic process	Mbtd1; Dicer1; Sfmbt1; Irf2; Ptch1; Tnks1bp1
3.49E-02	GO:0048523	negative regulation of cellular process	Mbtd1; Ptpn11; Dicer1; Sfmbt1; Enpp7; Brd4; Dhrs2; Tpx2; Irf2; Rnf213; Ptch1; Tnks1bp1
5.88E-02	GO:0051093	negative regulation of developmental process	Ptpn11; Dicer1; Sfmbt1; Ptch1
5.64E-02	GO:0010629	negative regulation of gene expression	Tdrd7; Ptpn11; Dicer1; Tnks1bp1

2.47E-02	GO:0010558	negative regulation of macromolecule biosynthetic process	Mbtd1; Dicer1; Sfmbt1; Irf2; Ptch1; Tnks1bp1
5.00E-02	GO:0048666	neuron development	Ptpn11; Dicer1; Kif20b; Ptch1
4.58E-02	GO:0070925	organelle assembly	Fitm2; Atp2a2; Tpx2; Rnf213
5.74E-02	GO:0045937	positive regulation of phosphate metabolic process	Ptpn11; Enpp7; Tpx2; Tnks1bp1
5.74E-02	GO:0010562	positive regulation of phosphorus metabolic process	Ptpn11; Enpp7; Tpx2; Tnks1bp1
4.82E-02	GO:0042327	positive regulation of phosphorylation	Ptpn11; Tpx2; Tnks1bp1
2.03E-02	GO:0043933	protein-containing complex organization	Atp2a2; Mbtd1; Dicer1; Sfmbt1; Brd4; Tpx2
3.12E-02	GO:0042127	regulation of cell population proliferation	Dicer1; Enpp7; Dhrs2; Kif20b; Ptch1

APPENDIX B. Over-represented pathways and GO terms in CPDB networks

Table B1. Over-represented GO pathways in kidney proteins of rainbow trout significantly affected by nickel treatment. The list of 275 significantly affected by nickel treatment was search against the Consensus Pathway database (CPDB) to find over-represented gene ontology (GO) biological processes involved in response to nickel exposure (p-value < 0.05). The list here only includes manually selected terms from all the over-represented pathways that best represent the networks of interest.

P-value	Pathway ID	GO Term	Protein from Input List
0.003685994	hsa04210	Apoptosis	Ngf; Tp53; Atm; Dab2ip; Akt2; Itpr2; Aifm1
0.004195897	R-HSA-349425	Autodegradation of the E3 ubiquitin ligase COP1	Atm; Tp53
0.009209869	R-HSA-1474244	Extracellular matrix organization	Mmp14; Bcan; Ltbp2; Itgb6; Adamts2; Dspp; Itgam; Mmp24; Fgg; Col20a1
0.007126153	WP2261	Glioblastoma signaling pathways	Akt2; Atm; Tp53; Igf1r; Gab1
0.005474524	PWY66-399	gluconeogenesis	Pc; Eno2; Pgam2
0.004388344	WP4674	Head and Neck Squamous Cell Carcinoma	Akt2; Fat1; Tp53; Igf1r; Gab1
0.003784348	p53hypoxiapathway	hypoxia and p53 in the cardiovascular system	Atm; Tp53; Taf1
0.005541249	R-HSA-5632681	Ligand-receptor interactions	Cdon; Ptch1
0.007056692	R-HSA-8875555	MET activates RAP1 and RAC1	Rapgef1; Gab1
0.00173747	hsa04722	Neurotrophin signaling pathway	Ngf; Tp53; Ntrk3; Akt2; Rapgef1; Mapk13; Gab1
0.004447567	hsa04928	Parathyroid hormone synthesis, secretion and action	Pth1r; Mmp14; Slc9a3r1; Akap13; Itpr2; Mmp24
0.002176107	WP3651	Pathways affected in adenoid cystic carcinoma	Atm; Bcorl1; Kdm6b; Tp53; Atrx
0.002197711	hsa04611	Platelet activation	Prkg2; Mylk; Akt2; Mapk13; Itpr2; Fgg; Pla2g4f
0.003056769	hsa05205	Proteoglycans in cancer	Igf1r; Fzd3; Tp53; Gab1; Ptch1; Akt2; Mapk13; Itpr2; Hpse2
0.008256269	WP15	Selenium Micronutrient Network	Saa2; Xdh; Fgg; Txnrd3; Cat
0.009919974	R-HSA-9659379	Sensory processing of sound	Ripor2; Epb41l3; Chrna9; Triobp
0.005888794	R-HSA-69541	Sensory processing of sound by outer hair cells of the cochlea	Ripor2; Epb41l3; Chrna9; Triobp
0.008737055	hsa05202	Stabilization of p53	Atm; Tp53
0.006774014	hsa04210	Transcriptional misregulation in cancer	Igf1r; Tp53; Atm; Cd40; Itgam; Prom1; Pbx3; Pbx1

Table B2. Over-represented GO pathways in liver proteins of rainbow trout significantly affected by nickel treatment. The list of 26 affected by nickel treatment was search against the Consensus Pathway database (CPDB) to find over-represented gene ontology (GO) biological processes involved in response to nickel exposure (p-value < 0.05). The list here only includes manually selected terms from all the over-represented pathways that best represent the networks of interest.

P-value	Pathway ID	GO Term	Protein from Input List
0.001156699	aurora_a_pathway	Aurora A signaling	Tpx2; tdrd7
0.001011939	WP2361	Gastric Cancer Network 1	Tpx2; kif20b
0.004121212	R-HSA-109582	Hemostasis	Irf2; ptpn11; serping1; kif20b; atp2a2
0.000302977	----------	IGF-Ncore	Ptpn11; ppp4r3a
0.006105267	R-HSA-909733	Interferon alpha/beta signaling	Irf2; ptpn11
0.008418503	R-HSA-418346	Platelet homeostasis	Ptpn11; atp2a2
0.00164687	WP619	Type II interferon signaling (IFNG)	Irf2; ptpn11

APPENDIX C. Over-represented pathways and GO terms in Cytoscape

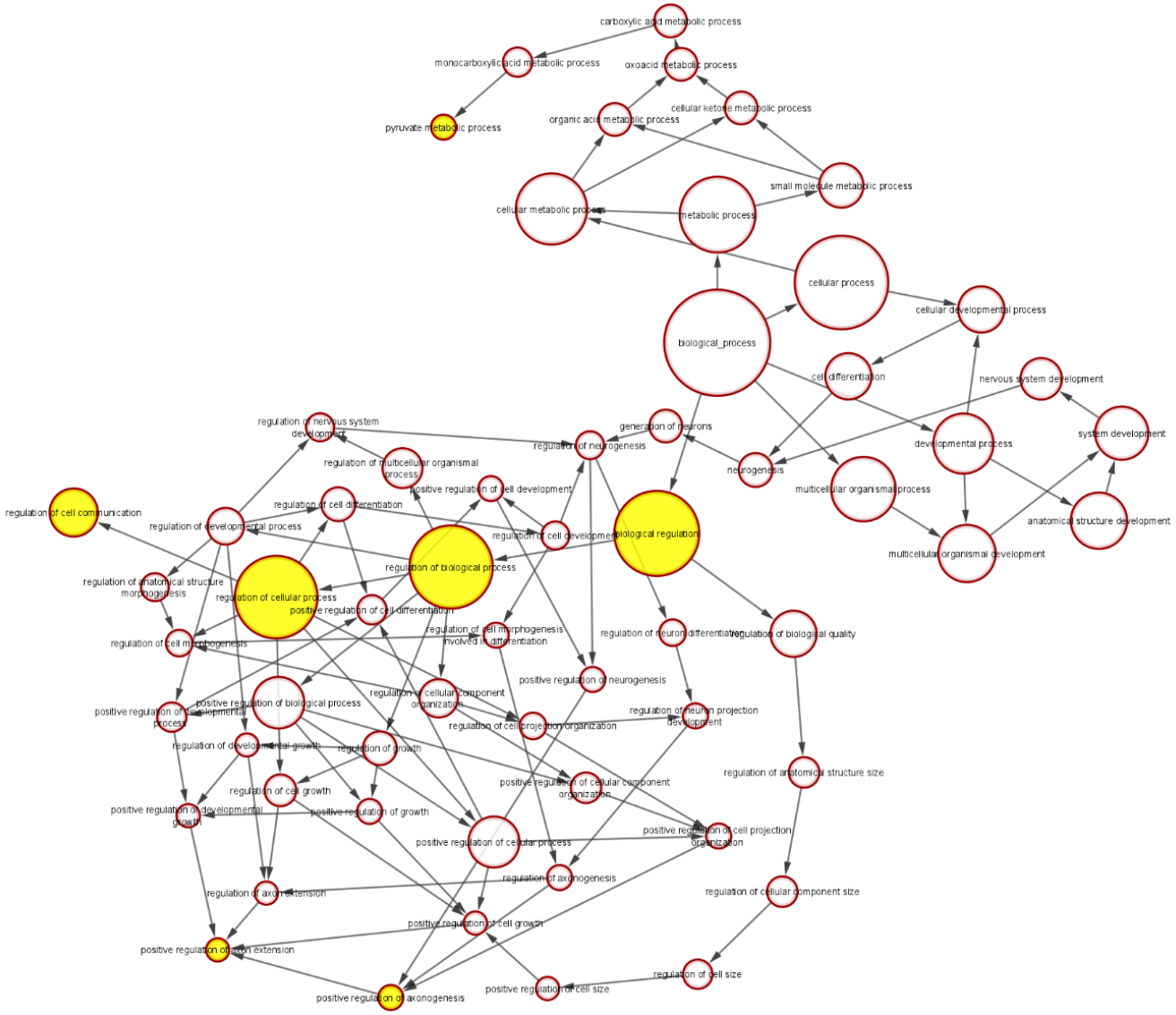

Figure C1. Network of over-represented pathways and processes in the kidney proteome of rainbow trout affected by nickel treatment. The list of 275 proteins significantly affected by nickel treatment were searched in Cytoscape 3.9.1 to find over-represented pathways and gene ontology (GO) biological processes involved in the response to nickel exposure ($p < 0.10$). Each node represents a pathway/process, where the greater the intensity of solid colour (yellow → orange → red) means the more significant the process. The larger the node represents processes with larger gene sets. The nodes are connected with edges, where the width of the edge represents the proteins shared between the nodes and the input list. A relative minimum overlap filter of 25% was applied to the edges (FDR < 0.25, p-value < 0.10). A background protein list was not used.

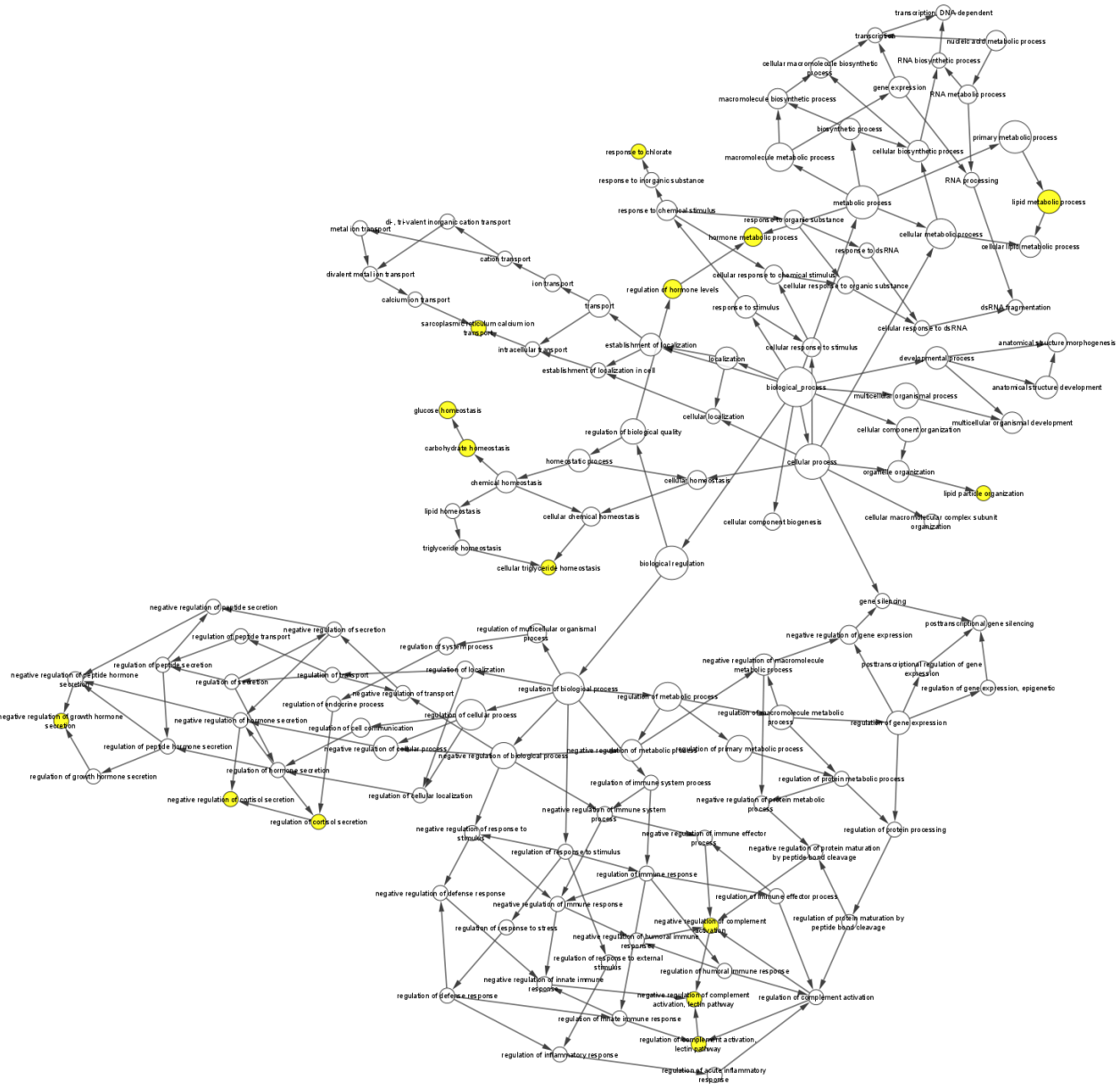

Figure C2. Network of over-represented pathways and processes in the liver proteome of rainbow trout affected by nickel treatment. The list of 26 proteins significantly affected by nickel treatment were searched in Cytoscape 3.9.1 to find over-represented pathways and gene ontology (GO) biological processes involved in the response to nickel exposure ($p < 0.10$). Each node represents a pathway/process, where the greater the intensity of solid colour (yellow → orange → red) means the more significant the process. The larger the node represents processes with larger gene sets. The nodes are connected with edges, where the width of the edge represents the proteins shared between the nodes and the input list. A relative minimum overlap filter of 25% was applied to the edges (FDR < 0.25, p-value < 0.50). A background protein list was not used.

Due to the inaccuracy and lack of significant proteins affected by nickel in the liver proteome, this figure was not used in the analysis of the liver in regards to affected pathways and biological functions. An extremely high FDR and p-value were required to see any pathway connections. This indicates that this is not a reliable analysis of affected pathways.